國 立 交 通 大 學

電信工程研究所

碩 士 論 文

正交分頻多工毫微微細胞系統子載波分配與
功率控制之研究

Joint Subcarrier Allocation and
Power Control for OFDMA Femtocells

研究生：李橋

指導教授：王蒞君 教授

中 華 民 國 九十九 年 七 月

正交分頻多工毫微微細胞系統子載波分配與功率控制之研究

Joint Subcarrier Allocation and Transmit Power Control for OFDMA Femtocells

研 究 生：李橋　　Student：Chiao Lee

指導教授：王蒞君　　Advisor：Li-Chun Wang

國 立 交 通 大 學

電信工程研究所

碩 士 論 文

A Thesis

Submitted to Department of Electrical Engineering

Institute of Communication Engineering

College of Electrical and Computer Engineering

National Chiao Tung University

in partial Fulfillment of the Requirements

for the Degree of

Master of Science

In

Communication Engineering

July 2010

Hsinchu, Taiwan, Republic of China

中華民國九十九年七月

正交分頻多工毫微微細胞系統子載波分配與功率控制之研究

學生: 李橋　　指導教授: 王蒞君教授

國立交通大學

電信工程研究所

摘要

毫微微細胞 (Femtocell) 被視為下世代無線系統的重要技術。因為毫微微細胞可以利用較低的傳輸功率 (Transmit Power) 及生產成本達到有效改善無線通訊於室內環境的資料傳輸速率 (Data Transmission Rate) 與信號涵蓋範圍 (Signal Coverage)。然而，當毫微微細胞系統被廣泛應用的時候，蜂巢式巨細胞基地台 (Macrocell) 及其他毫微微細胞對毫微微細胞的干擾影響甚巨。這種複雜的異質跨層干擾 (Two-tier Interference) 則成為不可忽視的因素。因此，當我們面對這個問題時，如何設計一個自主式及分散式的通道選取機制來克服異質跨層干擾將會是一項挑戰。在此論文中，我們針對正交分頻多工存取 (Orthogonal Frequency Division Multiple Access, OFDMA) 之毫微微細胞系統，提出分散式通道選取機制以減少干擾、並提升傳輸速率及信號可靠度 (Link Reliability)。我們提出通道增益導向之通道選取機制 (Gain-oriented Subchannel Selection Scheme) 及干擾避免導向之通道選取機制 (Interference-Avoidance Oriented Subchannel Selection Scheme)。經由模擬的結果顯示，來自巨細胞及其它毫微微細胞的干擾對於傳輸速率及信號可靠度有極大的影響。藉由適當調整傳輸的子通道數量 (Channel Usage Ratio)，我們所提出來的分散式通道選取機制可以顯著改善傳輸速率及信號可靠度。

此外，我們在論文中也針對毫微微細胞系統，分析異質跨層干擾影響。經由數學推導，在已知鄰近毫微微細胞基地台及巨細胞基地台位置與屏蔽

效應的影響 (Shadowing Standard Deviation)，我們可以估算出毫微微細胞使用者的信號可靠度。同時我們也可以分析毫微微細胞的通道使用率及可適用之巨細胞的半徑範圍。

最後我們探討當毫微微細胞系統使用時，如何同時尋找適當傳輸功率與子通道使用率的共同設計法則。我們比較『通道控制優先』與『功率控制優先』這兩種法則。雖然兩種法則皆可以找到適當的傳輸功率與通道使用率以提供最大功率效益。然而，經由模擬測試，我們發現『通道使用比例控制優先法則』比『功率控制優先法則』可以用更少的調整次數來找到適當的傳輸功率與子通道使用率以滿足最大能量效益。因為通道控制的影響比起功率控制的影響有所不同，通道使用比例控制可以視為對全部資源的巨觀分配法則，功率控制則是針對所分配資源的微觀使用法則。

總體而言，本論文之貢獻包括下列三項：

- 分散式通道選取機制：使毫微微細胞可以依據不同毫微微細胞的佈建密度與巨細胞距離的遠近提供適當的通道選取機制。且針對所在區域室外使用者出現的頻率給予毫微微細胞與蜂巢式巨細胞是否使用相同頻段之建議。
- 信號可靠度的分析架構：藉由毫微微細胞所處的環境分析其使用者信號可靠度的數學方法，並藉由模擬驗證。
- 傳輸功率與通道使用率的選取流程：針對毫微微細胞開機後如何找到適用的傳輸功率與通道使用率不僅可以維持毫微微細胞使用者傳輸速率與信號可靠度並滿足最大功率效益。

綜合以上，從毫微微細胞系統剛開機時，該如何找到適用的傳輸功率與通道使用率開始，至開機完成後，該以何種方式選取通道，本論文皆提出相關的共同設計法則與選取機制，本篇論文所討論之議題可以供未來毫微微細胞系統設計及佈建法則的重要參考。

Joint Subcarrier Allocation and Transmit Power Control
for OFDMA Femtocells

Student：Chiao Lee　　Advisors：Dr. Li-Chun Wang

Institute of Communication Engineering
National Chiao Tung University

Abstract

It goes without saying that femtcoells are the important technology in the next generation wireless networks since the femtocell can improve indoor capacity and coverage with lower power and less cost. However, as femtocells become popular, the indoor and outdoor users suffer from the complicated interference, including the interference from macrocells and other femtocells. Therefore, the femtocells pose a lot of challenge on managing the two-tier interference in an autonomous and distributed manner. In this thesis, we investigate how to distributedly select the subchannels for the OFDMA-based femtocell systems to reduce interference, improve indoor capacity, and ensure the link reliability requirement of indoor and outdoor user. We develop the gain-oriented and interference-avoidance-oriented distributed channel selection schemes. Simulation results show that the interference from the macrocell and other femtocells significantly degrades both femtocell and macrocell user's link reliability and capacity. However, by properly adjusting the number of used subchannels, the developed channel selection schemes can improve capacity and ensure the link reliability.

Moreover, we analyze the outage probability of the distribution channel selection for femtcoell with two-tier interference in OFDMA system. We can calculate the femtocell outage probability if we know the information of macrocell's and neighboring femtocells' location and the shadowing standard deviation. Besides, we also analyze the relationship between the femtocell

channel usage ratio and the macrocell radius. Therefore, we can know that in what macrocell radius, how much channel usage ratio of femtocell should be used.

Finally, We develop the joint sub-carrier allocation and power control principle for OFDMA femtocells. We compare the channel usage ratio oriented principle and transmit power oriented principle. Although the both principles can satisfy the capacity, link reliability, and achieve the highest energy efficiency for femtocell. The visimulation results shows that average adjusting times of the channel usage ratio oriented method is lower than the transmit power oriented method. The channel usage ratio effect on femtocell is different from power control. We can consider that the channel usage ratio allocate and limit the resource from whole wireless resource, and the power control allocates and adjusts the resource under the limited wireless resource.

Overall, the contribution for femtocell in this thesis contains:

- **Distributed channel selection principle:** Develop the distributed channel selection principles in different femtocell deployments and different macrocell radius. In addition, we suggest that the macrocell and femtocell should or should not use the same spectra by the existing probability of the outdoor users and femtocell deployment.
- **Outage probability analyzing:** Provide an analysis framework to analyze theoutage probability of femtocell with two-tier interference in OFDMA systems.
- **Joint sub-carrier allocation and power control principle:** Develop the joint sub-carrier allocation and power control principle for femtocell to find the suitable operating channel usage ratio and transmission power.

To summarize, this thesis discusses the channel selection, allocation of sub-carrier for each subchannel, and power control in OFDMA femtocells, which can provide important insight into the system design and deployment principles for future femtocell systems.

Acknowledgments

I would like to thank my parents and younger brother. They always give me endless supports. I especially would like to thank professor Li-Chun Wang who gave me many valuable suggestions in my research during these two years. I would not finish this work without his guidance and comments.

In addition, I am deeply grateful to my elder laboratory mates, Jane-Hwa Huang, Ang-Hsun Tsai, and Chu-Jung Yeh at Wireless System Labratory at the Institute of Electrical Engineering in National Chiao-Tung University. They provide me a lot of assistance and share happiness with me.

Contents

List of Tables

List of Figures

CHAPTER 1

Introduction

1.1 Problem and Solution

Cellular wireless systems have been used by over 1.4 billion subscribers. Cellular systems were initially designed for only voice communications. The traditional macrocell system serve the users in large coverage area with high transmission power. However, the number of cellular users continuously increases, and the applications of cellular systems can also provide data services. Cellular users can use their handsets for sending E-mail, watching video, and browsing the internet. Obviously, the traffic loading on the wireless communications will become heavier in the future. In addition, penetration loss reduce the signal strength in the indoor environments. For example, basement or underground have the poor coverage for the mobile cellular systems. Therefore, the heavier traffic loading and the dead zone of indoor region are challenging for macrocells. The femtocell networks is considered as one of important solutions for these problems in the traditional macrocell cellular systems [1].

It goes without saying that the femtocells will be widely employed in the next generation wireless networks since the femtocells improve indoor capacity and coverage. However, as the femtocells become popular, the indoor and outdoor users suffer from the complicated two-tier interference, including the interference from the macrocell and other femtocells. Therefore, the femtocells pose a lot of challenges on

managing the interference in an autonomous and distributed manner [2].

1.1.1 Distributed Channel Selection Principle for Femtocell with Two-tier Interference

As femtocells become popular, the indoor and outdoor users suffer from the complicated interference. Therefore, we investigate how to distributedly select the subchannels for the OFDMA-based femtocell systems to reduce interference, improve indoor capacity, and ensure the link reliability requirement for the indoor and outdoor users. We develop the gain-oriented and interference-avoidance-oriented distributed channel selection schemes. In the gain-oriented scheme, the femtocell selects the subchannels with higher link gain to transmit data. For the interference-avoidance-oriented scheme, the femtocell chooses subchannels with lower interference. We compare the two schemes with random selection scheme, which selects subchannels randomly.

1.1.2 Analysis the Outage Probability of OFDMA-based Femtocell

When femtocells are widely used in the future, the two-tier interference to indoor and outdoor users must not be disregarded. Therefore, we are interested in the QoS (Quality of Service) for femtocell users. By analyzing the outage probability of OFDMA based femtocells, we can know that the outage probability for the femtocell users, and the suitable channel usage ratio for femtocells [3]. We consider the effects of pathloss, shadowing, and frequency selective fading. We discuss the random and gain-oriented selection oriented methods. We apply order statistics theorem, to analyze the femtocell outage probability.

1.1.3 The Joint Sub-carrier Allocation and Power Control for Maximizing Energy Efficiency in OFDMA Based Femtocells

In the femtocell networks, we are interested in what channel usage ratio and the transmission power should be designed. In the viewpoint of the channel usage ratio, when a femtocell uses a higher ratio of subchannel for sending information, femtocell interfere to the macrocell's and the other femtocells' users with high probability. However, if the femtocell transmit data with a low ratio of channel usage ratio, a femtocell interfere other femtocell base stations with lower probability, but will serve its users with low capacity. In the viewpoint of the transmission power, when the femtocell face the strongly mactocell-to-femtocell interference, adjusting the transmission power to the higher level is useful to ensure the link quality. Nevertheless, when the femtocell face the femtocell-to-femtocell interference, adjusting the transmission power to the large level is useless because the large transmission power becomes the heavier interference to the other femtocells. The others femtocell will increase power to the higher level for ensure the link quality. Therefore, femtocells compete with each other and increase the power level until to the highest level. In this case, adjusting the femtocell with lower channel usage ratio is more useful than increasing the transmission power to the higher level [4].

1.2 Thesis Outline

The rest of this thesis is organized as follows. Chapter 2 introduces the background of femtocell and the OFDMA systems. Chapter 3 shows the system architecture, channel models and SINR for the femtocell systems. In Chapter 4 and [5], different distributed channel selection principle are proposed. We investigate the ef-

fect of two-tier interference in OFDMA femtocell systems with various sub-carrier allocation methods. In Chapter 5, outage analysis for femtocells of OFDMA systems with single carrier case are discussed. Chapter 6 discusses the analysis for femtocell outage in OFDMA systems in the multicarrier case. The joint transmit power management and sub-carrier allocation for maximizing energy efficiency in OFDMA based femtocells are shown in Chapter 7. Concluding remarks are given in Chapter 8.

CHAPTER 2

Background

2.1 Femtocell

2.1.1 The Concept of Femtocell

In cellular communications, femtocells can be considered as a small cellular base station. The femtocell is designed for the indoor areas like a home or campus/ community environments. It connects to the network of service provider via broadband, like asymmetrical digital subscriber loop (ADSL) or cable networks. Today, 1 to 4 active mobile phones in a residential setting, and 8 to 16 active mobile phones in enterprise settings are supported in typical femtocell. The femtocell is a very promising technique to improve indoor coverage and capacity for the next-generation mobile system with the benefits of low power, low cost, backward compatibility, and single-mode device. The femtocell base station is a simple and low-priced plug-and-play device with smaller coverage. This means that femtocell may have the opportunity on using the licensed spectrum again in the indoor environments. Compared to the macrocell base station, the femtocell base station can use lower power to achieve higher data rate due to the shorter communication distance [6].

Femtocells operated in the licensed spectrum and may use the same or different frequency as macrocells. Their coverage may overlap with a macrocell. Femtocells aim to serve the public users like an open subscriber group (OSG), or to serve a closed

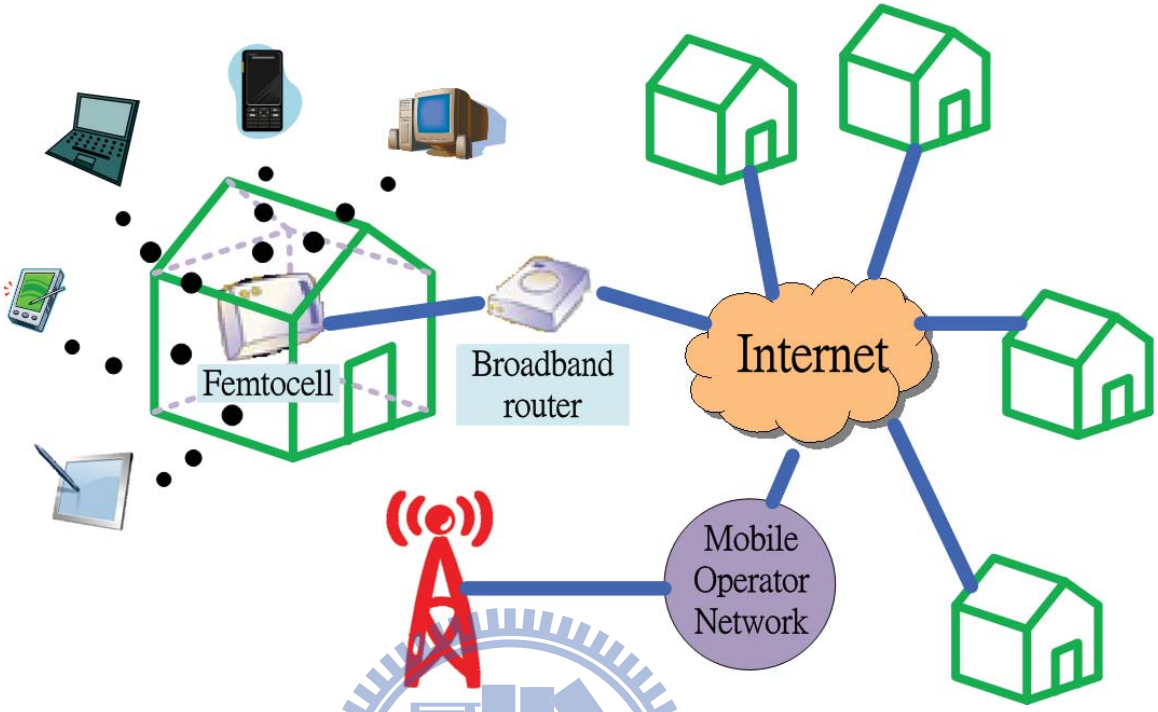

Figure 2.1: The concept of femtocell.

subscriber group (CSG), which is a set of subscribers authorized by the femtocell owner or the network service provider. CSG can be modified by the service level agreement between the subscriber and the network service provider [7, 8].

2.1.2 Femtocell Subscription Types

A femtocell base station may belong to one of the following three subscription types:

- **Closed Subscriber Group Femtocell:** A CSG femtocell is accessible only to the mobile users, which belong to its CSG. Mobile users which are not the members of the CSG should not try to access CSG femtocell.
- **Open Subscriber Group Femtocell:** An OSG femtocell is accessible to any mo-

bile users.

- **Hybrid Subscriber Group Femtocell:** A hybrid femtocell is primarily accessible to the mobile user that belongs to its CSG femtocell, while other mobile user outside CSG femtocell may also access such femtocell, and will be served at lower priority. Hybrid femtocell will provide services to such a mobile user as long as the QoS of mobile users in its CSG is not compromised.

2.2 Orthogonal Frequency Division Multiple Access

2.2.1 Basic Principle

Orthogonal frequency division multiplexing (OFDM) is a multiplexing technique that divides the bandwidth into multiple frequency sub-carriers. The input data stream is divided into several parallel substreams of a reduced data rate and each substream is modulated and transmitted on the separate orthogonal sub-carrier in an OFDM system. The increased symbol duration improves the robustness of OFDM to delay spread. Furthermore, the introduction of the cyclic prefix (CP) can completely discard the inter-symbol interference (ISI) when the CP duration is longer than the channel delay spread. The CP is typically a repetition of the last samples of data portion of the block that is appended to the beginning of the data payload. Figure 2.2 shows the last v samples of data portion of the block with N samples. The CP prevents the inter-block interference and makes the channel appear circular and permits low-complexity frequency domain equalization. The drawback of CP is that it increases overhead, and reduces bandwidth efficiency. Since OFDM has a very sharp, almost "brick-wall" spectrum, a large fraction of the allocated channel

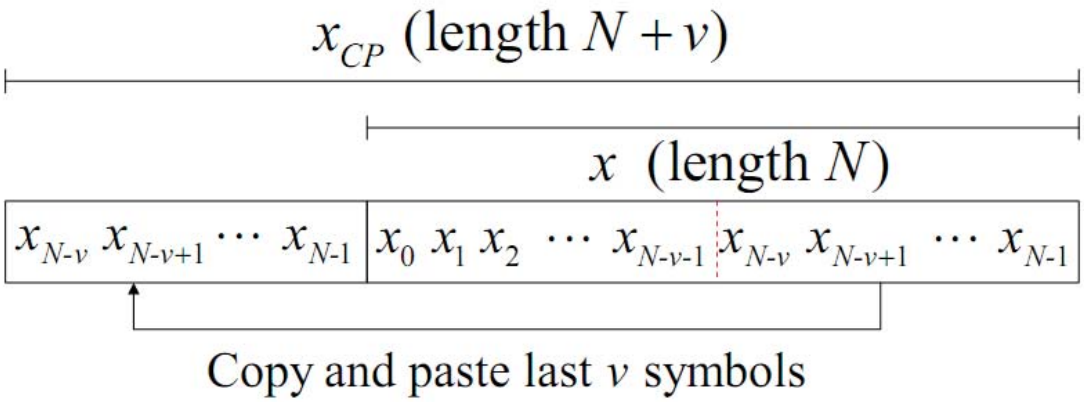

Figure 2.2: Cyclic prefix with last v samples in a OFDM data portion of the block.

bandwidth can be utilized for data transmission, which helps compensate the loss in efficiency due to the cyclic prefix.

OFDM takes advantage of the frequency diversity of the multipath channel by coding and interleaving the information across the sub-carriers to transmissions. OFDM modulation can be realized with the inverse fast Fourier transform (IFFT), which enables a large number of sub-carriers and low complexity. Resources are available in the time domain by means of OFDM symbols and in the frequency domain by means of sub-carriers in an OFDM system. The time and frequency resources can be organized into subchannels for allocation to each users. Orthogonal frequency division multiple access (OFDMA) is a multiple-access/multiplexing scheme that supplies multiplexing operation of data streams from multiple users onto the downlink subchannels and uplink multiple access by means of uplink subchannels.

2.2.2 Sub-carrier Permutation

Permutation is the way to allocate the sub-carrier in a subchannel. There are two types of permutation: Continuous sub-carrier and randomly distributed sub-carrier permutation methods. Figure 2.3 shows the continuous sub-carrier and randomly distributed sub-carrier permutation methods. The usage of subchannel can save the size of the header in MAC layer. For a 1024-point FFT, we need 10 bits to allocate a sub-carrier. For a 64-QAM modulation, there are only 6 information bits in a sub-carrier. The huge size for indexing sub-carrier is not practical. For a subchannel with 18 sub-carriers, one can only use 6 bits to index the total 40 subchannels.

In the IEEE 802.16m evaluation methodology [9], the PUSC permutation is suggested. PUSC is used together with the Wide-Beam Trisector Cell with Pentagon-Shaped Sector antenna pattern. For comparison, Band AMC is also discussed as the adjacent type permutation, which is the continuous sub-carrier permutation method. FUSC is suitable for the broadcast messages since FUSC uses the whole band of bandwidth. The pilots are common among all the subchannels. All the sectors must sent all the sub-carriers and pilots into the air. Usually FUSC is used with omni-directional antenna in broadcast situation as shown in Table 2.1.

2.2.3 IEEE 802.16m WiMAX System

A scalable physical layer enables standard-based solutions to deliver optimum performance in channel bandwidths ranging from 1.25 MHz to 20 MHz with fixed sub-carrier spacing for both fixed and portable/mobile usage models, while keeping the product with low cost. The architecture is based on a scalable subchannelization structure with variable Fast Fourier Transform (FFT) sizes according to the channel bandwidth. Coherence time, Doppler shift, and coherence bandwidth of the channel forms the basis for the consideration of a scalable structure where the FFT sizes scale

Table 2.1: **Permutation Types in WiMAX System.**

Sub-carrier Permutation Type	Example
Randomly Distributed	PUSC (Partial Usage of the Sub-carrier)
	OPUSC (Optional PUSC)
	FUSC (Full Usage of the Sub-carrier)
	OFUSC (Optional FUSC)
Continuous	Band AMC (Band Adaptive Modulation and Coding)

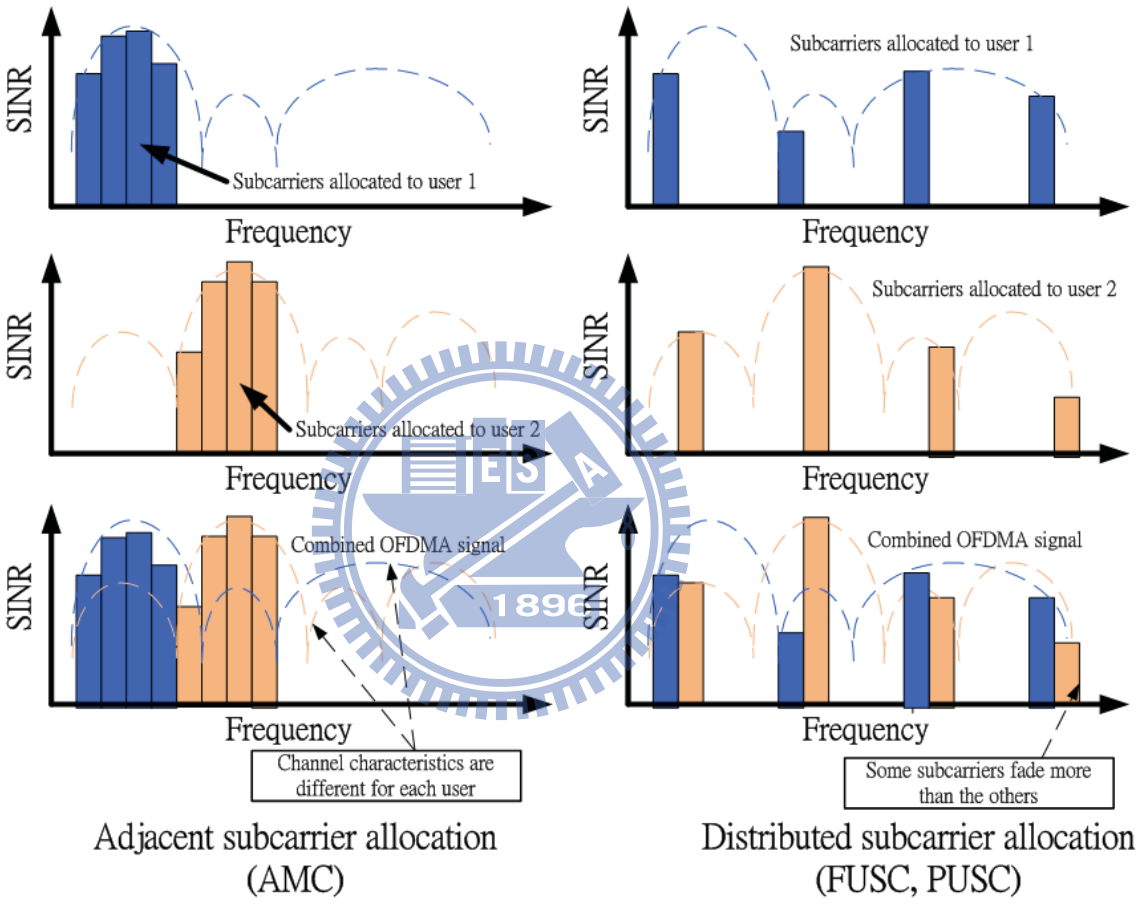

Figure 2.3: Localized and Distributed Resource Allocation.

Table 2.2: **OFDMA scalability parameters.**

Parameters	**Values**						
System bandwidth(MHz)	1.25	5	10	20	3.5	7	8.75
Sampling factor	28/25				8/7		
Sampling frequency(MHz)	1.4	5.6	11.2	22.4	4	8	10
Sampling time(nsec)	714.3	178.6	89.3	44.6	250	125	100
FFT size	128	512	1024	2048	512	1024	1024
Sub-carrier frequency spacing (kHz)	10.93				128		102.4
Guard time	11.4				16		12.8
OFDMA symbol time	102.8				144		115.2

with bandwidth to keep the sub-carrier spacing fixed. Table 2.2 shows the scalability range proposed in the corresponding 802.16 standard.

2.2.4 3GPP Long Term Evolution (LTE)

Long term evolution (LTE) is the project name of the 3-rd generation partnership project (3GPP). LTE is designed to increase the capacity in mobile telephone networks. The LTE specification provides downlink peak rates of at least 100 Mbps, an uplink of at least 50 Mbps and a frame time is less than 10 ms. LTE supports scalable carrier bandwidths, from 1.4 MHz to 20 MHz and supports both frequency division duplexing (FDD) and time division duplexing (TDD). Part of the LTE standard is the system architecture evolution, a flat IP-based network architecture de-

Table 2.3: **LTE parameters in femtocell system.**

Parameter	**Assumption**
Operating frequency	same/different as macrocell
System bandwidth	10 MHz
Channel bandwidth	same as macrocell
Min separation MS to femtocell	20 cm
Number of Tx antennas	1 (baseline) / 2x2 MIMO (optional)
Number of Rx antennas	2
Antenna gain	0/3/5 dBi
Exterior wall penetration loss	10/20 dB
Log-normal shadowing standard deviation	4 dB in rural / 10 dB in urban
Noise figure	8 dB
Min/Max Tx power	0/20 dBm

signed to replace the general packet radio service (GPRS) core network and ensure support for some old communication system or non-3GPP systems, like GPRS and WiMax. The main advantages with LTE are high throughput, low latency, plug and play, FDD and TDD in the same platform, an improved end-user experience and a simple architecture resulting in low operating costs. The next step for LTE evolution is LTE Advanced and is currently being standardized in 3GPP Release 10. Table 2.3 show the femtocell parameters in LTE system.

2.3 Literature Survey

2.3.1 Distributed Channel Selection Principle for Femtocell with Two-tier Interference

In the literature, the capacity and coverage of femtocells are studied in some depth. The work in [1] investigated the capacity of a CDMA-based femtocell, with considering the transmit power configuration for femtocells. In [3], the capacity and coverage for the OFDMA-based femtocell was investigated. Both the work in [1] and [3] considered a full-loaded case. That is, the femtocell users are busy all the time and use the whole spectrum to transmit their data. In addition, the channel selection is not considered. In [10], the authors compared channel selection methods in a OFDMA-based femtocell system. In [10], the whole spectrum is divided into three segments, and each femtocell user can choose one segment. However, only the femtocell-to-femtocell interference is considered in [10].

Different from the works in [1,3,10], this thesis develops the distributed channel selection schemes for the OFDMA-based femtocell networks with considering two-tier interference. In addition, the impact of the number of the subchannels allowed to be used by a femtocell user on link reliability and capacity is investigated.

2.3.2 Outage Probability Analysis for OFDMA-based Femtocell

In [11], the concept of OFDMA system and WiMAX was introduced. In [12], the outage probability of CSMA-based wireless local area network. The mathematical methods for the CSMA-based wireless local area network are modeled in the paper. In [13], it developed an uplink capacity analysis and interference avoidance strategy in such a two-tier CDMA network. The capacity analysis characterized the uplink

outage probability, accounting for power control, path loss and shadowing effects.

Compare to these works in [11–13], this thesis analyze the outage probability for OFDMA-based femtocell networks with considering two-tier interference. Besides, the relationship between the femtocell channel usage ratio and the macrocell radius are also analyze in the thesis.

2.3.3 The Joint Sub-carrier Allocation and Power Control for Maximizing Energy Efficiency in OFDMA-Based Femtocells

The work in [14] illustrated the power control from the downlink reception power of pilot sub-carrier. The upper/lower limit value of the transmit power are considered in this work. In [15], to achieve the tradeoff between energy efficiency and goodput, they suggested a fast channel-driven rate and power adaptation algorithm. They developed a physical/medium access control cross-layer analytical method to evaluate goodput and energy efficiency. In [16], this paper derived a fundamental relation providing the largest feasible cellular Signal-to-Interference-Plus-Noise Ratio (SINR), given any set of feasible femtocell SINRs. It provided a link budget analysis which enables simple and accurate performance insights in a two-tier network.

Different from the works in [14–16], this thesis proposes the joint sub-carrier allocation and power control for maximizing energy efficiency in OFDMA-based femtocells. Moreover, the channel usage ratio oriented method and transmit power oriented method are discussed in this thesis.

CHAPTER 3

System Models

3.1 System Architecture

We consider the OFDMA-based femtocell system in the campus/community environment as shows in Fig. 3.1. We consider the regular grid topology of 25 femtocells. This group of 25 femtocells is uniformly distributed in the macrocell with the coverage radius D_M of 500 m. The house size is 10 meters $\times$ 10 meters. Each house has four rooms, and the femtocell base station is located at the bottom-left corner of the top-right room with a (0.1 m, 0.1 m) shift from the center of the house. The separation distance between two neighboring femtocell base stations is d_{sf} (m). Each femtocell serves one user uniformly distributed in the house. In addition, we assume that there is at most one outdoor user around the considered femtocell. The outdoor user is uniformly distributed in the outdoor region with radius $(d_{sf} - 10)/2$ of the center femtocell, as shown in Fig. 3.2.

We consider the exclusive spectrum and shared spectrum allocation schemes. In the exclusive spectrum allocation scheme, macrocell and femtocell systems have different frequency bands, each allocated with 10 MHz bandwidth. With the shared spectrum allocation scheme, macrocell and femtocell systems are allocated with the same 10-MHz spectrum. The exclusive spectrum allocation scheme can reduce mutual interference, but may have lower spectrum efficiency. On the contrary, the shared

spectrum scheme can increase the spectrum efficiency. Nevertheless, this scheme faces the serious two-tier interference.

We consider the CSG and OSG access methods for femtocells in the shared-spectrum allocation scheme. The CSG femtocell system can serve only the authorized users, and thus the system has better privacy and security. However, the unauthorized users can not access the CSG femtocell base station, even if the femtocell can provide stronger signal than the macrocell. Consequently, the unauthorized user may suffer a stronger interference from the CSG femtocells. The OSG femtocell system is open for all the users, and the outdoor user can select the stronger signal among the macrocell and the closest femtocell. Therefore, the outdoor user can have better signal quality and link reliability. Nevertheless, the privacy and security are difficult issues for the OSG access method. Beside, the OSG method may result in frequent unnecessary handoffs between femtocells and macrocells.

The OFDMA-based femtocell system experiences two-tier interference. This paper considers the downlink case. As shown in Fig. 3.1, an indoor femtocell user has the interference from the macrocell and adjacent femtocells. Fig. 3.2 shows the interference for the outdoor users. If served by the macrocell, the outdoor user has the interference from all adjacent femtocells. As connecting to the femtocell, the outdoor user suffers the macro-to-femto and femto-to-femto interference, as shown in Fig. 3.2.

3.1.1 Location-Aware Femtocells

Location awareness can help reduce the interference from femtocells to the outdoor users. With the capability of location awareness, the femtocells are aware of the location of outdoor users. Therefore, if there is an outdoor user near the considered femtocell, this femtocell should decrease the used sub-carriers to reduce the interference to the outdoor users. The IEEE 802.16m system has the location

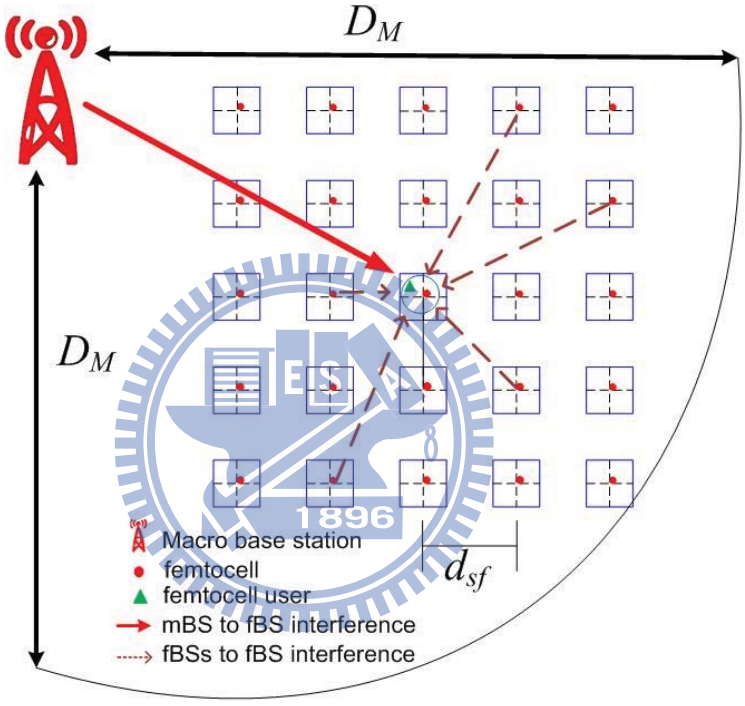

Figure 3.1: Femtocell layout in regular grids and two-tier interference to indoor user.

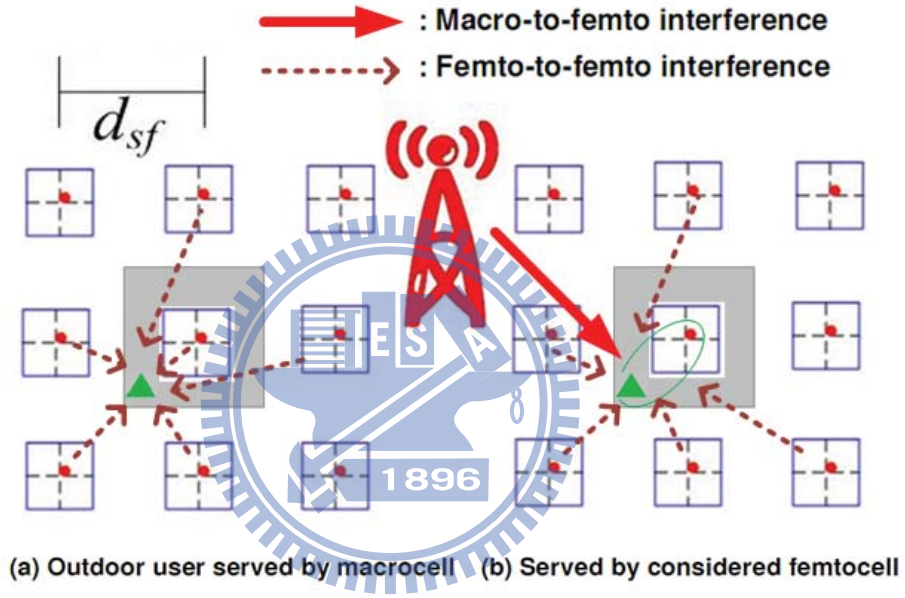

Figure 3.2: Two-tier interference for an outdoor user: (a) femtocell-to-macrocell interference; (b) femtocell-to- femtocell and macrocell-to-femtocell interference.

capability to accurately estimate and report the location of the outdoor user, as stated in the system description document (SDD) [17]. The location capability combined with network level signaling for supporting the location based services (LBS) and emergency location services (such as E-911 calls) can be also used to implement the location-aware femtocells [18].

The IEEE 802.16m system provides four positioning methods in: the network-determining, MS-determining, femtocell-detecting, and global-positioning-system-based methods [17]. For example, in the network-determining method, the system can measure the uplink time of arrival (TOA) and angle of arrival (AOA) to locate the outdoor user by the cooperation of several macrocells. These measurements can be supported via existing uplink transmissions (e.g. ranging sequence) or the signals used for the LBS measurements. The implementation of the location determination is out of the scope of this paper. The detailed information can be obtained in the IEEE 802.16m system description document.

3.2 Radio Channel Effects

This paper considers the impacts of pathloss, shadowing and frequency selective fading channel as follows.

- **Pathloss:** The pathloss decays with the propagation distance d between the transmitter and the receiver [19, 20]. That is,

$$L(d) = \begin{cases} L_{FS}(d) = 20\log_{10}(\frac{4\pi d}{\lambda}) \ , & \text{for } d \leq d_{BP} \\ L_{FS}(d_{BP}) + 35\log_{10}(\frac{d}{d_{BP}}) \ , & \text{for } d > d_{BP} \end{cases} \tag{3.1}$$

  where λ is the wavelength of operating frequency. The break point distance is $d_{BP} = 5$ m for the indoor link and 30 m for the outdoor-to-indoor link. $L_{FS}(d)$ is the free space pathloss.

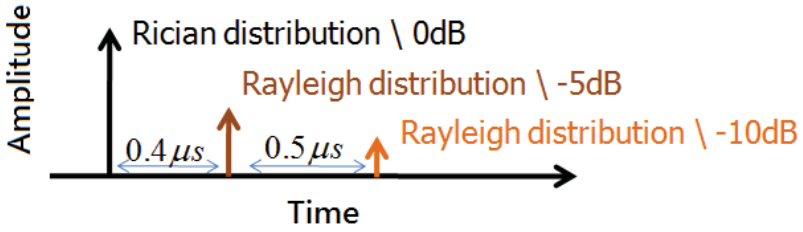

Figure 3.3: Time domain response of Stanford University interim channel model type 3 (SUI-3).

- **Penetration Loss:** The penetration loss is assumed to be 5 dB per internal wall for indoor link; and 10 dB per external wall for outdoor-to-indoor link [10].
- **Shadowing:** Shadowing is modeled by a log-normal random variable $10^{\frac{X}{10}}$, where X is a Gaussian distributed random variable with zero mean. The standard deviation is 5 dB for the indoor link between the femtocell and the indoor user; and 10 dB for the other links.
- **Frequency-Selective Multi-Path Fading:** Figure 3.3 shows that the frequency-selective multi-path fading is described by the Stanford University interim-3 (SUI-3) channel model, which assumes 3 taps with non-uniform delays [21].

3.3 Exponential Effective SINR Mapping (EESM)

We consider the two-tier interference including the femto-to-femto, macro-to-femto, femto-to-macro interference. Let $P_{j,m}$ and $p_{j,m}^{(k)}$ be the transmission power of

macrocell and that of the k-th femtocell at the m-th sub-carrier of the j-th subchannel. Moreover, G_{BS} and G_{FS} are the antenna gains of macrocell and femtocell. The channel gain between macrocell and the considered user is $H_{j,m}$, and that between the k-th femtocell and the considered user is $h_{j,m}^{(k)}$, which include the effects of shadowing and frequency-selective multi-path fading. Therefore, the signal to interference-and-noise ratio (SINR) of the m-th sub-carrier in the j-th subchannel for the user served by macrocell is defined as

$$\Gamma_{j,m} = \frac{\frac{P_{j,m} G_{BS} H_{j,m}}{L(D)}}{\sum_{k=1}^{K} \frac{p_{j,m}^{(k)} G_{FS} h_{j,m}^{(k)}}{L(d_k)} + N_0}, \tag{3.2}$$

where the first term of the denominator is the total interference from K neighboring femtocells, $L(d)$ is the path-loss, and N_0 is the noise power. The SINR of the m-th sub-carrier in the j-th subchannel for the user served by the i-th femtocell is defined as

$$\gamma_{j,m}^{(i)} = \frac{\frac{p_{j,m}^{(i)} G_{FS} h_{j,m}^{(i)}}{L(d_i)}}{\frac{P_{j,m} G_{BS} H_{j,m}}{L(D)} + \sum_{k=1, k\neq i}^{K} \frac{p_{j,m}^{(k)} G_{FS} h_{j,m}^{(k)}}{L(d_k)} + N_0}, \tag{3.3}$$

where the denominator considers the interference from the macrocell and the neighboring femtocells.

The exponential effective SINR mapping (EESM) method is to map a vector of the per sub-carrier SINR level to a single AWGN-equivalent SINR [22]. Suppose that there are M individual sub-carriers in a subchannel with the SINR for each sub-carrier $\{\gamma_1, \gamma_2, \ldots, \gamma_M\}$. The AWGN-equivalent SINR for the subchannel j can be expressed as

$$\gamma_{eff,j}(\gamma_1, \gamma_2, \ldots, \gamma_M) = -\beta \cdot ln(\frac{1}{M} \sum_{m=1}^{M} e^{-\frac{\gamma_m}{\beta}}), \tag{3.4}$$

where β is an EESM calibration factor to minimize the mean square error between the effective SINR calculated by EESM method and the equivalent SINR obtained from

Table 3.1: **Modulation Coding Schemes and EESM parameter (β).**

Modulation	Code Rate (Repetition: default=1)	Spectrum Efficiency σ (bit/s/Hz)	Minimum SINR	EESM factor (β, dB)
QPSK	**1/2(4)**	**0.25**	**-2.5 dB**	**2.18**
QPSK	**1/2(2)**	**0.5**	**0.5 dB**	**2.28**
QPSK	**1/2**	**1**	**3.5 dB**	**2.46**
QPSK	**3/4**	**1.5**	**6.5 dB**	**2.56**
16-QAM	**1/2**	**2**	**9 dB**	**7.45**
16-QAM	**3/4**	**3**	**12.5 dB**	**8.93**
64-QAM	**1/2**	**3**	**14.5 dB**	**11.31**
64-QAM	**2/3**	**4**	**16.5 dB**	**13.8**
64-QAM	**3/4**	**4.5**	**18.5 dB**	**14.71**

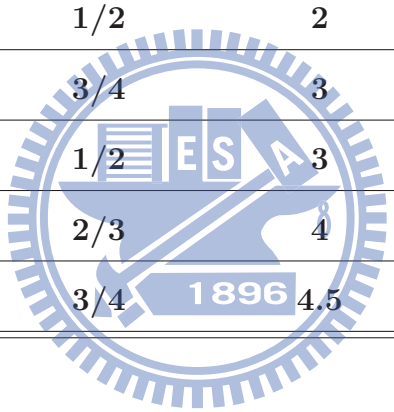

simulation. Table 3.1 shows the considered modulation coding schemes (MCS), the corresponding SINR threshold, and the EESM parameter β. According to Table 3.1, we can determine the MCS and the spectrum efficiency σ_j for the used channel with the effective SINR $\gamma_{eff,j}(\gamma_1, \gamma_2, \ldots, \gamma_M)$.

3.4 Performance Metrics

3.4.1 Link Reliability

The link reliability is the probability that effective SINR for the considered user is greater than a predefined SINR threshold γ_{th}. Consider that there are total J subchannels. We define the subchannel usage ratio ρ as the ratio of used subchannels to the total subchannels. One user selects ρJ subchannels for downlink transmission. Let ε_j denote the utility function. According to the channel selection scheme, if the subchannel j is selected to transmit data, $\varepsilon_j = 1$; otherwise, $\varepsilon_j = 0$. Then, we define the average link reliability for the considered user as

$$\overline{P_{rel}} = \frac{1}{\rho J} \sum_{j=1}^{J} \varepsilon_j P_r\{\gamma_{eff,j} \geq \gamma_{th}\}, \tag{3.5}$$

where $P_r\{\gamma_{eff,j} \geq \gamma_{th}\}$ is the link reliability of the j-th subchannel. The SINR threshold γ_{th} means the minimum SINR requirement for data transmission.

3.4.2 Femtocell Capacity

The femtocell capacity C is defined as the average throughput of a femtocell, which depends on the channel selection scheme, the number of used subchannels, and the adopted MCS of each subchannel. According to the equivalent SINR $\gamma_{eff,j}$ from the EESM method, we can determine the used MCS and then the spectrum efficiency σ_j. Assume that B_m is the bandwidth of a sub-carrier and there are M sub-carriers in a subchannel. The subchannel bandwidth is $B_j = MB_m$. Then, the femtocell capacity is equal to

$$C = \frac{1}{1+G} \sum_{j=1}^{J} \varepsilon_j B_j \sigma_j, \tag{3.6}$$

where G is the guard fraction.

3.4.3 Effective Spectrum Efficiency

The effective spectrum efficiency of the exclusive and shared spectrum allocation schemes for the femtocells are calculated in the following. In the exclusive-spectrum scheme, the total allocated bandwidth is $2B$ since the femtocells and macrocells are allocated with different frequency bands. Assume that the achieved femtocell capacity under the link reliability requirement is C_{ex}. The effective spectrum efficiency of one femtocell in the exclusive-spectrum scheme is defined as

$$SE_{ex} = \frac{C_{ex}}{2B}. \tag{3.7}$$

In the shared spectrum scheme, the femtocells use the same frequency band of bandwidth B as the macrocells. Let C_{sh} be the achieved capacity of one femtocell with the link reliability requirement. Therefore, the effective spectrum efficiency for the shared- spectrum scheme is de ned as

$$SE_{sh} = \frac{C_{sh}}{B}. \tag{3.8}$$

Indeed, SE_{ex} and SE_{sh} defined in (3.7) and (3.8) are the measurements of spectrum efficiency improvement by one femtocell. Although the effective spectrum efficiency SE_{ex} and SE_{sh} are not the actual spectrum efficiency of a heterogeneous macrocell/femtocell system, they can be used to quantitatively compare the spectrum efficiency of the exclusive and shared allocation schemes. Intuitively, with the double bandwidth, the exclusive-spectrum allocation scheme may have less spectrum efficiency than the shared scheme. However, in the shared-spectrum scheme, femtocells must reduce the used sub-carriers for ensuring the link reliability of all the users. This signi cantly reduces the effective spectrum efficiency. Hence, we suggest employing the location awareness capability in the femtocell system to improve the effective spectrum efficiency of the shared spectrum scheme.

Thanks to the location awareness capability as discussed in Section 3.1.1, the femtocells are aware of the existence of an outdoor user. Therefore, only the femtocells close to the outdoor user should decrease the used sub-carriers to reduce the interference. In this situation, the achieved femtocell capacity is C_{sh1}. On the contrary, the femtocells far away from the outdoor user can still use more sub-carriers with higher capacity C_{sh0}. Suppose that for the considered femtocell, the probability that there is an outdoor user around it is p. Therefore, with the location awareness, the average spectrum efficiency for the shared scheme can increase to

$$SE_{LA} = \frac{pC_{sh1} + (1-p)C_{sh0}}{B}. \tag{3.9}$$

The existing probability p of outdoor user around a femtocell depends on the population density, femtocell density, femtocell transmission power and so on. This probability can be estimated from the long-term statistics.

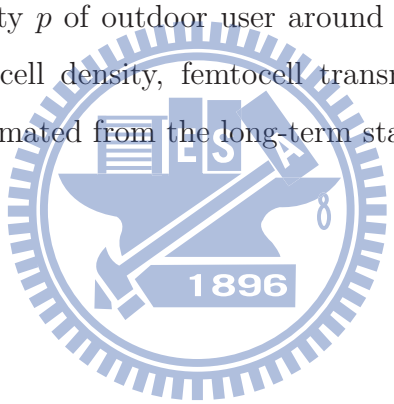

CHAPTER 4

Distributed Channel Selection for Femtocell with Two-tier Interference

4.1 Femtocell Capacity Maximization

Capacity and link reliability are both essential factors in the distributed channel selection principle for the OFDMA-based femtocell systems. From a link reliability perspective, decreasing the number of subchannels allocated to a femtocell can decrease the interference for the users around the femtocells. However, from the link capacity standpoint, increasing the number of subchannels allocated to a femtocell can provide higher data rate.

To improve the tradeoff between capacity and link reliability, we formulate an optimization problem to determine the optimal number of subchannels allocated to a femtocell, aiming to maximize femtocell capacity subject to the link reliability requirement of indoor and outdoor users.

The decision variable in the optimization problem is the channel usage ratio ρ. Based on these considerations, we formulate the capacity maximization issue as a nonlinear programming problem in the following:

$$\max_{0\leq\rho\leq 1} C = \frac{1}{1+G}\sum_{j=1}^{J}\varepsilon_j B_j \sigma_j \tag{4.1}$$

subject to:

$$\rho = \frac{1}{J}\sum_{j=1}^{J}\varepsilon_j \tag{4.2}$$

$$\overline{P_{rel}} \geq Rel_{th} \tag{4.3}$$

where $\varepsilon_j \in \{0, 1\}$, and Rel_{th} is the link reliability requirement for all the users.

4.2 Distributed Channel Selection Scheme

We develop two distributed channel selection principles for the femtocell systems [23]: the gain-oriented and interference-avoidance-oriented channel selection schemes. The first scheme aims to transmit data in the subchannel with higher link gain. By contrary, the second one transmits data in the subchannel with lower interference. Both schemes operate in a distributed manner. Each femtocell can select the subchannels for transmission by itself. The key parameter is the subchannel usage ratio ρ as shown in (7.1). We detail the developed channel selection schemes as follows [24].

4.2.1 Max-Min Gain-Oriented Subchannel Selection Scheme

We explain the procedures in the following.

(S1) Compare the link gain of individual sub-carrier in a subchannel. The minimum sub-carrier link gain in a subchannel is

$$h_j = \min_{m=1,2,\ldots,M}\{h_{j,m}^{(i)}\}, \text{ for } j = 1, \ldots, J \tag{4.4}$$

where M is the total number of sub-carriers in a subchannel, and J is the the total number of subchannels.

(S2) Number all the subchannels according to the minimum sub-carrier link gain, by the order $h_1 \geq h_2 \geq ... \geq h_{\rho J} \geq ... \geq h_J$.

(S3) Select the first ρJ subchannels with higher link gain for transmission. That is, i-th subchannel will be selected, if $h_i \geq h_{\rho J}$.

For example, there are 4 subchannels in the OFDMA-based femtocell system, and each subchannel has 3 sub-carriers. The link gains for the sub-carriers in each subchannel are SCH_1 = {0.2, 0.5, 0.4}, SCH_2 = {-1.4, -0.3, -0.6}, SCH_3 = {-0.1, 0.7, 1.1} and SCH_4 = {-0.4, -0.8, 0.3} (dB), respectively. According to (S1), the minimum link gain h_j for four subchannels are {0.2, -1.4, -0.1, -0.8} (dB). Assume that we need to choose two subchannels for transmission. Then, according to (S2) and (S3), we select SCH_1 and SCH_3 since these subchannels have higher minimum link gains.

4.2.2 Max-Avg Gain-Oriented Subchannel Selection Scheme

This scheme selects the subchannels according to the average sub-carrier link gain.

(S1) Compute the average sub-carrier link gain of each subchannel.

$$h_j = \frac{1}{M} \sum_{m=1}^{M} h_{j,m}^{(i)}, \text{ for } j = 1, \ldots, J. \tag{4.5}$$

(S2) Number all the subchannels according to the average sub-carrier link gain, by the order $h_1 \geq h_2 \geq ... \geq h_{\rho J} \geq ... \geq h_J$.

(S3) Follow the step **(S3)** in Section 4.2.1.

Consider the example in Section 4.2.1. The average link gain h_j for the four subchannels are {0.37, -0.74, 0.59, -0.28} (dB), respectively. Following (S2) and (S3) in Section 4.2.1, we will select SCH_1 and SCH_3, since these subchannels have higher average link gain.

4.2.3 Min-Max Interference Avoidance Subchannel Selection Scheme

The procedures are described in the following. We consider the interference from macrocell and other femtocells.

(S1) Compare the interference of each sub-carrier in a subchannel. The maximum interference for the sub-carriers in a subchannel is

$$I_j = \max_{m=1,2,...,M} \{ \frac{P_{j,m} G_{BS} H_{j,m}}{L(D)} + \sum_{k=1,k\neq i}^{K} \frac{p_{j,m}^{(k)} G_{FS} h_{j,m}^{(k)}}{L(d_k)} \}. \tag{4.6}$$

(S2) Number all the subchannels according to the maximum sub-carrier interference, by the order $I_1 \leq I_2 \leq ... \leq I_{\rho J} \leq ... \leq I_J$.

(S3) Select the first ρJ subchannels with lower interference for transmission. That is, i-th subchannel will be selected, if $I_i \leq I_{\rho J}$.

Assume that the total interference power for the sub-carriers in each subchannel are SCH_1 = {-70, -91, -83}, SCH_2 = {-81, -72, -102}, SCH_3 = {-81, -113, -102} and SCH_4 = {-89, -108, -75} (dBm), respectively. According to (S1), the maximum sub-carrier interference I_j for four subchannels are {-70, -72, -81, -75} (dBm). According to (S2) and (S3), we will select SCH_3 and SCH_4 due to lower maximum interference.

4.2.4 Min-Avg Interference Avoidance Subchannel Selection Scheme

This scheme selects the subchannels according to the average interference for the sub-carriers of a subchannel.

(S1) Compute the average interference of a subchannel.

$$I_j = \frac{1}{M} \sum_{m=1}^{M} \left(\frac{P_{j,m} G_{BS} H_{j,m}}{L(D)} + \sum_{k=1,k\neq i}^{K} \frac{p_{j,m}^{(k)} G_{FS} h_{j,m}^{(k)}}{L(d_k)} \right). \tag{4.7}$$

(S2) Number all the subchannels according to the average interference, by the order $I_1 \leq I_2 \leq ... \leq I_{\rho J} \leq ... \leq I_J$.

(S3) Follow the step **(S3)** in Section 4.2.3.

Considering the example in Section 4.2.3, the average interference I_j for four subchannels are {-74.5, -76.3, -85.7, -79.6} (dBm). Then, following (S2) and (S3), we select SCH_3 and SCH_4 due to lower average interference power.

4.3 Simulation Results

We investigate the downlink capacity and link reliability of the OFDMA-based femtocells by simulations. We consider the shared spectrum allocation and the exclusive spectrum allocation schemes for the femtocells and macrocell. In the shared spectrum allocation scheme, we consider a fully-loaded macrocell system where the macrocell uses all the subcahnnels to send data. Hence, the macrocell must interfere with the femtocell on each subchannel. We assume the femtocell layout as shown in Fig. 3.1. There are 24 femtocells around the considered femtocell, and the group of 25 femtocells is uniformly distributed in a macrocell with the coverage of 500 meters. The separation distance between femtocells is $d_{sf} = 20$ m, unless otherwise specified. The nominal system parameters are listed in Table 4.1. There are total $J = 40$ subchannels. The link reliability requirement is $Rel_{th} = 90\%$. The SINR threshold for link reliability is $\gamma_{th} = -2.5$ dB as an example. Based on the above simulation setup, we compare the gain-oriented and interference-avoidance-oriented distributed channel selection schemes.

Table 4.1: **Parameters in the OFDMA-based IEEE 802.16m WiMAX system.**

Parameter	Value
Carrier frequency	2.5 GHz
mBS/fBS Tx power	43,14 dBm
Noise figure (mBS/fBS/MS)	5dB/7dB/5dB
mBS radius, D_M	500 m
Separation distance between fBSs, d_{sf}	20 m/40 m
Antenna gain (mBS/fBS/MS)	8dB/3dB/3dB
System bandwidth	10 MHz
Sampling frequency	11.2 MHz
FFT size	1024
sub-carrier bandwidth, B_j	10.9375 kHz
Number of null/pilot/data sub-carriers	184,120,720
Number of subchannels, J	40
sub-carriers of each subchannel, M	18
Link reliability requirement, Rel_{th}	90%

4.3.1 Link Reliability and Capacity in Exclusive Spectrum Allocation

Figure 4.1 shows the femtocell link reliability against the channels usage ratio ρ for the exclusive spectrum allocation schemes, where $d_{sf} = 20$ m. In the figure, the femto-to-femto interference significantly affects the link reliability. As the channel usage ratio ρ increases, the link reliability probability decreases due to the increasing interference from other femtocells. Compared to the random selection scheme, the developed distributed channel selection schemes has better link reliability. Therefore, given the link reliability requirement, the developed channel selection schemes can use more subchannels. In this example, under the link reliability requirement $\overline{P_{rel}} \geq 90\%$, the maximum allowable channel usage ratio of the random selection scheme is 0.8. The maximum allowable channel usage ratio of the developed channel selection scheme can increase to 0.9. The figure also shows that for a lower ρ, the interference-avoidance-oriented scheme can choose the subchannels with lower interference to improve the link reliability. However, with a higher ρ, the femtocell will use almost all the subchannels, and the interference from neighboring cannot be avoided. In this situation, the gain-oriented scheme to select the subchannel with higher gain can achieve higher link reliability.

Figure 4.2 shows the femtocell capacity against the channel usage ratio ρ in the exclusive spectrum scheme, where $d_{sf} = 20$ m. In general, as the femtocell uses more data subchannels with a larger ρ, the femtocell can provide higher capacity. Noteworthily, the capacity for the gain-oriented scheme is the concave function of ρ. In this example, the optimal femtocell capacity is 10.7 Mbps at $\rho = 0.8$. This is because as ρ increases to a larger value, the increasing femto-to-femto interference degrades link reliability and thereby diminishes the femtocell capacity. In this figure, the proposed channel selection schemes can achieve higher capacity than the random

selection scheme. For example, if the link reliability requirement $\overline{P_{rel}} \geq 90\%$ is given, the gain-oriented channel selection scheme with $\rho = 0.8$ can achieve 17% higher femtocell capacity than the random selection scheme with $\rho = 0.8$. This figure also shows that the interference-avoidance-oriented channel selection scheme has higher femtocell capacity for the case with a lower ρ. With a lower ρ, each femtocell only uses a fewer subchannels The interference-avoidance-oriented channel selection scheme can choose the subchannels with lower interference. In this case, the link reliability and then the femtocell capacity can be improved.

In Figs. 4.1 and 4.2, it is shown that the Max-Min and Max-Avg methods for gain-oriented scheme have comparable link reliability and femtocell capacity. In the interference-avoidance-oriented scheme, the performance of Min-Max method and that of Min-Avg method are almost the same.

4.3.2 Link Reliability and Capacity in Shared Spectrum Allocation

Figure 4.3 illustrates the indoor user's reliability probability for various channel usage ratio ρ, where $d_{sf} = 20$ m. We consider the shared spectrum allocation scheme and two-tier interference. Compared to Fig. 4.1, this figure shows that the interference from macrocell remarkably degrades the link reliability of indoor user. For example, the link reliability probability for the random channel selection scheme at $\rho = 0.8$ decreases by 8% as the macrocell and femtocells share the same spectrum. It is shown that the proposed channel selection schemes still can improve the link reliability. The gain-oriented selection scheme has higher link reliability. In the shared spectrum scheme, it can be observed from the simulation results that the macro-to-femto interference dominates the two-tier interference. Since the macrocell uses all the subchannels to serve macrocell users, the interference from macrocell cannot be

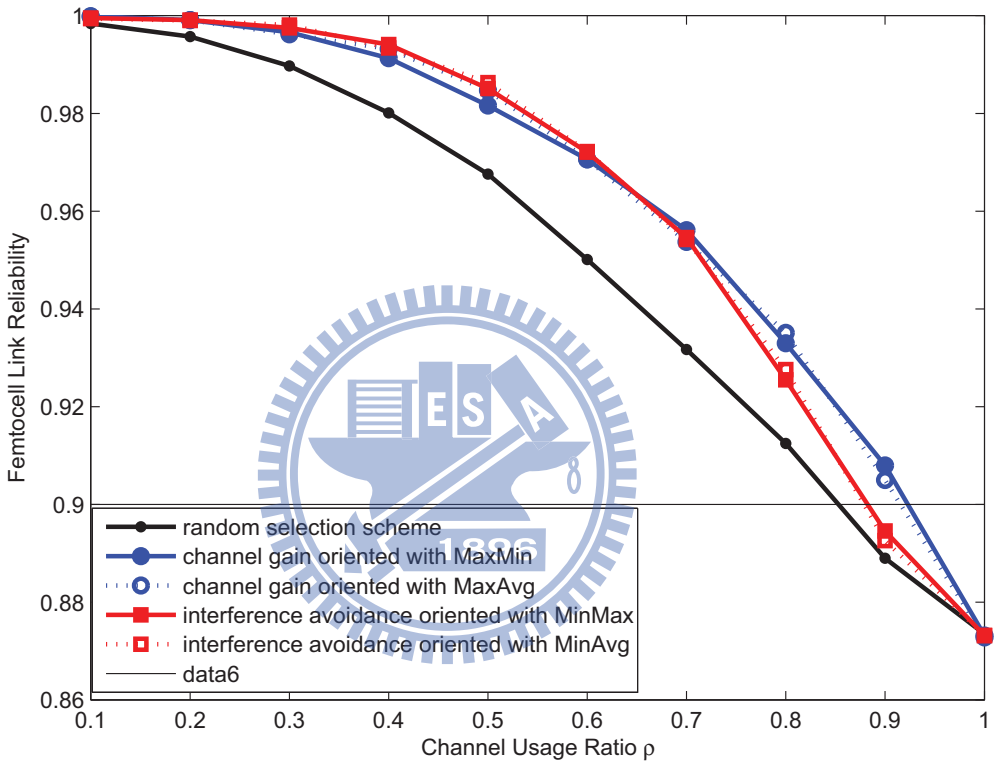

Figure 4.1: Link reliability versus the channel usage ratio ρ with the exclusive spectrum scheme.

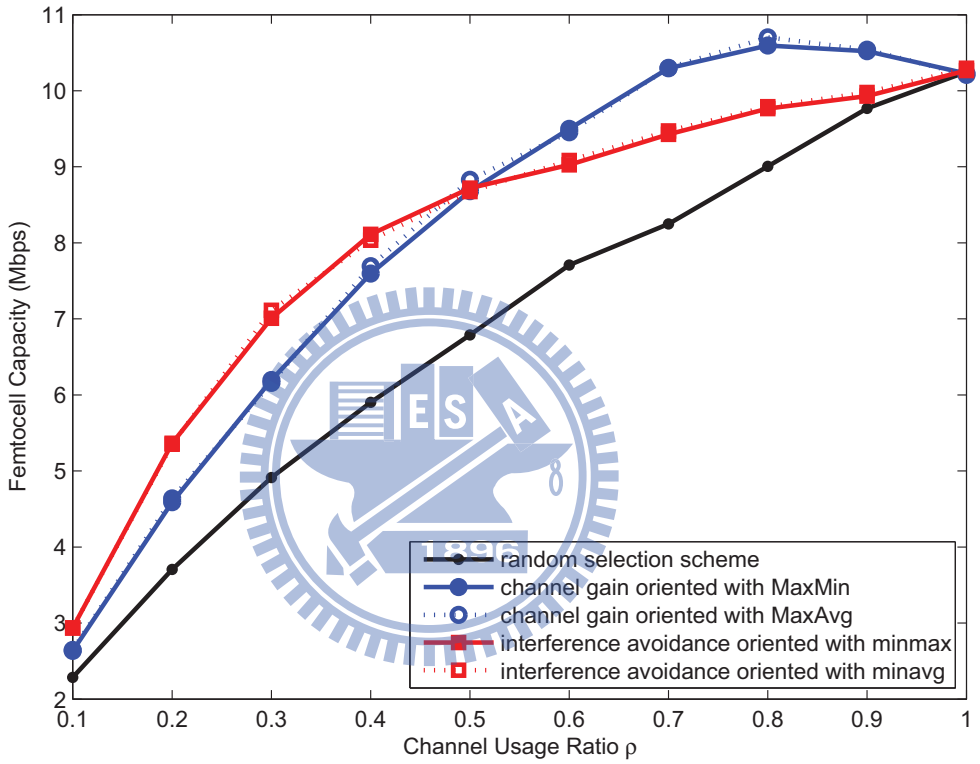

Figure 4.2: Femtocell capacity versus the channel usage ratio ρ with the exclusive spectrum allocation scheme.

avoided. In this situation, the gain-orient selection scheme to select the subchannels with higher link gain can achieve better link reliability. Therefore, under a link reliability requirement, the gain-oriented selection scheme can use more subchannels with higher femtocell capacity. For example, the channel usage ratio ρ for the random selection scheme should be less than 0.3 to meet the link reliability requirement $\overline{P_{rel}} \geq 90\%$. The gain-oriented selection scheme can use nearly twice subchannels for data transmission.

Figure 4.4 illustrates the outdoor user's reliability probability for the various number of data subchannels in femtocells, where $d_{sf} = 20$ m. Compare to the Fig 4.3, this figure shows that interference from femtocells remarkably degrades the outdoor link reliability. When femtcoells increase channel usage ratio ρ, the interference effect on the outdoor user's link reliability significantly. Therefore, femtocell have to decrease the transmitted subchannels by a low value for ensuring the macrocell user's link reliability requirement $\overline{P_{rel}} \geq 90\%$. In this case, the shared spectrum allocation scheme and two-tier interference are considered. We compare different distributed channel selection schemes and different subscription types. In this figure, the OSG femtocell can allow more subchannels for transmission than CSG femtocell under the condition of the macrocell user's link reliability requirement. When the outdoor users face to the two-tier interference, the OSG femtocell can provide a opportunity to connect with stronger link no matter the femtocell or macrocell. However, if outdoor user choose the femtocell for communication, the outdoor user have to face stronger two-tier interference than indoor user without the protect by the wall. The CSG femtocell can provide more subchannel for transmission by gain-oriented selection scheme because that could makes the macrocell user transmit by different subchannel from other femtocells. Moreover, if we consider the factor of distributed channel selection schemes, we can find out the channel gain and interference-avoidance-oriented selection scheme provide different performance to OSG and CSG femtocells. The OSG

femtocell can provide more subchannel for transmission by interference-avoidance-oriented selection scheme. Because the femtocells will choose the different subchannels from the neighboring femtocell by the interference-avoidance-oriented selection scheme, the outdoor users have less interference when it connect to the femtocell. This figure also shows that the performance of random selection scheme and gain-oriented selection scheme are the same. For the outdoor user, each indoor user choose their higher link gain is independent to each other and to the outdoor user. Therefore, when the indoor user is served by the femtocell with gain-oriented selection scheme, it is look like the randomly selection to the outdoor users.

Figure 4.5 shows the femtocell capacity for the various number of data subchannels in the shared spectrum allocation scheme, where $d_{sf} = 20$ m. It is shown that the macrocell-to-femtocell interference degrades the femtocell capacity remarkably. Since the macrocell interferes with the femtocell, the femtocell have to use fewer subchannels to ensure link reliability. In this situation, the interference-avoidance-oriented scheme is preferred, because it can effectively decrease interference and improve capacity. In this case, under the link reliability requirement $\overline{P_{rel}} \geq 90\%$. the interference-avoidance-oriented scheme for $\rho = 0.5$ can achieve 103% higher capacity than the random selection scheme for $\rho = 0.3$.

4.3.3 Spectrum Efficiency Improvement by Location Awareness

Figure 4.6 shows the average effective spectrum efficiency against the existing probability of the outdoor user nearby the femtocell p. From Fig. 4.4, we know that the femtocell has to pose their channel usage ratio ρ in a very low value for ensuring the link reliability of outdoor users in the shared spectrum allocation scheme. Therefore, effective spectrum efficiency of the femtocells in the shared spectrum allocation

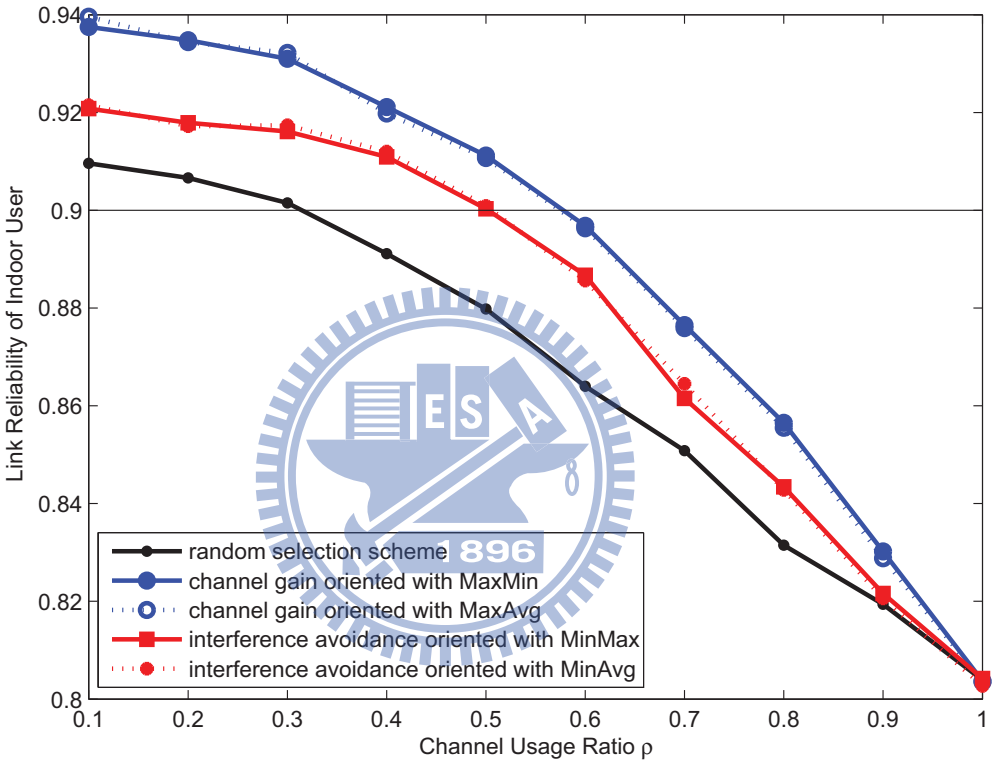

Figure 4.3: Link reliability of indoor user versus the channel usage ratio ρ with the shared spectrum allocation scheme.

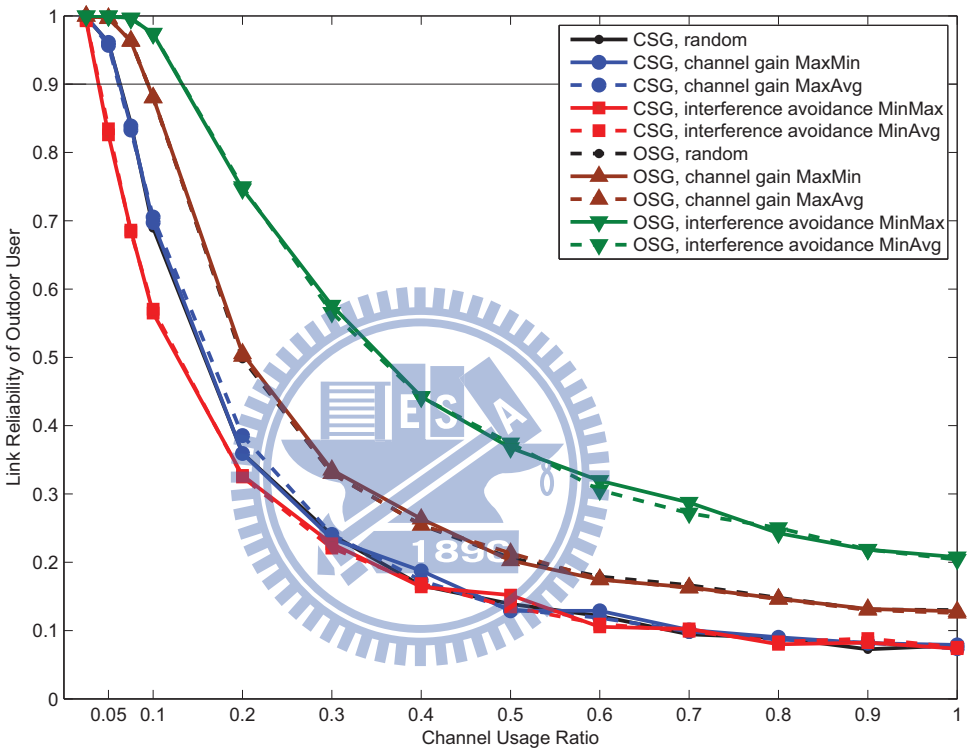

Figure 4.4: Link reliability of outdoor user versus the channel usage ratio ρ with the shared spectrum allocation scheme.

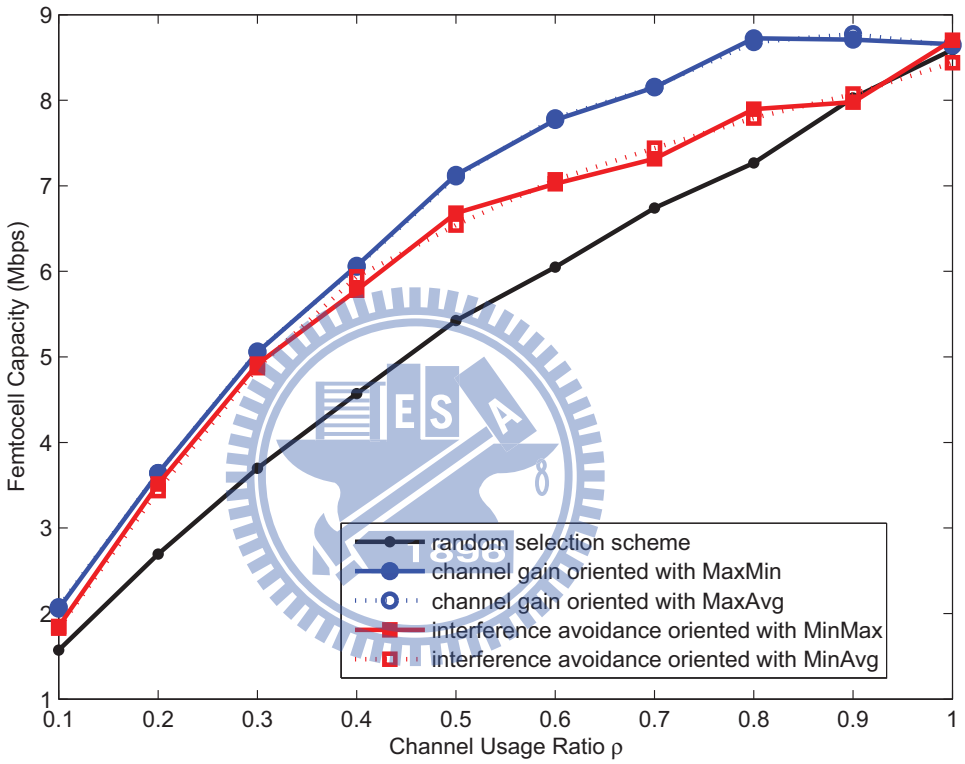

Figure 4.5: Femtocell capacity versus the channel usage ratio ρ with the shared spectrum allocation scheme.

scheme are much lower than the femtocell in the exclusive spectrum allocation scheme. However, if the femtocell has the capability of location awareness, then the femtocell can reduce the channel usage ratio ρ only when the femtocell notice the outdoor users is nearby this area. Therefore, the femtocell with location awareness capability can make the effective spectrum efficiency of the shared spectrum allocation scheme has probability higher than the exclusive spectrum allocation scheme. In this figure, if the femtocell has the capability of location awareness, the effective spectrum efficiency of the CSG and OSG femtocells decreases as the existing probability p increases. Besides, the effective spectrum efficiency of the exclusive spectrum scheme has the cross point with that of the shared spectrum scheme. The cross point corresponds an existing probability of the outdoor user p^*. That means that the shared spectrum scheme has better effective spectrum efficiency than the exclusive spectrum scheme as $p \leq p^*$. Moreover, the cross points in Fig. 4.6 can be calculated as we assume the average effective spectrum efficiency of the shared spectrum scheme equals that of the exclusive spectrum scheme.

$$SE_{LA} = \frac{pC_{sh1} + (1-p)C_{sh0}}{B} = SE_{ex} = \frac{C_{ex}}{2B}\bigg|_{p=p^*} \tag{4.8}$$

Therefore, the cross point is calculated as

$$p^* = \frac{C_{sh0} - \frac{1}{2}C_{ex}}{C_{sh0} - C_{sh1}} \tag{4.9}$$

4.3.4 Impacts of Location Awareness on Spectrum Efficiency

Figure 4.7 illustrates the spectrum efficiency versus the femtocell density in different spectrum allocation schemes and different subscription types. This figure shows that when the denser of femtocells deployment, the spectrum efficiency decrease due to the heavier interference from the neighboring femtocells. In the exclusive spectrum allocation scheme, the existing probability of the outdoor user does not effect

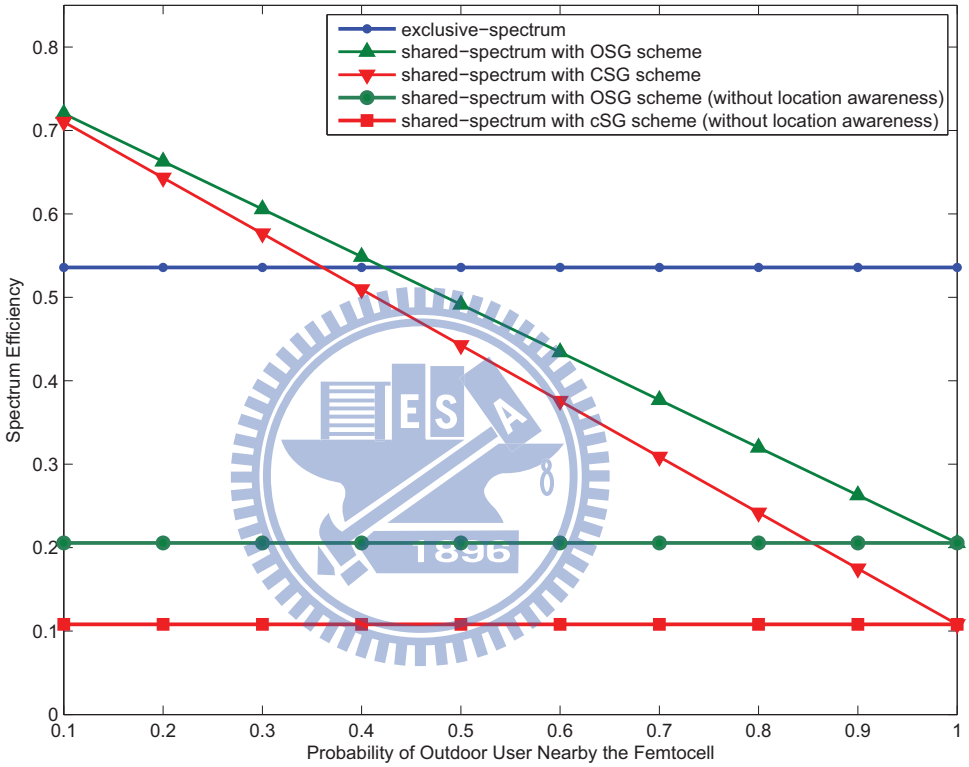

Figure 4.6: Spectrum efficiency versus the femtocell density for shared and exclusive allocation schemes.

on the femtocell spectrum efficiency because the outdoor user and the femtocell user are using the different spectra. When we consider the femtocell with the capability of location awareness in the shared spectrum allocation scheme, the existing probability of the outdoor user effect on the femtocell spectrum efficiency significantly. When we assume that there are no outdoor users around the femtocell area, that means the femtocell can provide as higher capacity as possible and do not consider the link reliability of outdoor user. In this case, the shared spectrum allocation scheme can achieve higher spectrum efficiency than exclusive spectrum allocation scheme. However, when the existing probability of the outdoor user is higher, and ensure the link reliability of outdoor users, the spectrum efficiency in the shared spectrum allocation scheme is much lower than the exclusive spectrum allocation scheme no matter the femtocell with the closed subscriber group or closed subscriber group. From the Fig. 4.4, we know that femtocells have to pose the transmission subchannels in a very low value for ensuring the outdoor user's link quality. Therefore, The existing probability of the outdoor user is a important factor if we consider the macrocell and femtocell are allocated in the same spectrum.

Figure 4.8 illustrates the probability of outdoor user nearby the femtocell versus the femtocell density in different femtocell subscription types. When the femtocell has the capability of location aware function, it means that the femtocell can get the information that if the outdoor users are nearby the femtocell. The femtocell can provide the highest capacity to their users if there is no outdoor user nearby and reduce the number of subchannels for transmission when the outdoor user is nearby the femtocell. These lines in the Fig. 4.8 show that in what probability of outdoor user nearby the femtocell, the shared spectrum and exclusive spectrum allocation scheme have the same spectrum efficiency in the same density of femtocell deployment. This lines also cut up the figure in three parts and these parts help us to know what is the more suitable allocation scheme in each situations. For example, when we knows

that the density of femtocell is 1500 femtocells per $1km^2$ and probability of outdoor user nearby the femtocell is 60%, and it located in the upper area of this figure, then we suggest that exclusive spectrum allocation scheme is suitable because the higher capacity can be achieve in this allocation scheme. Moreover, When we knows that the femtocell deployment and probability of outdoor user nearby the femtocell is located in the middle or lower area of this figure, the shared spectrum allocation scheme can make OSG femtocell with better spectrum efficiency. However, when we have to use the CSG femtocell in shared spectrum allocation scheme, the femtocell deployment and probability of outdoor user nearby the femtocell is located in the lower area of this figure can provide the higher capacity than exclusive spectrum allocation scheme.

4.4 Conclusions

In this chapter, we developed the distributed channel selection principle to ensure the link reliability and improve capacity in the OFDMA-based femtocell systems. We consider the impact on indoor user and outdoor user with different spectrum allocation. For the femtocells, the femtocell-to-femtocell and the macrocell-to-femtocell interference significantly degrade the link reliability and capacity. We develop gain-oriented and interference-avoidance-oriented channel selection principles to improve capacity and link reliability. When we request the indoor user under the link reliability requirement $\overline{P_{rel}} \geq 90\%$, the simulation results show that the developed channel selection scheme can achieve at most 103% higher capacity than the random selection scheme. Moreover, for guaranteeing the link quality of macrocell user, femtocells have to use very low ratio of subchannels for transmission. However, location awareness can help femtocells be aware of the location of outdoor users. Then femtocells can reduce their channel usage ratio only when the outdoor users in the femtocells' coverage. Femtocells can service their user with whole capability without interfering the

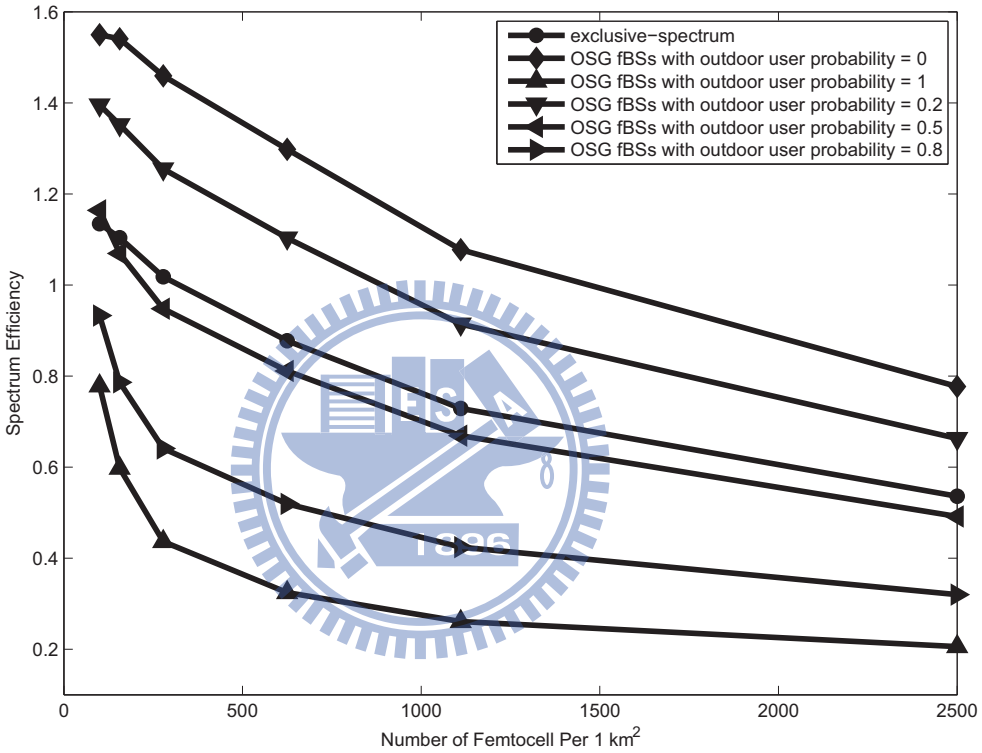

Figure 4.7: Spectrum efficiency versus the probability of outdoor user nearby the femtocell in different allocation schemes.

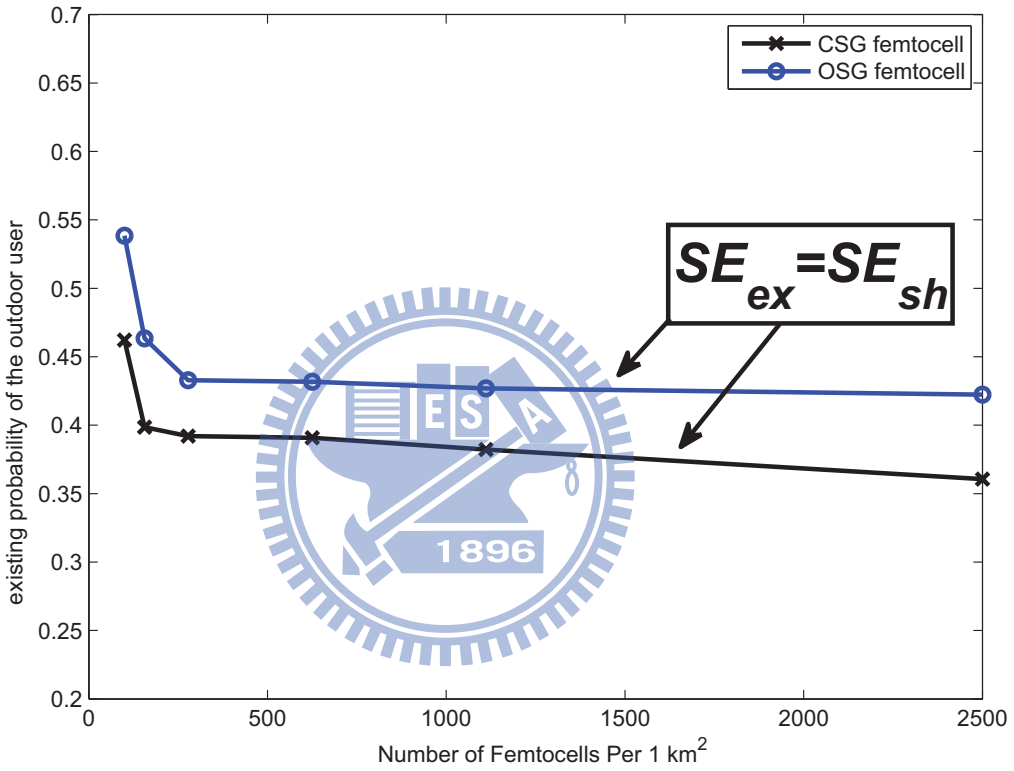

Figure 4.8: Probability of outdoor user nearby the femtocell versus the femtocell density.

neighbour macrocell users. Furthermore, from the viewpoint of spectrum efficiency, the exclusive spectrum allocation scheme is suitable for the area having outdoor user with high probability. The shared spectrum allocation scheme can provide the higher spectrum efficiency when the probability of serving outdoor users is low.

CHAPTER 5

Analysis of Distributed Channel Selection for Femtocell with Two-tier Interference: Single Carrier Case

In this chapter, our goal is to analyze the outage of femtocell with two-tier interference in the single carrier case. Besides, we investigate the impacts of channel usage ratio and the macrocell radius on the outage probability of femtocell users.

5.1 Assumptions

5.1.1 Sub-carrier Allocation

There are two main categories of subchannel allocation scheme in OFDMA systems: contiguous and randomly distributed sub-carrier permutation method. Contiguous sub-carrier permutation allocates contiguous sub-carriers into one subchannel. Randomly distributed sub-carrier permutation allocates non-contiguous sub-carriers distributed over the entire bandwidth into subchannels. The objective of randomly distributed permutations is to achieve the inter-cell interference averaging for the moving users. The contiguous sub-carrier permutation is more suitable for the fixed wireless communications. Femtocell is used for a small area and indoor environment

like campus/community environment. Therefore, the contiguous sub-carrier permutation is better for the femtocell systems with the low mobility communication [25].

5.1.2 Radio Channel

Path loss and Penetration Loss

The path loss decays with the propagation distance d between the transmitter and the receiver [19, 20]. That is,

$$L_{pathloss}(d) = \begin{cases} L_{FS}(d) = 20\log_{10}(\frac{4\pi d}{\lambda}) \ , & \text{for } d \leq d_{BP} \\ L_{FS}(d_{BP}) + 35\log_{10}(\frac{d}{d_{BP}}) \ , & \text{for } d > d_{BP} \end{cases}, \tag{5.1}$$

where λ is the wavelength of operating frequency. The break point distance is $d_{BP} =$ 5 meters for the indoor link and 30 meters for the outdoor-to-indoor link. $L_{FS}(d)$ is the free space pathloss.

The penetration loss $L_{penetration}$ is assumed to be 5 dB per internal wall for indoor link, and 10 dB per external wall for outdoor-to-indoor link. That is,

$$L_{penetration} = 5W_{in} + 10W_{out}, \tag{5.2}$$

where the W_{in} is the number of the crossed internal wall, and W_{out} is the number of the crossed external wall.

From (5.1) and (5.2), we can know the pathloss and the penetration loss. Therefore, the total loss by the transmission path is defined as

$$L(d) = L_{pathloss}(d) + L_{penetration}. \tag{5.3}$$

Shadowing

Shadowing is modeled by a log-normal random variable $10^{\frac{\xi}{10}}$, where ξ is a Gaussian distributed random variable with zero mean. The standard deviation is 5

dB for the indoor link between the femtocell and the indoor user, and 10 dB for the other links.

Multipath Fading on Subchannel

Rayleigh fading is used in the outage probability analysis of femtocells with the two-tier interference. Rayleigh fading characterizes the impact of multipath propagation distribution. The probability of density function for Rayleigh distributed random variable h as

$$f_h(h) = 2he^{-h^2}. \tag{5.4}$$

Let $Y = h^2$. Then the cumulative density function of Y can be written as

$$F_Y(y) = 1 - e^{-y}. \tag{5.5}$$

5.1.3 Signal to Interference and Noise Ratio

We consider the two-tier interference including the femto-to-femto, macro-to-femto, femto-to-macro interference. Let $P_{k,j}$ be the transmission power of the k-th base station at the j-th subchannel, respectively. Shadowing can be characterized by a log-normal random variable $10^{\frac{\xi_{k,j}}{10}}$, where $\xi_{k,j}$ is a Gaussian random variable on the j-th subchannel of the k-th femtocell. The subchannel gain between the k-th base station and the considered user is $y_{k,j}$. Therefore, the received signal power at the femtocell mobile terminal can be written as [12, 26, 27]

$$P_{i,j} = P_{k,j}10^{\frac{\xi_{k,j}}{10}} y_{k,j}/L(r_k). \tag{5.6}$$

Assume that there are K base stations that include the $(K-1)$ femtocells and a macrocell in the system, labeled from 2 to K. Let the desired user be indexed with

1. Then the total interference P_{I_j} received from the other $(K-1)$ base stations of subchannel j can be expressed as

$$P_{I_j} = \sum_{k=2}^{K} \varepsilon_{k,j} P_{k,j} 10^{\xi/10} y_{k,j} / L(r_k), \tag{5.7}$$

where ε_j is the utility function. If the subchannel j is selected to transmit data, $\varepsilon_j = 1$; otherwise, $\varepsilon_j = 0$.

Then, the signal-to-interference noise ratio (SINR) on the j-th subchannel of the first femtocell can be express as

$$SINR = \frac{P_{1,j}}{P_{I_j} + N_0}, \tag{5.8}$$

where N_0 is the noise power.

5.2 Outage Probability of Single Femtocell

We consider a scenario that only a femtocell in this area, none other macrocell or femtocells. By setting the required received threshold γ_{th}, the outage probability can be expressed as

$$\begin{aligned}
&P_{outage} \\
&= \Pr[SNR < \gamma_{th}] \\
&= \Pr[\frac{P_{i,j} 10^{\frac{\xi_{i,j}}{10}} y_{i,j} / L(r_i)}{N_0} < \gamma_{th}] \\
&= \Pr[y_{i,j} < \gamma_{th} \frac{N_0}{P_{i,j}} 10^{-\frac{\xi_{i,j}}{10}} L(r_i)] \\
&= \int_{-\infty}^{\infty} \int_{0}^{R} F_Y[\gamma_{th} \frac{N_0}{P_{i,j}} 10^{-\frac{\xi_{i,j}}{10}} L(r_i)] f_{r_i}(r_i) f_\xi(\xi) dr_i d\xi
\end{aligned}$$

$$= \int_{-\infty}^{\infty} \int_{0}^{R} [1 - e^{-\gamma_{th} \frac{N_0}{P_{i,j}} 10^{-\frac{\xi_{i,j}}{10}} L(r_i)}] \frac{2r_i}{R^2} \frac{e^{-\frac{\xi^2}{2\sigma^2}}}{\sqrt{2\pi}\sigma} dr_i d\xi, \tag{5.9}$$

where R is the cell radius and there are no other femtocells and macrocell in the neighboring area.

5.3 Outage Probability of Random Channel Selection Principle for Femtocell with Two-tier Interference

In this case, we consider the two-tier interference including the femto-to-femto, macro-to-femto, femto-to-macro interference. The effect of noise may be neglected (i.e. $N_0 = 0$) in the interference limited system. Thus, the outage probability of random selection principle for femtocell with two-tier interference can be written as

$$\begin{aligned}
&P_{outage,random} \\
&= \Pr[SIR_{1,j} < \gamma_{th}] \\
&= \Pr[\frac{P_{1,j} 10^{\xi_{i,j}/10} y_{i,j} / L(r_i)}{\sum_{k=2}^{K} \varepsilon_{k,j} P_{k,j} 10^{\xi_{k,j}/10} y_{k,j} / L(r_k)} < \gamma_{th}] \\
&= \Pr[\frac{P_{1,j} 10^{\xi_{i,j}/10} y_{i,j}}{L(r_i)} < \gamma_{th} \sum_{k=2}^{K} \frac{\varepsilon_{k,j} P_{k,j} 10^{\xi_{k,j}/10} y_{k,j}}{L(r_k)}] \\
&= \Pr[y_{i,j} < \gamma_{th} \sum_{k=2}^{K} \frac{\varepsilon_{k,j} P_{k,j}}{P_{1,j}} 10^{\frac{\xi_{k,j} - \xi_{1,j}}{10}} \frac{L(r_1)}{L(r_k)} y_{k,j}].
\end{aligned} \tag{5.10}$$

Let $r = (r_2, r_3, ..., r_K)$ and $\xi = (\xi_2, \xi_3, ..., \xi_K)$. Then the outage probability of random selection principle for femtocell user 1 can be written as

$$
\begin{aligned}
& P_{outage,random}(r_1, \xi_1 | r, \xi) \\
& = \int_0^\infty ... \int_0^\infty [1 - \exp(-\gamma_{th} \sum_{k=2}^{K} \frac{\varepsilon_{k,j} P_{k,j}}{P_{1,j}} 10^{\frac{\xi_{k,j} - \xi_{1,j}}{10}} \frac{L(r_1)}{L(r_k)} y_{k,j})] \\
& \cdot e^{-y_{2,j}} \cdots e^{-y_{K,j}} \cdot dy_2 \cdots dy_K \\
& = \int_0^\infty ... \int_0^\infty e^{-y_{2,j}} \cdots e^{-y_{K,j}} dy_2 \cdots dy_K \\
& - \int_0^\infty ... \int_0^\infty \exp(-\sum_{k=2}^{K} y_{k,j} (1 + \gamma_{th} \frac{\varepsilon_{k,j} P_{k,j}}{P_{1,j}} 10^{\frac{\xi_{k,j} - \xi_{1,j}}{10}} \frac{L(r_1)}{L(r_k)})) dy_2 \cdots dy_K \\
& = 1 - \prod_{k=2}^{K} \frac{1}{(1 + \gamma_{th} \frac{\varepsilon_{k,j} P_{k,j}}{P_{1,j}} 10^{\frac{\xi_{k,j} - \xi_{1,j}}{10}} \frac{L(r_1)}{L(r_k)})}.
\end{aligned}
\tag{5.11}
$$

5.4 Outage Probability of Gain-Oriented Channel Selection Principle for Femtocell with Two-tier Interference

In Section. 4.2, we develop the gain-oriented channel selection principle for femtocell systems. The gain-oriented selection scheme aims to transmit data in the subchannel with higher link gain. This selection scheme operate in a distributed manner. Each femtocell can select the subchannels for transmission by itself. We detail the gain-oriented selection schemes in Sections. 4.2.1 and 4.2.2.

5.4.1 Outage Probability of Maximal Link Gain Channel for Femtocell with Two-tier Interference

We assume that the gain value of each subchannel is Rayleigh distribution. Recall Equations 5.4 and 5.5 in Section 5.1.2, we can have the distribution of received power Z as the cumulative density function of Z can be written as

$$f_Z(z) = e^{-z} \tag{5.12}$$

$$F_Z(z) = 1 - e^{-z}. \tag{5.13}$$

Consider that there are total N subchannels. If we use only one sebchannel for transmission, we will choose the highest link gain channel by the gain-oriented selection scheme. In this case, let $Y = max(z_1, z_2, ..., z_N)$ and $z_1, z_2, ..., z_N$ are independent and identically distributed (i.i.d.), then the cumulative density function of Y can be written as

$$\begin{aligned} F_Y(y) &= P\{z_1 \leq y, z_2 \leq y, ..., z_N \leq y\} \\ &= F_{z_1,z_2,...,z_N}(y, y, ..., y) \\ &= \prod_{i=1}^{N} F_{z_i}(y) \\ &= (1 - e^{-y})^N, \end{aligned} \tag{5.14}$$

and the probability density function is expressed as

$$\begin{aligned} f_Y(y) &= \frac{d}{dy} F_Y(y) \\ &= \frac{d}{dy}(1 - e^{-y})^N \\ &= Ne^{-y}(1 - e^{-y})^{N-1}. \end{aligned} \tag{5.15}$$

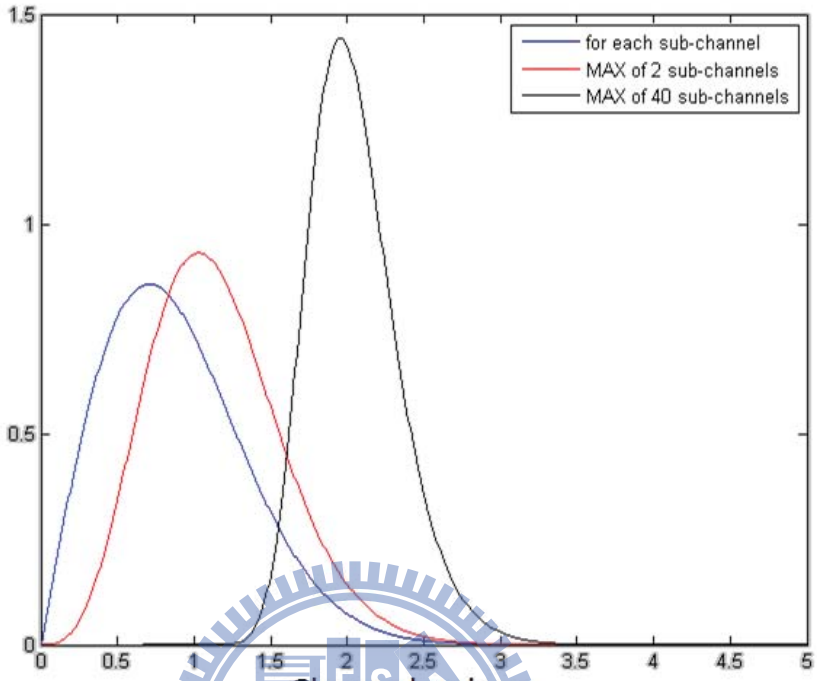

Figure 5.1: Probability density function for the max channel gain selection.

Figure 5.4.1 shows that the probability density function of the maximal subchannel link gain selection from 1 subchannel, 2 subchannels, and 40 subchannels. It also illustrates that if we can choose the maximal subchannel link gain from more subchannels, then the higher probability we can choose the subchannel with higher link.

When we assume all the femtocells with the capability of channel gain selection function. The interference from macrocell and femtocells should be considered. In this interference limited system, the effects of noise may be neglected. Thus, the outage probability of maximal link gain selection principle for femtocell with two-tier

interference can be written as

$$
\begin{aligned}
P_{outage,(1-st)} &= \Pr[SNR_{1,j} < \gamma_{th}] \\
&= \Pr[\frac{P_{1,j}10^{\xi_{i,j}/10}y_{i,j}/L(r_i)}{\sum_{k=2}^{K}\varepsilon_{k,j}P_{k,j}10^{\xi_{k,j}/10}y_{k,j}/L(r_k)} < \gamma_{th}] \\
&= \Pr[\frac{P_{1,j}10^{\xi_{i,j}/10}y_{i,j}}{L(r_i)} < \gamma_{th}\sum_{k=2}^{K}\frac{\varepsilon_{k,j}P_{k,j}10^{\xi_{k,j}/10}y_{k,j}}{L(r_k)}] \\
&= \Pr[y_{i,j} < \gamma_{th}\sum_{k=2}^{K}\frac{\varepsilon_{k,j}P_{k,j}}{P_{1,j}}10^{\frac{\xi_{k,j}-\xi_{1,j}}{10}}\frac{L(r_1)}{L(r_k)}y_{k,j}]. \qquad (5.16)
\end{aligned}
$$

Let $r = (r_2, r_3, ..., r_K)$ and $\xi = (\xi_2, \xi_3, ..., \xi_K)$. Then the outage probability of maximal link gain selection principle for femtocell user 1 can be written as

$$
\begin{aligned}
&P_{outage,(1-st)}(r_1, \xi_1 | r, \xi) \\
&= \int_0^\infty ... \int_0^\infty [1 - \exp(-\gamma_{th}\sum_{k=2}^{K}\frac{\varepsilon_{k,j}P_{k,j}}{P_{1,j}}10^{\frac{\xi_{k,j}-\xi_{1,j}}{10}}\frac{L(r_1)}{L(r_k)}y_{k,j})]^N \cdot e^{-y_{2,j}} \cdots e^{-y_{K,j}} \cdot dy_2 \cdots dy_K \\
&= \int_0^\infty ... \int_0^\infty \sum_{l=0}^{N}\binom{N}{l}(1)^l(-\exp(-\gamma_{th}\sum_{k=2}^{K}\frac{\varepsilon_{k,j}P_{k,j}}{P_{1,j}}10^{\frac{\xi_{k,j}-\xi_{1,j}}{10}}\frac{L(r_1)}{L(r_k)}y_{k,j}))^{N-l} \\
&\cdot e^{-y_{2,j}} \cdots e^{-y_{K,j}} \cdot dy_2 \cdots dy_K \\
&= \int_0^\infty ... \int_0^\infty \sum_{l=0}^{N}\binom{N}{l}(-1)^{N-l}\exp(-\gamma_{th}(N-l)\sum_{k=2}^{K}\frac{\varepsilon_{k,j}P_{k,j}}{P_{1,j}}10^{\frac{\xi_{k,j}-\xi_{1,j}}{10}}\frac{L(r_1)}{L(r_k)}y_{k,j}) \\
&\cdot e^{-y_{2,j}} \cdots e^{-y_{K,j}} \cdot dy_2 \cdots dy_K \\
&= \int_0^\infty ... \int_0^\infty \sum_{l=0}^{N}\binom{N}{l}(-1)^{N-l}\exp(-\sum_{k=2}^{K}y_{k,j}(1+\gamma_{th}(N-l)\frac{\varepsilon_{k,j}P_{k,j}}{P_{1,j}}10^{\frac{\xi_{k,j}-\xi_{1,j}}{10}}\frac{L(r_1)}{L(r_k)}))dy_2 \cdots dy_K
\end{aligned}
$$

$$= \sum_{l=0}^{N} [\begin{pmatrix} N \\ l \end{pmatrix} (-1)^{N-l} \prod_{k=2}^{K} \frac{1}{(1 + (N-l)\gamma_{th} \frac{\varepsilon_{k,j} P_{k,j}}{P_{1,j}} 10^{\frac{\xi_{k,j} - \xi_{1,j}}{10}} \frac{L(r_1)}{L(r_k)})}]. \quad (5.17)$$

5.4.2 Outage Probability of n-th Highest Link Gain Channel for Femtocell with Two-tier Interference

For the base station like femtocell, multiple subchannels are used in the same time. According to the gain-oriented principle, femtocell uses the top higher subchannel for sending information. In addition, the total N subchannels are considered in the femtocell system. If we use n subchannels for transmission, we choose the 1-st to n-th highest link gain channel by the gain-oriented selection scheme. In this case, let $Y = \{y_1, y_2, ..., y_N\}$ be the order statistics of independent and identically distributed (i.i.d.) random variable from $(z_1, z_2, ..., z_N)$ where $y_1 \leq y_2 \leq ... \leq y_N$, then the cumulative density function of Y_n can be written as

$$F_{Y_n}(y) = \sum_{i=n}^{N} \begin{pmatrix} N \\ i \end{pmatrix} [F_Z(y)]^i [1 - F_Z(y)]^{N-i}, \quad (5.18)$$

and the probability density function is expressed as

$$f_{Y_n}(y) = \frac{N!}{(N-n)!(n-1)!} f_Z(y) [F_Z(y)]^{N-n} [1 - F_Z(y)]^{n-1}. \quad (5.19)$$

In this case, the outage probability of n-th highest link gain selection principle for femtocell with two-tier interference can be written as

$$P_{outage,(n-th)}$$

$$= \Pr[SNR_{1,j} < \gamma_{th}]$$

$$= \Pr[\frac{P_{1,j} 10^{\xi_{i,j}/10} y_{i,j} / L(r_i)}{\sum_{k=2}^{K} \varepsilon_{k,j} P_{k,j} 10^{\xi_{k,j}/10} y_{k,j} / L(r_k)} < \gamma_{th}]$$

$$= \Pr[\frac{P_{1,j}10^{\xi_{i,j}/10}y_{i,j}}{L(r_i)} < \gamma_{th}\sum_{k=2}^{K}\frac{\varepsilon_{k,j}P_{k,j}10^{\xi_{k,j}/10}y_{k,j}}{L(r_k)}]$$

$$= \Pr[y_{i,j} < \gamma_{th}\sum_{k=2}^{K}\frac{\varepsilon_{k,j}P_{k,j}}{P_{1,j}}10^{\frac{\xi_{k,j}-\xi_{1,j}}{10}}\frac{L(r_1)}{L(r_k)}y_{k,j}]. \tag{5.20}$$

Let $r = (r_2, r_3, ..., r_K)$ and $\xi = (\xi_2, \xi_3, ..., \xi_K)$. Then the outage probability of n-th highest link gain selection principle for femtocell user 1 can be written as

$$P_{outage,(n-th)}(r_1, \xi_1|r, \xi)$$

$$= \int_0^\infty ... \int_0^\infty \sum_{l=n}^{N}\binom{N}{l}[1-\exp(-\gamma_{th}\sum_{k=2}^{K}\frac{\varepsilon_{k,j}P_{k,j}}{P_{1,j}}10^{\frac{\xi_{k,j}-\xi_{1,j}}{10}}\frac{L(r_1)}{L(r_k)}y_{k,j})]^l$$

$$\cdot [\exp(-\gamma_{th}\sum_{k=2}^{K}\frac{\varepsilon_{k,j}P_{k,j}}{P_{1,j}}10^{\frac{\xi_{k,j}-\xi_{1,j}}{10}}\frac{L(r_1)}{L(r_k)}y_{k,j})]^{N-l}\cdot e^{-y_{2,j}}\cdots e^{-y_{K,j}}\cdot dy_2\cdots dy_K$$

$$= \int_0^\infty ... \int_0^\infty \sum_{l=n}^{N}\{\binom{N}{l}\sum_{m=0}^{l}[\binom{l}{m}(-1)^{l-m}$$

$$\cdot \exp(-\gamma_{th}(l-m)\sum_{k=2}^{K}\frac{\varepsilon_{k,j}P_{k,j}}{P_{1,j}}10^{\frac{\xi_{k,j}-\xi_{1,j}}{10}}\frac{L(r_1)}{L(r_k)}y_{k,j})]$$

$$\cdot [\exp(-\gamma_{th}(N-l)\sum_{k=2}^{K}\frac{\varepsilon_{k,j}P_{k,j}}{P_{1,j}}10^{\frac{\xi_{k,j}-\xi_{1,j}}{10}}\frac{L(r_1)}{L(r_k)}y_{k,j})]\}\cdot e^{-y_{2,j}}\cdots e^{-y_{K,j}}\cdot dy_2\cdots dy_K$$

$$= \int_0^\infty ... \int_0^\infty \sum_{l=n}^{N}\{\binom{N}{l}\sum_{m=0}^{l}[\binom{l}{m}(-1)^{l-m}$$

$$\cdot \exp(-\gamma_{th}(N-m)\sum_{k=2}^{K}\frac{\varepsilon_{k,j}P_{k,j}}{P_{1,j}}10^{\frac{\xi_{k,j}-\xi_{1,j}}{10}}\frac{L(r_1)}{L(r_k)}y_{k,j})]\}$$

$$\cdot e^{-y_{2,j}}\cdots e^{-y_{K,j}}\cdot dy_2\cdots dy_K$$

$$= \int_0^{\infty} \cdots \int_0^{\infty} \sum_{l=n}^{N} \{ \begin{pmatrix} N \\ l \end{pmatrix} \sum_{m=0}^{l} [\begin{pmatrix} l \\ m \end{pmatrix} (-1)^{l-m}$$

$$\mathrm{e}^{(-\sum_{k=2}^{K} y_{k,j}(1+\gamma_{th}(N-m)\frac{\varepsilon_{k,j}P_{k,j}}{P_{1,j}} 10^{\frac{\xi_{k,j}-\xi_{1,j}}{10}} \frac{L(r_1)}{L(r_k)}))}]\} \cdot dy_2 \cdots dy_K$$

$$= \sum_{l=n}^{N} \{ \begin{pmatrix} N \\ l \end{pmatrix} \sum_{m=0}^{l} [\begin{pmatrix} l \\ m \end{pmatrix} (-1)^{l-m} \prod_{k=2}^{K} \frac{1}{(1+(N-m)\gamma_{th}\frac{\varepsilon_{k,j}P_{k,j}}{P_{1,j}} 10^{\frac{\xi_{k,j}-\xi_{1,j}}{10}} \frac{L(r_1)}{L(r_k)})}]\}. \tag{5.21}$$

5.5 Simulation Results

We investigate the downlink outage of the OFDMA femtocells by analysis in Sections 5.3 and 5.4. We consider the exclusive spectrum allocation and the shared spectrum allocation schemes for the femtocells and macrocell. The gain-oriented distributed channel selection scheme and random selection scheme are considered. We assume the femtocell layout as shown in Fig. 3.1. There are 24 femtocells around the considered femtocell, and the group of 25 femtocells is uniformly distributed in a macrocell with the coverage of 500 meters. The separation distances between femtocells are $d_{sf} = 20$ meters. The link reliability requirement is larger than 90%. The nominal system parameters are listed in Table 4.1.

5.5.1 Outage Probability in Exclusive Spectrum Allocation

Fugure 5.2 shows the outage probability of different channels with different highest link gain against the femtocell sub-channel usage ratio ρ with the exclusive spectrum allocation, where $d_{sf} = 20$ meters. This figure shows the femtocell-to-femtocell interference in the exclusive spectrum allocation significantly impacts on the outage probability. As the subchannel usage ratio increases, the outage prob-

ability increases due to the increasing interference from other femtocells. In this figure, the subchannel with higher link gain can achieve lower outage probability. If the subchannel with the link gain is higher than the 15-th higher subchannel, those subchannels can ensure the link reliability requirement larger than 90% while other femtocell using all the subchannels. Compare to the random selection scheme, gain-oriented selection scheme can guarantee at least 25 suchannels perform better than randomly selection.

Fugure 5.3 shows the outage probability against the data sub-channel usage ratio ρ with the exclusive spectrum allocation, where $d_{sf} = 20$ meters. We consider the two channel selection schemes: gain-oriented and random selection schemes. The femtocell-to-femtocell interference in the exclusive spectrum allocation significantly impacts the link reliability probability. As the channel usage ratio increases, the outage probability increases due to the increasing interference from other femtocells. In this figure, the gain-oriented selection scheme has better performance than random selection scheme. If we request the outage probability requirement has to larger than 90%, the random selection scheme can use only channel usage ratio $\rho = 0.4$ for transmission and the gain-oriented selection scheme can transmission with channel usage ratio $\rho = 0.8$. That means we can use 100% more subchannels for communications if we use the gain-oriented selection scheme.

5.5.2 Outage Probability in Shared Spectrum Allocation

Fugure 5.4 shows the outage probability of different channels with different highest link gain against the femtocell sub-channel usage ratio ρ with the shared spectrum allocation, where $d_{sf} = 20$ meters. The two-tier interference is considered. Comparing Fig. 5.2, it is shown that the interference from macrocell significantly effects on the link reliability, and the outage probability increases. For example, in

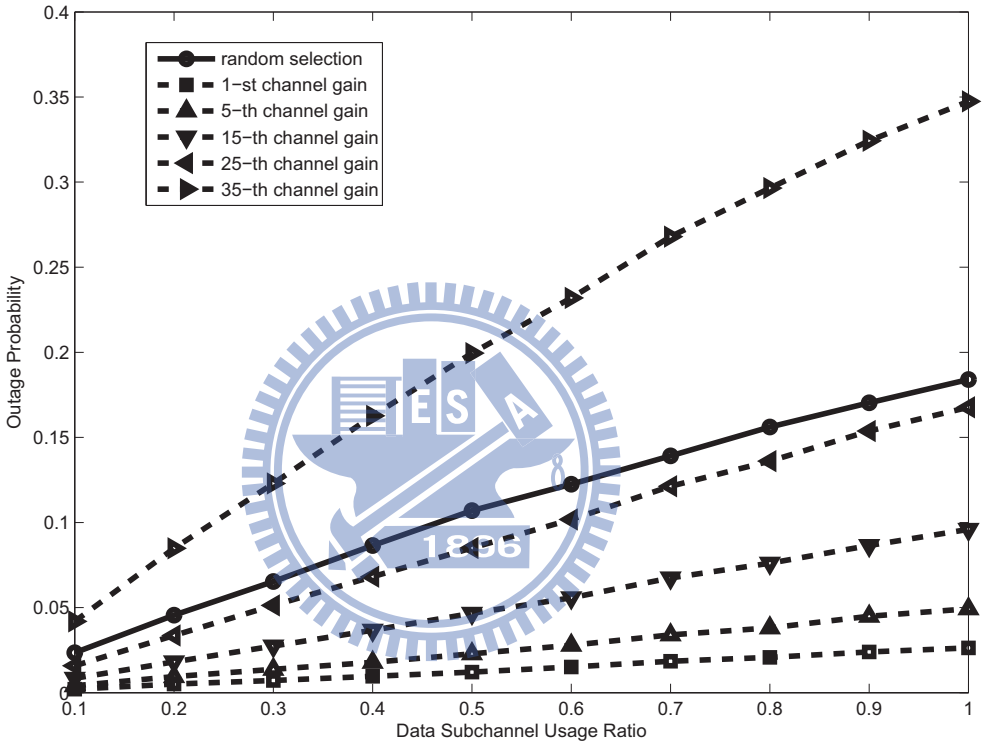

Figure 5.2: Outage probability with exclusive spectrum allocation scheme in different highest channel gain.

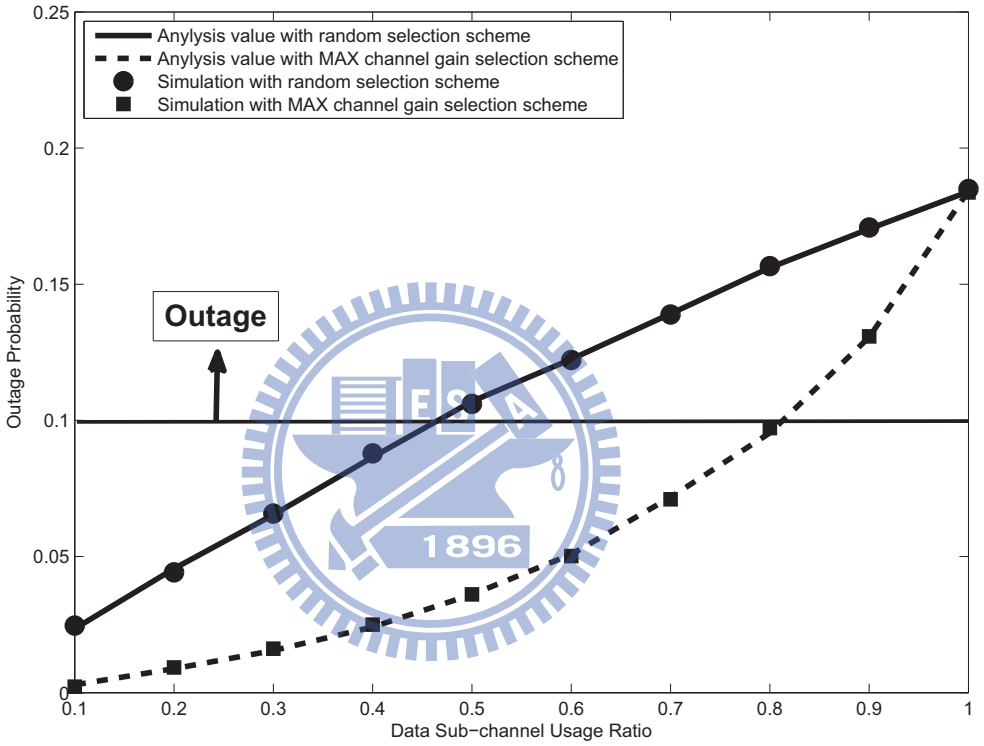

Figure 5.3: Outage probability with exclusive spectrum allocation scheme in random and channel-gain oriented selection schemes.

Fig. 5.2, when we request the link reliability requirement has to larger than 90%, the 50% subchannels can be used. However, only 30% channel usage ratio can be used when we allocate the macrocell and femtocells in the same spectrum.

Fugure 5.5 shows the outage probability against the data sub-channel usage ratio ρ with the shared spectrum allocation, where $d_{sf} = 20$ meters. We consider the gain-oriented and random selection schemes. Compared to Fig. 5.3, it is shown that the two-tier interference significantly impacts the link reliability probability. Random selection scheme can use 40% channel usage ratio for communication and guarantee the link reliability in the exclusive spectrum allocation scheme, but only 30% can use in the shared spectrum allocation scheme. That means femtocell use 25% lower subchannels because the extra interference from the macrocell. In addition, this figure illustrates the gain-oriented selection scheme has better performance than random selection scheme. If we request the outage probability requirement has to larger than 90%, the random selection scheme can use only channel usage ratio $\rho = 0.3$ for transmission and the gain-oriented selection scheme can transmission with channel usage ratio $\rho = 0.7$. That means we can use 133% more subchannels for communication if we use the gain-oriented selection scheme.

5.5.3 Impact of Macrocell Radius and Femtocell Channel Usage Ratio

In this subsection, we are interest in the relationship between the macrocell and the femtocell. In other words, we try to know the relationship between the femtocell channel usage ratio and the macrocell radius distance D_M. How many subchannels can be used while we know the information of the macrocell radius. From the analysis and the simulation results, the larger radius of macrocell, the higher channel usage ratio can be used by femtocells.

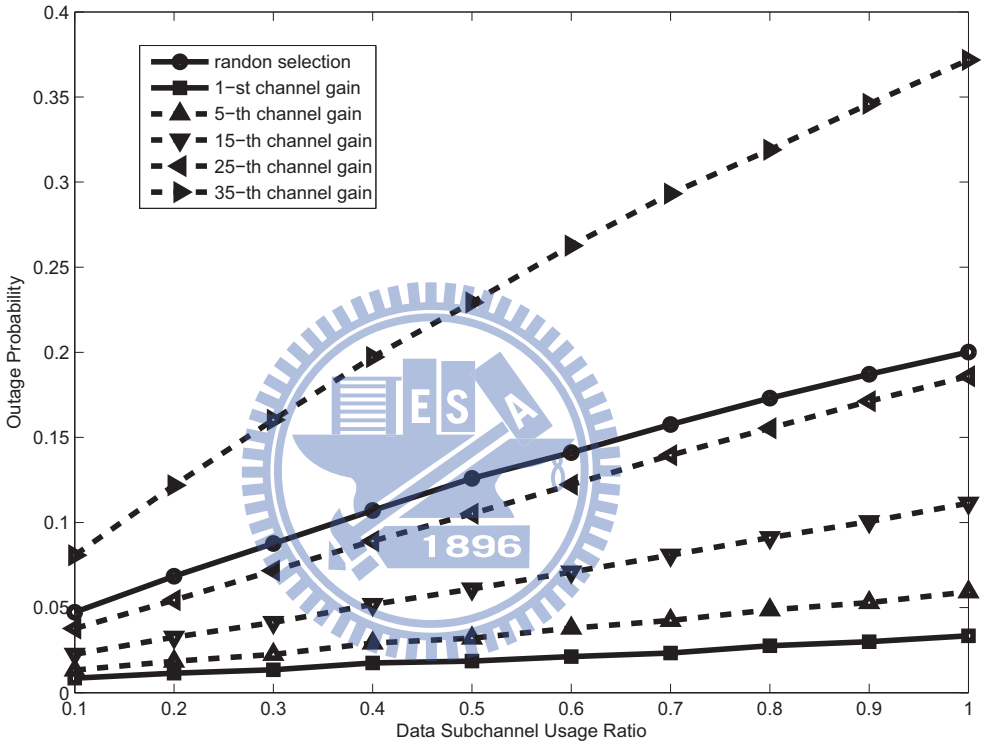

Figure 5.4: Outage probability with shared spectrum allocation scheme in different highest channel gain.

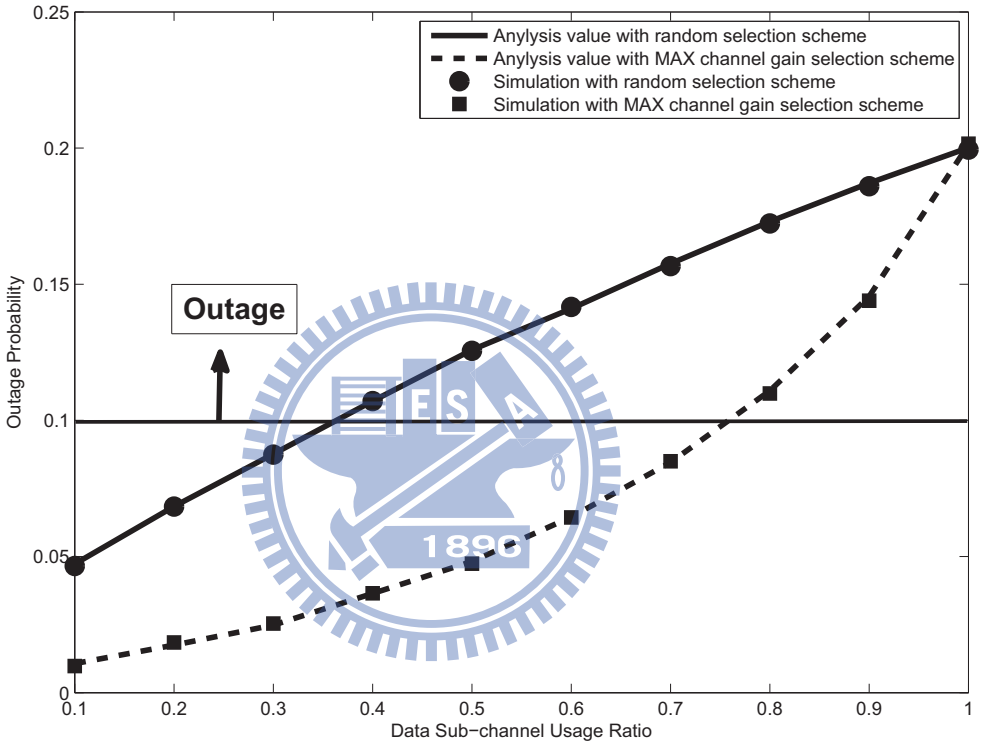

Figure 5.5: Outage probability with shared spectrum allocation scheme in random and gain-oriented selection schemes.

We investigate the downlink outage of the OFDMA femtocells by analysis in Sections 5.3 and 5.4. We consider the shared spectrum allocation schemes for the femtocells and macrocell. The gain-oriented distributed channel selection scheme and random selection scheme are considered. We assume that the femtocell layout as shown in Fig. 3.1. There are 24 femtocells around the considered femtocell, and the group of 25 femtocells is uniformly distributed in a macrocell with the coverage D_M. The separation distances between femtocells are $d_{sf} = 20$ meters. The link reliability requirement is larger than 90%. The nominal system parameters are listed in Table 4.1.

Fugure 5.6 shows the outage probability of different channel usage ratio ρ against the macrocell radius with the shared spectrum allocation, where $d_{sf} = 20$ meters. We consider the interference from macrocell and femtocells. The gain-oriented and random selection schemes are considered. It is shown that the two-tier interference significantly impacts the link reliability probability. As the macrocell radius D_M increases, the outage probability decreases because the interference from the macrocell decrease. In this figure, the lower channel usage ratio ρ can achieve lower outage probability and interfered from the others femtocells with lower probability. When we compare the gain-oriented selection scheme with random selection scheme, the gain-oriented selection scheme can achieve lower outage probability than random selection scheme when we use the same channel usage ratio. For example, as $D_M = 1000$ meters and the channel usage ratio is 50%, the outage probability is 10% by the random selection scheme, and 4% by gain-oriented selection scheme.

Table 5.1 shows the relationship between macrocell radius D_M and channel usage ratio ρ of femtocell. In this table, we know that the larger the macrocell radius, the higher the channel usage ratio used. The table also shows that the gain-oriented selection scheme can used more channel usage ratio ρ than randomly selected under the same macrocell radius D_M. If the macrocell radius D_M is shorter than 250 meters,

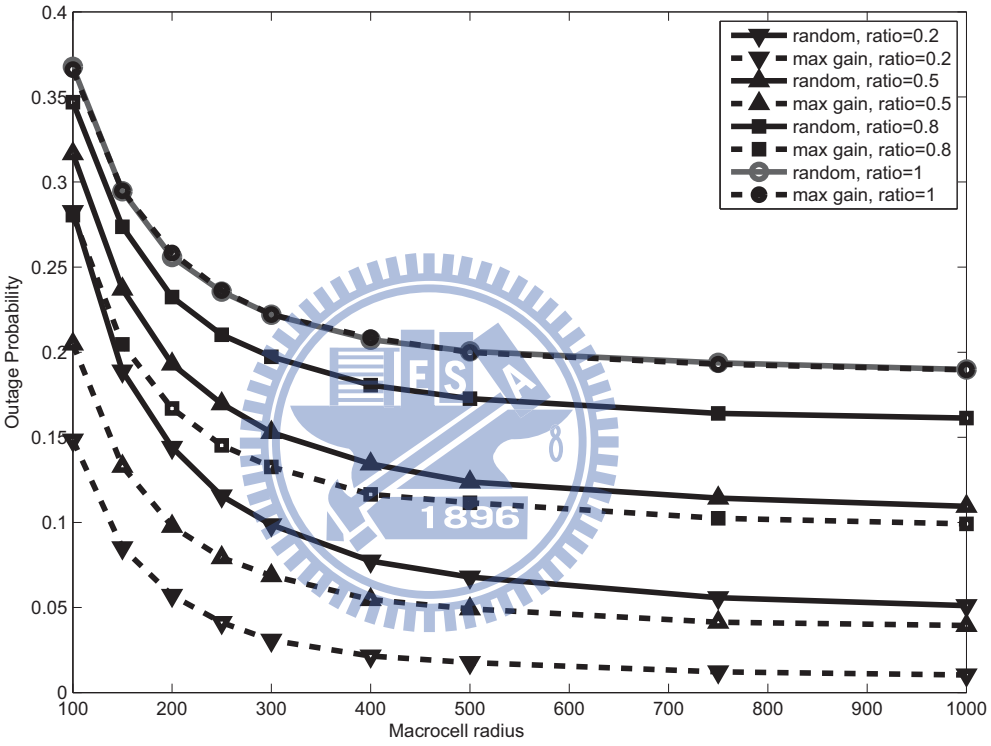

Figure 5.6: Outage probability in different macrocell radius.

the random selection scheme makes the femtocells is outage even femtocells use only the channel usage ratio $\rho = 0.1$. In the same condition of macrocell radius $D_M = 250$ meters, femtocells can transmission with channel usage ratio $\rho = 0.5$ if femtocells use the gain-oriented scheme. In addition, the channel usage ratio will be limited by the interference from the others femtocells. Even we ignore the macrocell interference, the fmetocell still cannot use all the bandwidth for transmission.

Table 5.2 shows that the relationship between channel usage ratio ρ and macrocell radius D_M. The table shows that the gain-oriented selection scheme is better for femtocell in the same macrocell radius under the same channel usage ratio ρ that femtocell is used. If we request the channel usage ratio $\rho = 0.4$, the macrocell radius D_M has to be longer than 647.39 meters if the femtocell use the random selection scheme, and if the femtocell use the gain-oriented selection scheme, the macrocell radius D_M has to be longer than 170.15 meters.

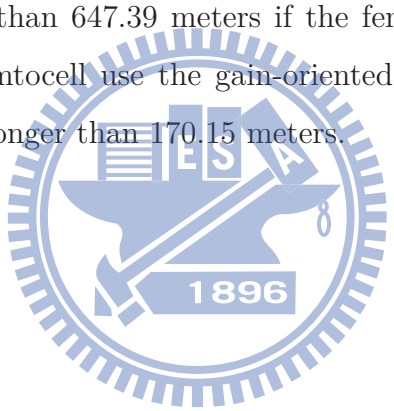

Table 5.1: **Macrocell radius versus channel usage ratio with different selection method.**

Macrocell Radius (D_M)	**Channel Usage Ratio with Random Selecion (Ratio ρ)**	**Channel Usage Ratio with Maximal Channel Gain Selecion (Ratio ρ)**
100	x	x
150	x	0.3
200	x	0.5
250	0.1	0.6
300	0.1	0.6
400	0.2	0.7
500	0.3	0.7
750	0.4	0.7
1000	0.4	0.8
∞	0.4	0.8

Table 5.2: **Channel usage ratio versus macrocell radius with different selection method.**

Channel Usage Ratio (ρ)	**Random Selecion on Macrocell Radius (D_M)**	**Maximal Channel Gain Selecion on Macrocell Radius (D_M)**
0.1	244.44	125.02
0.2	295.86	138.21
0.3	387.30	149.26
0.4	647.39	170.15
0.5	x	196.74
0.6	x	239.67
0.7	x	349.35
0.8	x	949.96
0.9	x	x
1	x	x

CHAPTER 6

Analysis of Distributed Channel Selection for Femtocell with Two-tier Interference: Multicarrier Case

In this chapter, we analyze the outage of femtocell with two-tier interference in multicarrier case. Both gain-oriented and random selection scheme are discussed. Moreover, we investigate the relationship between channel usage ratio and macrocell radius in the exclusive and shared spectrum allocation schemes.

6.1 Assumptions

6.1.1 Sub-carrier Allocation

Contiguous and randomly distributed sub-carrier permutation allocations are two main categories of subchannel allocation scheme in OFDMA systems. The contiguous sub-carrier permutation is already discussed in Chapter 5. Therefore, in this chapter, we focus on the randomly distributed permutations. The benefit of distributed permutations is to achieve frequency diversity and inter-cell interference averaging. In the chapter, we discuss the outage probability for femtocell of OFDMA systems with multicarrier case.

6.1.2 Radio Channel

We consider the radio channel effects of path loss, penetration loss, and shadowing, which are discussed in Section 5.1.2.

Multipath Fading on Sub-carrier

Rayleigh fading is used in the outage probability analysis of femtocell with two-tier interference. Rayleigh fading characterizes the impact of multipath propagation distribution. The probability of density function for Rayleigh distributed random variable h as

$$f_h(h) = 2he^{-h^2}. \tag{6.1}$$

Let $Y = h^2$. Then the cumulative density function of Y can be written as

$$F_Y(y) = 1 - e^{-y}. \tag{6.2}$$

6.1.3 Signal to Interference and Noise Ratio

We consider the two-tier interference. Let $P_{k,j,m}$ be the transmission power of the k-th base station on m-th sub-carrier of j-th subchannel. Shadowing can be characterized by a log-normal random variable $10^{\frac{\xi_{k,j}}{10}}$, where $\xi_{k,j}$ is a Gaussian random variable of j-th subchannel in the k-th femtocell. The sub-carrier gain between the k-th base station and the considered user is $y_{k,j,m}$. There are M sub-carriers in a subchannel. Therefore, the received signal power at the m-th sub-carrier in the femtocell mobile terminal can be written as

$$P_{r_{k,j,m}} = P_{k,j,m}10^{\xi_{k,j}/10}y_{k,j,m}/L(r_k), \tag{6.3}$$

and the total power of a subchannel in the femtocell mobile terminal is

$$P_{k,j} = \sum_{m=1}^{M} P_{r_{k,j,m}} \tag{6.4}$$

$$= P_{k,j,m} 10^{\xi_{k,j}/10} (\sum_{m=1}^{M} y_{k,j,m}) / L(r_k) \tag{6.5}$$

$$= P_{k,j,m} 10^{\xi_{k,j}/10} y_{k,j} / L(r_k), \tag{6.6}$$

where $y_{k,j}$ is the subcahnnel gain, which is the sum of the M sub-carriers gain. The probability density function for the link gain of a subchannel $y_{k,j}$ is

$$f_y(y) = e^{-y} \frac{y^{M-1}}{(M-1)!}, \tag{6.7}$$

and the cumulative density function of $y_{k,j}$ can be written as

$$F_Y(y) = 1 - \sum_{t=0}^{M-1} \frac{e^{-y} y^t}{t!}. \tag{6.8}$$

Assume that there are K base stations that include $(K-1)$ femtocells and a macrocell in the system, labeled from 2 to K. Without the loss of generality, let the desired user be indexed with 1. Then the total interference P_{I_j} received from the other $(K-1)$ femtocell of the j-th subchannel can be expressed as

$$P_{I_j} = \sum_{k=2}^{K} \varepsilon_{k,j} P_{k,j} 10^{\xi/10} y_{k,j} / L(r_k), \tag{6.9}$$

where ε_j is the utility function. If the subchannel j is selected to transmit data, $\varepsilon_j = 1$; otherwise, $\varepsilon_j = 0$.

The SINR on the j-th subchannel of the first femtocell can be express as

$$SINR = \frac{P_{1,j}}{P_{I_j} + N_0} \quad , \tag{6.10}$$

where N_0 is the noise power.

6.2 Outage Probability of Single Femtocell

First, we consider a scenario that only a femtocell 1 in this area, no other macrocell or femtocells. By setting the required received threshold γ_{th}, the outage probability with one femtocell can be expressed as

$$
\begin{aligned}
& P_{outage} \\
& = \Pr[SNR < \gamma_{th}] \\
& = \Pr[\frac{P_{1,j,m} 10^{\frac{\xi_{i,j}}{10}} y_{i,j} / L(r_i)}{N_0} < \gamma_{th}] \\
& = \Pr[y_{i,j} < \gamma_{th} \frac{N_0}{P_{1,j,m}} 10^{-\frac{\xi_{i,j}}{10}} L(r_i)] \\
& = \int_{-\infty}^{\infty} \int_{0}^{R} F_Y[\gamma_{th} \frac{N_0}{P_{1,j,m}} 10^{-\frac{\xi_{i,j}}{10}} L(r_i)] f_{r_i}(r_i) f_{\xi}(\xi) dr_i d\xi \\
& = \int_{-\infty}^{\infty} \int_{0}^{R} \{1 - e^{-\gamma_{th} \frac{N_0}{P_{1,j,m}} 10^{-\frac{\xi_{i,j}}{10}} L(r_i)} \sum_{t=0}^{M-1} \frac{[\gamma_{th} \frac{N_0}{P_{1,j,m}} 10^{-\frac{\xi_{i,j}}{10}} L(r_i)]^t}{t!} \} \frac{2r_i}{R^2} \frac{e^{-\frac{\xi^2}{2\sigma^2}}}{\sqrt{2\pi}\sigma} dr_i d\xi,
\end{aligned}
\tag{6.11}
$$

where R is the cell radius and there are no other femtocells and macrocell in the neighboring area.

6.3 Outage Probability of Random Channel Selection Principle for Femtocell with Two-tier Interference

6.3.1 Single Interference Case for Random Channel Selection Principle

First, we consider one interference only from the base station k. Assume the noise can be neglected (i.e. $N_0 = 0$) in this case. Thus, the outage probability of random selection principle for femtocell with two-tier interference can be written as

$$
\begin{aligned}
& P_{outage,random} \\
&= \Pr[SIR_{1,j} < \gamma_{th}] \\
&= \Pr[\frac{P_{1,j,m}10^{\xi_{i,j}/10}y_{i,j}/L(r_i)}{\varepsilon_{k,j}P_{k,j,m}10^{\xi_{k,j}/10}y_{k,j}/L(r_k)} < \gamma_{th}] \\
&= \Pr[\frac{P_{1,j,m}10^{\xi_{i,j}/10}y_{i,j}}{L(r_i)} < \gamma_{th}\frac{\varepsilon_{k,j}P_{k,j,m}10^{\xi_{k,j}/10}y_{k,j}}{L(r_k)}] \\
&= \Pr[y_{i,j} < \gamma_{th}\frac{\varepsilon_{k,j}P_{k,j,m}}{P_{1,j,m}}10^{\frac{\xi_{k,j}-\xi_{1,j}}{10}}\frac{L(r_1)}{L(r_k)}y_{k,j}] \\
&= \Pr[y_{i,j} < I_k y_{k,j}], \qquad (6.12)
\end{aligned}
$$

where $I_k = \gamma_{th}\frac{\varepsilon_{k,j}P_{k,j,m}}{P_{1,j,m}}10^{\frac{\xi_{k,j}-\xi_{1,j}}{10}}\frac{L(r_1)}{L(r_k)}$.

The outage probability of random selection principle for femtocell user 1 can be written as

$$P_{outage,random,2fBSs}$$

$$= \int_0^{\infty} [1 - e^{-I_k y_{k,j}} \sum_{t=0}^{M-1} \frac{(I_k y_{k,j})^t}{t!}] \cdot \frac{e^{-y_{k,j}} {y_{k,j}}^{M-1}}{(M-1)!} \cdot dy_{k,j}$$

$$= \int_0^{\infty} \frac{e^{-y_{2,j}} {y_{2,j}}^{M-1}}{(M-1)!} \cdot dy_{k,j} - \int_0^{\infty} \frac{e^{-I_k y_k} e^{-y_{k,j}} {y_{2,j}}^{M-1}}{(M-1)!} \sum_{t=0}^{M-1} \frac{(I_k y_{k,j})^t}{t!} dy_{k,j}$$

$$= 1 - \sum_{t=0}^{M-1} \frac{(I_k)^t (t+M-1)!}{(M-1)! t!} \int_0^{\infty} \frac{(y_{k,j})^{t+M-1}}{(t+M-1)!} e^{-(I_k+1)y_k} dy_{k,j} \tag{6.13}$$

$$= 1 - \sum_{t=0}^{M-1} \frac{(I_k)^t (t+M-1)!}{(M-1)! t!} \frac{1}{(I_k+1)^{t+M}}. \tag{6.14}$$

6.3.2 Multi-interference Case for Random Channel Selection Principle

We consider the two-tier interference, the interference from total $K-1$ base stations 2 to K. This means that the femtocell has to face the two-tier interference. In ths case, the noise effects may be neglected. Thus, the outage probability of random selection principle for femtocell with two-tier interference can be written as

$$P_{outage,random}$$

$$= \Pr[SIR_{1,j} < \gamma_{th}]$$

$$= \Pr[\frac{P_{1,j,m} 10^{\xi_{i,j}/10} y_{i,j} / L(r_i)}{\sum_{k=2}^{K} \varepsilon_{k,j} P_{k,j,m} 10^{\xi_{k,j}/10} y_{k,j} / L(r_k)} < \gamma_{th}]$$

$$= \Pr[\frac{P_{1,j,m}10^{\xi_{i,j}/10}y_{i,j}}{L(r_i)} < \gamma_{th}\sum_{k=2}^{K}\frac{\varepsilon_{k,j}P_{k,j,m}10^{\xi_{k,j}/10}y_{k,j}}{L(r_k)}]$$

$$= \Pr[y_{i,j} < \gamma_{th}\sum_{k=2}^{K}\frac{\varepsilon_{k,j}P_{k,j,m}}{P_{1,j,m}}10^{\frac{\xi_{k,j}-\xi_{1,j}}{10}}\frac{L(r_1)}{L(r_k)}y_{k,j}]$$

$$= \Pr[y_{i,j} < \sum_{k=2}^{K} I_k y_{k,j}]$$

$$\approx \Pr[y_{i,j} < y_I\sum_{k=2}^{K} I_k], \tag{6.15}$$

where $I_k = \gamma_{th}\frac{\varepsilon_{k,j}P_{k,j,m}}{P_{1,j,m}}10^{\frac{\xi_{k,j}-\xi_{1,j}}{10}}\frac{L(r_1)}{L(r_k)}$.

Let $r = (r_2, r_3, ..., r_K)$ and $\xi = (\xi_2, \xi_3, ..., \xi_K)$. Then the outage probability of random selection principle for femtocell user 1 can be written as

$$P_{outage,random}(r_1, \xi_1 | r, \xi)$$

$$= \int_0^\infty [1 - e^{-y_I\sum_{k=2}^{K} I_k}\sum_{t=0}^{M-1}\frac{(y_I\sum_{k=2}^{K} I_k)^t}{t!}][\frac{e^{-y_I}{y_I}^{M-1}}{(M-1)!}]dy_I$$

$$= \int_0^\infty \frac{e^{-y_I}{y_I}^{M-1}}{(M-1)!}dy_I - \int_0^\infty \frac{e^{-y_I\sum_{k=2}^{K} I_k}e^{-y_I}{y_I}^{M-1}}{(M-1)!}\sum_{t=0}^{M-1}\frac{(y_I\sum_{k=2}^{K} I_k)^t}{t!}dy_I$$

$$= 1 - \sum_{t=0}^{M-1}\int_0^\infty \frac{e^{-y_I(1+\sum_{k=2}^{K} I_k)}{y_I}^{M-1}}{(M-1)!}\frac{{y_I}^t(\sum_{k=2}^{K} I_k)^t}{t!}dy_I$$

$$= 1 - \sum_{t=0}^{M-1}\int_0^\infty \frac{{y_I}^{t+M-1}(\sum_{k=2}^{K} I_k)^t}{(M-1)!t!}e^{-y_I(1+\sum_{k=2}^{K} I_k)}dy_I$$

$$= 1 - \sum_{t=0}^{M-1} \frac{(\sum_{k=2}^{K} I_k)^t (t+M-1)!}{(M-1)!t!} \int_0^{\infty} \frac{{y_I}^{t+M-1}}{(t+M-1)!} e^{-y_I(1+\sum_{k=2}^{K} I_k)} dy_I$$

$$= 1 - \sum_{t=0}^{M-1} \frac{(\sum_{k=2}^{K} I_k)^t (t+M-1)!}{(M-1)!t!} \frac{1}{(1+\sum_{k=2}^{K} I_k)^{t+M}}. \quad (6.16)$$

6.4 Outage Probability of Gain-Oriented Channel Selection Principle for Femtocell with Two-tier Interference

6.4.1 Outage Probability of Maximal Link Gain Channel for Femtocell with Two-tier Interference

In Section. 4.2, we developed the gain-oriented selection principle for the femtocell systems. The gain-oriented selection scheme aims to use the subchannels with higher link gain for communication. The gain-oriented selection scheme operates in a distributed and autonomous manner. Each femtocell can select the subchannels for transmission by itself. We detail the gain-oriented selection schemes in Sections. 4.2.1 and 4.2.2.

Single Interference Case for Maximal Link Gain Channel Selection

In Section. 6.1.3, we know the probability density function for the link gain of a subchannel is

$$f_Z(z) = e^{-z} \frac{z^{M-1}}{(M-1)!}, \quad (6.17)$$

and the cumulative density function of a subchannel can be written as

$$F_Z(z) = 1 - \sum_{t=0}^{M-1} \frac{e^{-z} z^t}{t!}. \tag{6.18}$$

Consider that there are total N subchannels. If we use only one sebchannel for transmission, we choose the highest link gain channel by the gain-oriented selection scheme. In this case, let $Y = max(z_1, z_2, ..., z_N)$ and $z_1, z_2, ..., z_N$ are independent and identically distributed (i.i.d.). Then the cumulative density function of Y can be written as

$$\begin{aligned} F_Y(y) &= P\{z_1 \le y, z_2 \le y, ..., z_N \le y\} \\ &= F_{z_1, z_2, ..., z_N}(y, y, ..., y) \\ &= \prod_{i=1}^{N} F_{z_i}(y) \\ &= (1 - \sum_{t=0}^{M-1} \frac{e^{-y} y^t}{t!})^N. \end{aligned} \tag{6.19}$$

First, we consider a interference only from the base station k, and assume the effect of noise can be neglected. The outage probability of maximal link gain selection principle for femtocell with two-tier interference can be written as

$$\begin{aligned} & P_{outage,(1-st)} \\ &= \Pr[SIR_{1,j} < \gamma_{th}] \\ &= \Pr[\frac{P_{1,j,m} 10^{\xi_{i,j}/10} y_{i,j} / L(r_i)}{\varepsilon_{k,j} P_{k,j,m} 10^{\xi_{k,j}/10} y_{k,j} / L(r_k)} < \gamma_{th}] \\ &= \Pr[\frac{P_{1,j,m} 10^{\xi_{i,j}/10} y_{i,j}}{L(r_i)} < \gamma_{th} \frac{\varepsilon_{k,j} P_{k,j,m} 10^{\xi_{k,j}/10} y_{k,j}}{L(r_k)}] \end{aligned}$$

$$= \Pr[y_{i,j} < \gamma_{th} \frac{\varepsilon_{k,j} P_{k,j,m}}{P_{1,j,m}} 10^{\frac{\xi_{k,j}-\xi_{1,j}}{10}} \frac{L(r_1)}{L(r_k)} y_{k,j}]$$

$$= \Pr[y_{i,j} < y_{k,j} I_k], \tag{6.20}$$

where $I_k = \gamma_{th} \frac{\varepsilon_{k,j} P_{k,j,m}}{P_{1,j,m}} 10^{\frac{\xi_{k,j}-\xi_{1,j}}{10}} \frac{L(r_1)}{L(r_k)}$.

Let $r = (r_2, r_3, ..., r_K)$ and $\xi = (\xi_2, \xi_3, ..., \xi_K)$. Then the outage probability of maximal link gain selection principle for femtocell 1 can be written as

$P_{outage,(1-st)}(r_1, \xi_1 | r, \xi)$

$$= \int_0^\infty [1 - e^{-y_{k,j} I_k} \sum_{t=0}^{M-1} \frac{(y_{k,j} I_k)^t}{t!}]^N \frac{e^{-y_{k,j}} {y_{k,j}}^{M-1}}{(M-1)!} dy_{k,j}$$

$$= \int_0^\infty \sum_{l=0}^{N} \binom{N}{l} (1)^l (-e^{-y_{k,j} I_k} \sum_{t=0}^{M-1} \frac{(y_{k,j} I_k)^t}{t!})^{N-l} \frac{e^{-y_{k,j}} {y_{k,j}}^{M-1}}{(M-1)!} dy_{k,j}$$

$$= \int_0^\infty \sum_{l=0}^{N} \binom{N}{l} (-1)^{N-l} (\frac{e^{-y_{k,j}(I_k(N-l)+1)} {y_{k,j}}^{M-1}}{(M-1)!}) (\sum_{t=0}^{M-1} \frac{(y_{k,j} I_k)^t}{t!})^{N-l} dy_{k,j}$$

$$= \int_0^\infty \sum_{l=0}^{N} \binom{N}{l} (-1)^{N-l} (\frac{e^{-y_{k,j}(I_k(N-l)+1)} {y_{k,j}}^{M-1}}{(M-1)!}) (\sum_{t=0}^{M-1} \frac{(N-l)^t (y_{k,j} I_k)^t}{t!}) dy_{k,j}$$

$$= \int_0^\infty \sum_{l=0}^{N} \binom{N}{l} (-1)^{N-l} (\sum_{t=0}^{M-1} \frac{e^{-y_{k,j}(I_k(N-l)+1)} {y_{k,j}}^{M-1}}{(M-1)!} \frac{(N-l)^t (y_{k,j} I_k)^t}{t!}) dy_{k,j}$$

$$= \sum_{l=0}^{N} \binom{N}{l} (-1)^{N-l} \sum_{t=0}^{M-1} \frac{{I_k}^t (N-l)^t (t+M-1)!}{(M-1)! t!} \int_0^\infty \frac{{y_{k,j}}^{t+M-1}}{(t+M-1)!} e^{-y_{k,j}(I_k(N-l)+1)} dy_{k,j}$$

$$= \sum_{l=0}^{N} \binom{N}{l} (-1)^{N-l} \sum_{t=0}^{M-1} \frac{{I_k}^t (N-l)^t (t+M-1)!}{(M-1)! t! (I_k(N-l)+1)^{t+M}}. \tag{6.21}$$

Multi-interference Case for Maximal Link Gain Channel Selection

When we consider the interference from other $K-1$ base stations 2 to K, the noise effects may be neglected in the interference limited system. Thus, the outage probability of maximal link gain selection principle for femtocell with two-tier interference can be written as

$$
\begin{aligned}
& P_{outage,(1-st)} \\
& = \Pr[SIR_{1,j} < \gamma_{th}] \\
& = \Pr[\frac{P_{1,j,m}10^{\xi_{i,j}/10}y_{i,j}/L(r_i)}{\sum_{k=2}^{K}\varepsilon_{k,j}P_{k,j,m}10^{\xi_{k,j}/10}y_{k,j}/L(r_k)} < \gamma_{th}] \\
& = \Pr[\frac{P_{1,j,m}10^{\xi_{i,j}/10}y_{i,j}}{L(r_i)} < \gamma_{th}\sum_{k=2}^{K}\frac{\varepsilon_{k,j}P_{k,j,m}10^{\xi_{k,j}/10}y_{k,j}}{L(r_k)}] \\
& = \Pr[y_{i,j} < \gamma_{th}\sum_{k=2}^{K}\frac{\varepsilon_{k,j}P_{k,j,m}}{P_{1,j,m}}10^{\frac{\xi_{k,j}-\xi_{1,j}}{10}}\frac{L(r_1)}{L(r_k)}y_{k,j}] \\
& = \Pr[y_{i,j} < \sum_{k=2}^{K}y_{k,j}I_k] \\
& \approx \Pr[y_{i,j} < y_I\sum_{k=2}^{K}I_k], \qquad (6.22)
\end{aligned}
$$

where $I_k = \gamma_{th}\frac{\varepsilon_{k,j}P_{k,j,m}}{P_{1,j,m}}10^{\frac{\xi_{k,j}-\xi_{1,j}}{10}}\frac{L(r_1)}{L(r_k)}$.

Let $r = (r_2, r_3, ..., r_K)$ and $\xi = (\xi_2, \xi_3, ..., \xi_K)$. Then the outage probability of maximal link gain selection principle for femtocell user 1 can be written as

$P_{outage,(1-st)}(r_1, \xi_1 | r, \xi)$

$$= \int_0^\infty [1 - e^{-y_I \sum_{k=2}^{K} I_k} \sum_{t=0}^{M-1} \frac{(y_I \sum_{k=2}^{K} I_k)^t}{t!}]^N \frac{e^{-y_I} {y_I}^{M-1}}{(M-1)!} dy_I$$

$$= \int_0^\infty \sum_{l=0}^{N} \binom{N}{l} (1)^l (-e^{-y_I \sum_{k=2}^{K} I_k} \sum_{t=0}^{M-1} \frac{(y_I \sum_{k=2}^{K} I_k)^t}{t!})^{N-l} \frac{e^{-y_I} {y_I}^{M-1}}{(M-1)!} dy_I$$

$$= \int_0^\infty \sum_{l=0}^{N} \binom{N}{l} (-1)^{N-l} (\frac{e^{-y_I(1+(N-l)\sum_{k=2}^{K} I_k)} {y_I}^{M-1}}{(M-1)!}) (\sum_{t=0}^{M-1} \frac{(y_I \sum_{k=2}^{K} I_k)^t}{t!})^{N-l} dy_I$$

$$= \int_0^\infty \sum_{l=0}^{N} \binom{N}{l} (-1)^{N-l} (\sum_{t=0}^{M-1} e^{-y_I(1+(N-l)\sum_{k=2}^{K} I_k)} {y_I}^{M-1} \frac{(N-l)^t (y_I \sum_{k=2}^{K} I_k)^t}{t!}) dy_I$$

$$= \sum_{l=0}^{N} \binom{N}{l} (-1)^{N-l} \sum_{t=0}^{M-1} \frac{(\sum_{k=2}^{K} I_k)^t (N-l)^t (t+M-1)!}{(M-1)!t!} \int_0^\infty \frac{{y_I}^{t+M-1}}{(t+M-1)!} e^{-y_I(1+(N-l)\sum_{k=2}^{K} I_k)} dy_I$$

$$= \sum_{l=0}^{N} \binom{N}{l} (-1)^{N-l} \sum_{t=0}^{M-1} \frac{(\sum_{k=2}^{K} I_k)^t (N-l)^t (t+M-1)!}{(M-1)!t!(1+(N-l)\sum_{k=2}^{K} I_k)^{t+M}}. \quad (6.23)$$

6.4.2 Outage Probability of n-th Highest Link Gain Channel for Femtocell with Two-tier Interference

For femtocell systems, the femtocells use multiple subchannels for serving their users. By gain-oriented principle, femtocells choose the subchannels with higher link gain for communication. There are total N subchannels in a femtocell system. If we use n subchannels for transmission, we will choose the highest n link gain channel

by the gain-oriented selection scheme. In this case, let $Y = \{y_1, y_2, ..., y_N\}$ be the order statistics of independent and identically distributed (i.i.d.) random variable from $(z_1, z_2, ..., z_N)$ where $y_1 \leq y_2 \leq ... \leq y_N$, than the cumulative density function and probability density function of Y_n can be written as

$$F_{Y_n}(y) = \sum_{i=n}^{N} \begin{pmatrix} N \\ i \end{pmatrix} [F_Z(y)]^i [1 - F_Z(y)]^{N-i} \tag{6.24}$$

$$f_{Y_n}(y) = \frac{N!}{(N-n)!(n-1)!} f_Z(y) [F_Z(y)]^{N-n} [1 - F_Z(y)]^{n-1}. \tag{6.25}$$

Single Interference Case for n-th Highest Link Gain Channel Selection

Two femtocell base stations 1 and k are considered in this scenario, and the interference is only come from the femtocell k. There are N subchannels in a femtocell system, and we consider each subchannel individually. The outage probability of the n-th highest link gain subchannel for femtocells with two-tier interference can be written as

$$\begin{aligned}
&P_{outage,(n-th)} \\
&= \Pr[SNR_{1,j} < \gamma_{th}] \\
&= \Pr[\frac{P_{1,j,m} 10^{\xi_{i,j}/10} y_{i,j} / L(r_i)}{\varepsilon_{k,j} P_{k,j,m} 10^{\xi_{k,j}/10} y_{k,j} / L(r_k)} < \gamma_{th}] \\
&= \Pr[\frac{P_{1,j,m} 10^{\xi_{i,j}/10} y_{i,j}}{L(r_i)} < \gamma_{th} \frac{\varepsilon_{k,j} P_{k,j,m} 10^{\xi_{k,j}/10} y_{k,j}}{L(r_k)}] \\
&= \Pr[y_{i,j} < \gamma_{th} \frac{\varepsilon_{k,j} P_{k,j,m}}{P_{1,j,m}} 10^{\frac{\xi_{k,j} - \xi_{1,j}}{10}} \frac{L(r_1)}{L(r_k)} y_{k,j}] \\
&= \Pr[y_{i,j} < y_{k,j} I_k],
\end{aligned} \tag{6.26}$$

where $I_k = \gamma_{th}\frac{\varepsilon_{k,j}P_{k,j,m}}{P_{1,j,m}}10^{\frac{\xi_{k,j}-\xi_{1,j}}{10}}\frac{L(r_1)}{L(r_k)}$.

Let $r = (r_2, r_3, ..., r_K)$ and $\xi = (\xi_2, \xi_3, ..., \xi_K)$. Then the outage probability of n-th highest link gain selection principle for femtocell user 1 can be written as

$$P_{outage,(n-th)}(r_1, \xi_1 | r, \xi)$$

$$= \int_0^\infty \sum_{l=n}^{N} \binom{N}{l} [1 - e^{-y_{k,j}I_k} \sum_{t=0}^{M-1} \frac{(y_{k,j}I_k)^t}{t!}]^l [e^{-y_{k,j}I_k} \sum_{t=0}^{M-1} \frac{(y_{k,j}I_k)^t}{t!}]^{N-l} \frac{e^{-y_{k,j}} {y_{k,j}}^{M-1}}{(M-1)!} dy_{k,j}$$

$$= \int_0^\infty \sum_{l=n}^{N} \binom{N}{l} \sum_{m=0}^{l} \binom{l}{m} (-1)^{l-m} (e^{-y_{k,j}I_k} \sum_{t=0}^{M-1} \frac{(y_{k,j}I_k)^t}{t!})^{l-m}$$

$$\cdot (e^{-y_{k,j}I_k} \sum_{t=0}^{M-1} \frac{(y_{k,j}I_k)^t}{t!})^{N-l} \frac{e^{-y_{k,j}} {y_{k,j}}^{M-1}}{(M-1)!} dy_{k,j}$$

$$= \int_0^\infty \sum_{l=n}^{N} \binom{N}{l} \sum_{m=0}^{l} \binom{l}{m} (-1)^{l-m} (e^{-y_{k,j}I_k} \sum_{t=0}^{M-1} \frac{(y_{k,j}I_k)^t}{t!})^{N-m} \frac{e^{-y_{k,j}} {y_{k,j}}^{M-1}}{(M-1)!} dy_{k,j}$$

$$= \int_0^\infty \sum_{l=n}^{N} \binom{N}{l} \sum_{m=0}^{l} \binom{l}{m} (-1)^{l-m} (\frac{e^{-y_{k,j}I_k(N-m)} e^{-y_{k,j}} {y_{k,j}}^{M-1}}{(M-1)!}) (\sum_{t=0}^{M-1} \frac{(y_{k,j}I_k)^t}{t!})^{N-m} dy_{k,j}$$

$$= \int_0^\infty \sum_{l=n}^{N} \binom{N}{l} \sum_{m=0}^{l} \binom{l}{m} (-1)^{l-m} (\sum_{t=0}^{M-1} \frac{e^{-y_{k,j}(1+I_k(N-m))} {y_{k,j}}^{t+M-1}}{(M-1)!} \frac{(N-m)^t (I_k)^t}{t!}) dy_{k,j}$$

$$= \sum_{l=n}^{N} \binom{N}{l} \sum_{m=0}^{l} \binom{l}{m} (-1)^{l-m} (\sum_{t=0}^{M-1} \frac{(N-m)^t (I_k)^t (t+M-1)!}{(M-1)!t!}$$

$$\cdot \int_0^\infty \frac{{y_{k,j}}^{t+M-1} e^{-y_{k,j}(1+I_k(N-m))}}{(t+M-1)!} dy_{k,j})$$

$$= \sum_{l=n}^{N} \binom{N}{l} \sum_{m=0}^{l} \binom{l}{m} (-1)^{l-m} \left(\sum_{t=0}^{M-1} \frac{(N-m)^t (I_k)^t (t+M-1)!}{(M-1)!t!(1+I_k(N-m))^{t+M}} \right). \quad (6.27)$$

Multi-interference Case for n-th Highest Link Gain Channel Selection

There are total K base stations in this scenario, and the femtocell 1 has to face the interference from macrocell and femtocell 2 to K. There are N subchannels in a femtocell system. We consider each subchannel individually. The outage probability of n-th highest link gain subchannel for femtocell with two-tier interference can be written as

$$\begin{aligned}
&P_{outage,(n-th)} \\
&= \Pr[SNR_{1,j} < \gamma_{th}] \\
&= \Pr\left[\frac{P_{1,j,m} 10^{\xi_{i,j}/10} y_{i,j} / L(r_i)}{\sum_{k=2}^{K} \varepsilon_{k,j} P_{k,j,m} 10^{\xi_{k,j}/10} y_{k,j} / L(r_k)} < \gamma_{th}\right] \\
&= \Pr\left[\frac{P_{1,j,m} 10^{\xi_{i,j}/10} y_{i,j}}{L(r_i)} < \gamma_{th} \sum_{k=2}^{K} \frac{\varepsilon_{k,j} P_{k,j,m} 10^{\xi_{k,j}/10} y_{k,j}}{L(r_k)}\right] \\
&= \Pr\left[y_{i,j} < \gamma_{th} \sum_{k=2}^{K} \frac{\varepsilon_{k,j} P_{k,j,m}}{P_{1,j,m}} 10^{\frac{\xi_{k,j}-\xi_{1,j}}{10}} \frac{L(r_1)}{L(r_k)} y_{k,j}\right] \\
&\approx \Pr\left[y_{i,j} < y_I \sum_{k=2}^{K} I_k\right], \quad (6.28)
\end{aligned}$$

where $I_k = \gamma_{th} \frac{\varepsilon_{k,j} P_{k,j,m}}{P_{1,j,m}} 10^{\frac{\xi_{k,j}-\xi_{1,j}}{10}} \frac{L(r_1)}{L(r_k)}$.

Let $r = (r_2, r_3, ..., r_K)$ and $\xi = (\xi_2, \xi_3, ..., \xi_K)$. Then the outage probability of n-th highest link gain selection principle for femtocell user 1 can be written as

$P_{outage,(n-th)}(r_1, \xi_1 | r, \xi)$

$$= \int_0^\infty \sum_{l=n}^{N} \binom{N}{l} [1 - e^{-y_I \sum_{k=2}^{K} I_k} \sum_{t=0}^{M-1} \frac{(y_I \sum_{k=2}^{K} I_k)}{t!}^t]^l [e^{-y_I \sum_{k=2}^{K} I_k} \sum_{t=0}^{M-1} \frac{(y_I \sum_{k=2}^{K} I_k)}{t!}^t]^{N-l} \frac{e^{-y_I} {y_I}^{M-1}}{(M-1)!} dy_I$$

$$= \int_0^\infty \sum_{l=n}^{N} \binom{N}{l} \sum_{m=0}^{l} \binom{l}{m} (-1)^{l-m} (e^{-y_I \sum_{k=2}^{K} I_k} \sum_{t=0}^{M-1} \frac{(y_I \sum_{k=2}^{K} I_k)}{t!}^t)^{l-m}$$

$$\cdot (e^{-y_I \sum_{k=2}^{K} I_k} \sum_{t=0}^{M-1} \frac{(y_I \sum_{k=2}^{K} I_k)}{t!}^t)^{N-l} \frac{e^{-y_I} {y_I}^{M-1}}{(M-1)!} dy_I$$

$$= \int_0^\infty \sum_{l=n}^{N} \binom{N}{l} \sum_{m=0}^{l} \binom{l}{m} (-1)^{l-m} (e^{-y_I \sum_{k=2}^{K} I_k} \sum_{t=0}^{M-1} \frac{(y_I \sum_{k=2}^{K} I_k)}{t!}^t)^{N-m} \frac{e^{-y_I} {y_I}^{M-1}}{(M-1)!} dy_I$$

$$= \int_0^\infty \sum_{l=n}^{N} \binom{N}{l} \sum_{m=0}^{l} \binom{l}{m} (-1)^{l-m} (\frac{e^{-y_I(N-m) \sum_{k=2}^{K} I_k} e^{-y_I} {y_I}^{M-1}}{(M-1)!}) (\sum_{t=0}^{M-1} \frac{(y_I \sum_{k=2}^{K} I_k)}{t!}^t)^{N-m} dy_I$$

$$= \int_0^\infty \sum_{l=n}^{N} \binom{N}{l} \sum_{m=0}^{l} \binom{l}{m} (-1)^{l-m} (\sum_{t=0}^{M-1} \frac{e^{-y_I(1+(N-m) \sum_{k=2}^{K} I_k)} {y_I}^{t+M-1}}{(M-1)!} \frac{(N-m)^t (\sum_{k=2}^{K} I_k)}{t!}^t) dy_I$$

$$= \sum_{l=n}^{N} \binom{N}{l} \sum_{m=0}^{l} \binom{l}{m} (-1)^{l-m} (\sum_{t=0}^{M-1} \frac{(N-m)^t (\sum_{k=2}^{K} I_k)^t (t+M-1)!}{(M-1)! t!}$$

$$\cdot \int_0^\infty \frac{{y_I}^{t+M-1} e^{-y_{k,t}(1+(N-m) \sum_{k=2}^{K} I_k)}}{(t+M-1)!} dy_I)$$

$$= \sum_{l=n}^{N} \begin{pmatrix} N \\ l \end{pmatrix} \sum_{m=0}^{l} \begin{pmatrix} l \\ m \end{pmatrix} (-1)^{l-m} \left(\sum_{t=0}^{M-1} \frac{(N-m)^t \left(\sum_{k=2}^{K} I_k\right)^t (t+M-1)!}{(M-1)!t!(1+(N-m)\sum_{k=2}^{K} I_k)^{t+M}} \right). \tag{6.29}$$

6.5 Simulation Results

We analyze the downlink outage probability of the OFDMA-based femtocells in this chapter. We consider the exclusive spectrum allocation and the shared spectrum allocation schemes for the femtocells and macrocell. The gain-oriented distributed channel selection scheme and random selection scheme are considered. We assume the femtocell layout as shown in Fig. 3.1. There are 24 femtocells around the considered femtocell, and the group of 25 femtocells is uniformly distributed in a macrocell with the coverage of 500 meters. The separation distances between femtocells are $d_{sf} = 20$ meters. The link reliability requirement is larger than 90%. The nominal system parameters are listed in Table 4.1.

6.5.1 Outage Probability in Exclusive Spectrum Allocation

Fugure 6.1 shows the outage probability of different channels with different highest link gain against the femtocell sub-channel usage ratio ρ with the exclusive spectrum allocation, where $d_{sf} = 20$ meters. This figure shows the outage of subchannels with different highest link gain in the femtocell system. In the exclusive spectrum allocation scheme, only the femtocell-to-femtocell interference effect on outage probability. The outage probability increases when the sub-channel usage ratio increases and interfere to other femtocells with higher probability. In this figure, the subchannel with higher the link gain can ensure the outage probability. If the subchannel with the link gain is higher than the 15-th higher subchannel, those subchannels can

ensure the link reliability requirement is larger than 90% while other femtocell using all the subchannels.

Fugure 6.2 shows the outage probability against the data sub-channel usage ratio ρ with the exclusive spectrum allocation, where $d_{sf} = 20$ meters. The gain-oriented and random selection schemes are considered. When the sub-channel usage ratio increases, the outage probability increases due to the increasing interference from other femtocells. In this figure, the gain-oriented selection method has better performance than random selection method. Lower outage probability can be consummated by the gain-oriented selection method. However, the both method make no difference when the channel usage ratio is 1 because both of them use all the subchannels for communication.

6.5.2 Outage Probability in Shared Spectrum Allocation

Fugure 6.3 shows the outage probability of different channels with different highest link gains against the femtocell sub-channel usage ratio ρ with the shared spectrum allocation, where $d_{sf} = 20$ meters. We consider the two-tier interference. Comparing Fig. 6.1, it is shown that the interference form macrocell significantly impacts the link reliability, and the outage probability increases. For example, in Fig. 6.1, when we request the link reliability requirement has to larger than 90%, the 90% subchannels can be used. However, only 70% channel usage ratio can be used when we allocate the macrocell and femtocells in the same spectrum.

Fugure 6.4 shows the outage probability against the data sub-channel usage ratio ρ with the shared spectrum allocation, where $d_{sf} = 20$ meters. We consider the two channel selection schemes: gain-oriented and random selection schemes. This figure shows the two-tier interference significantly impacts on the outage probability. Compared to the Fig. 6.2, it is shown that the two-tier interference in the shared spec-

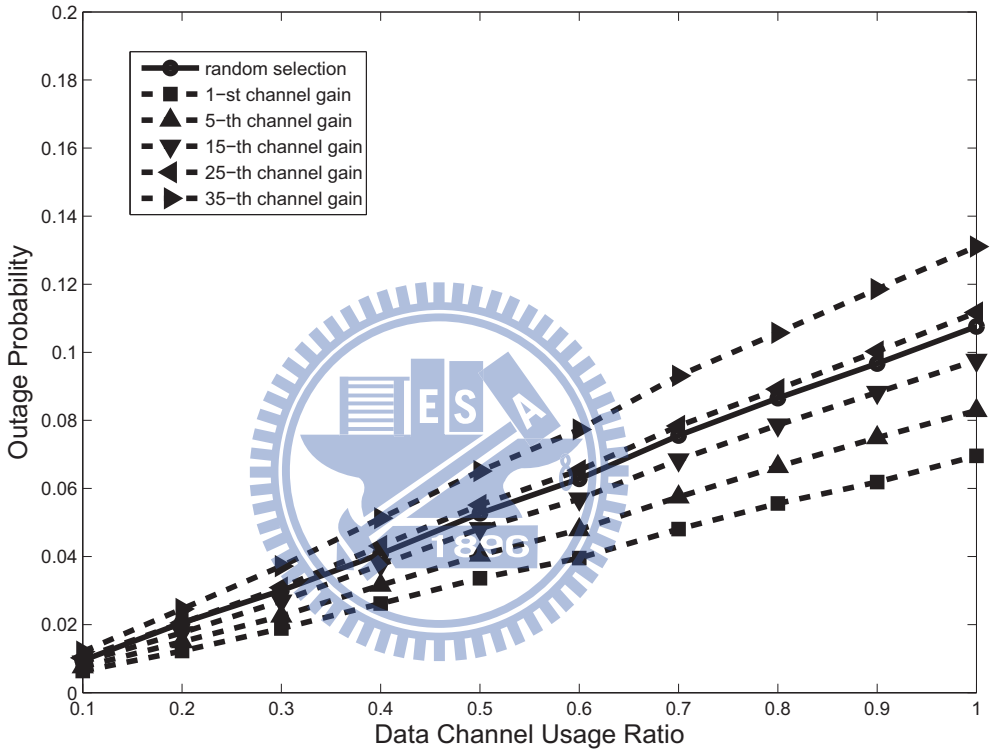

Figure 6.1: Outage probability with exclusive spectrum allocation scheme in different highest channel gain.

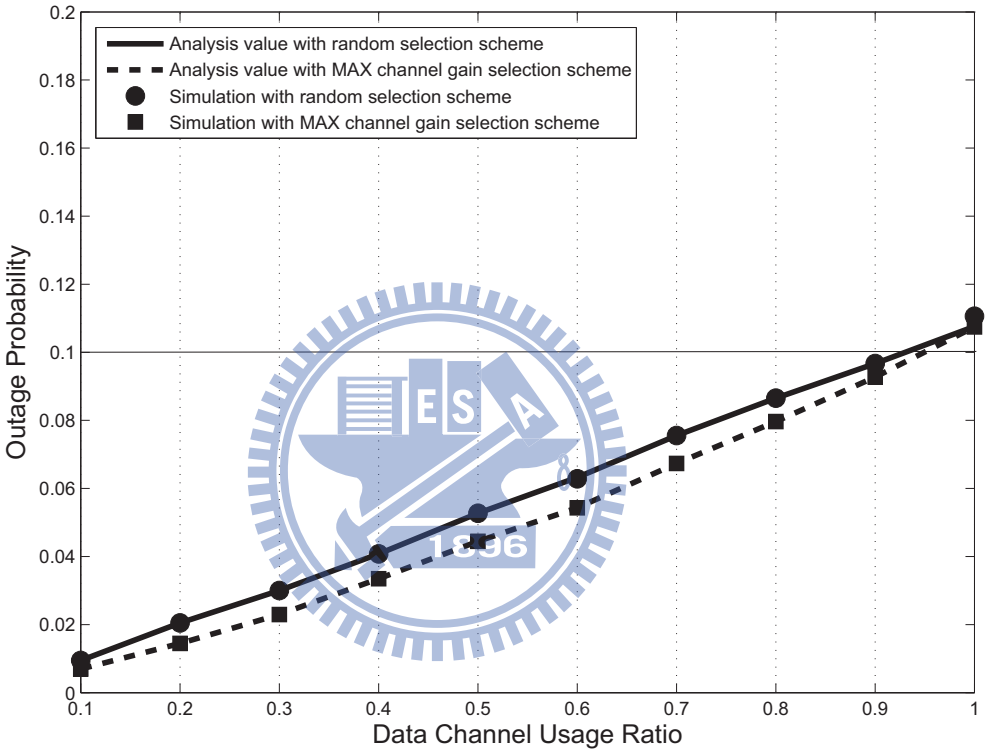

Figure 6.2: Outage probability with exclusive spectrum allocation scheme in random and gain-oriented selection schemes.

trum allocation scheme significantly effect on the link reliability probability. Random selection scheme can use 90% channel usage ratio for communication and guarantee the link reliability in the exclusive spectrum allocation scheme, but only 70% can use in the shared spectrum allocation scheme. That means femtocell use 22.2% lower subchannels because the extra interference from the macrocell. In addition, this figure illustrates the gain-oriented selection scheme has better performance than random selection scheme. If we request the outage probability requirement $Rel_{th} = 90\%$, the random selection scheme can use only channel usage ratio $\rho = 0.8$ for transmission and the gain-oriented selection scheme can transmission with channel usage ratio $\rho = 0.9$. That means we can use 25% more subchannels for communication if we use the gain-oriented selection scheme.

6.5.3 Impact of Macrocell Radius and Femtocell Channel Usage Ratio

In this subsection, we are interested in the relationship between the macrocell and the femtocell. In the future, when femtocells become popular, the femtocell users suffer from the complicated two-tier interference. Therefore, the femtocells pose a many challenges on managing the interference to increase the capacity and maintain the link reliability. In this subsection, we examine in the relationship between the macrocell radius and the femtocell channel usage ratio. From the analysis and the simulation results, the larger the radius of macrocell, the higher the channel usage ratio can be used by femtocells.

We analyze the downlink outage of the OFDMA-based femtocells. We consider the shared spectrum allocation schemes for the femtocells and macrocell. The gain-oriented distributed channel selection scheme and random selection scheme are considered. We assume that the femtocell layout as shown in Fig. 3.1. There are

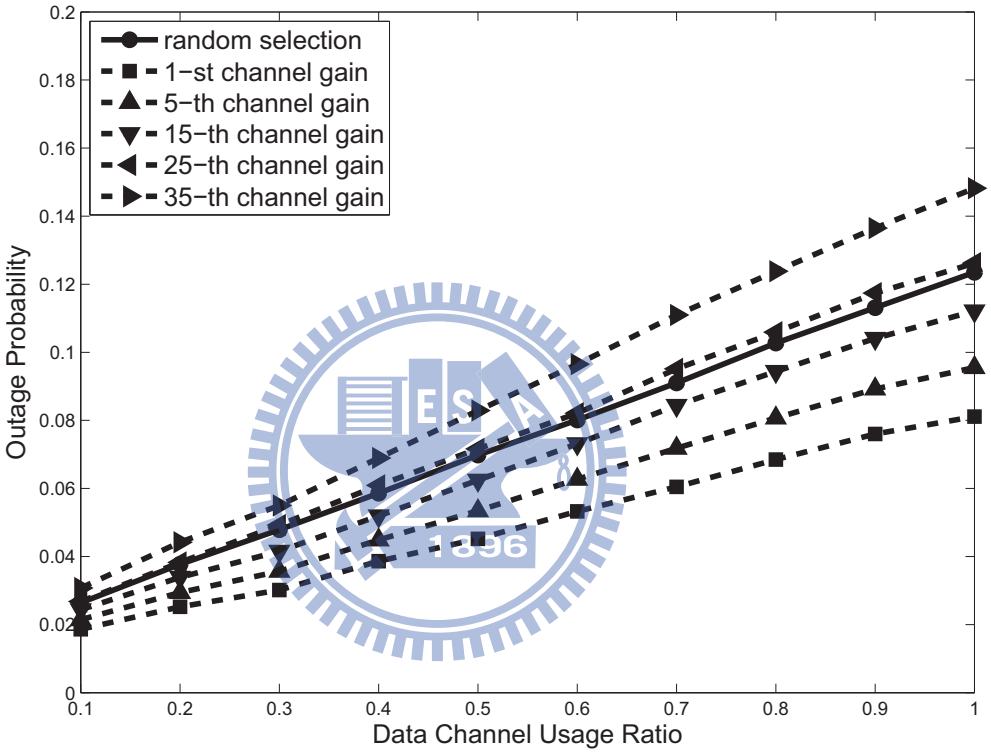

Figure 6.3: Outage probability with shared spectrum allocation scheme in different highest channel gain.

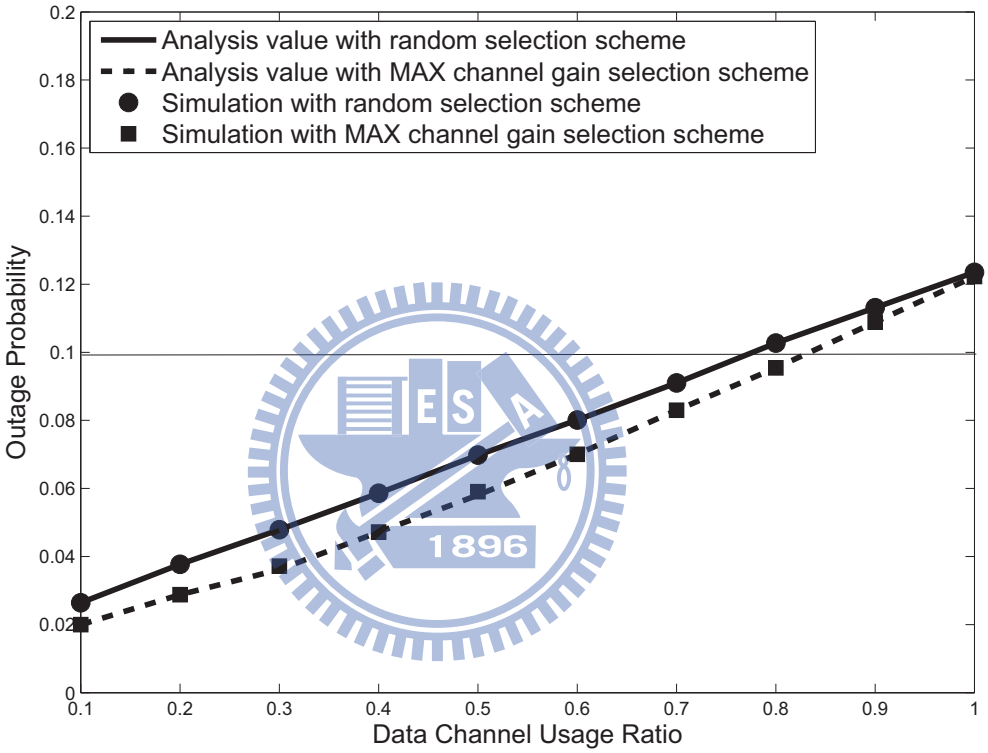

Figure 6.4: Outage probability with shared spectrum allocation scheme in random and gain-oriented selection schemes.

24 femtocells around the considered femtocell, and the group of 25 femtocells is uniformly distributed in a macrocell with the coverage D_M. The separation distances between femtocells are $d_{sf} = 20$ meters. The link reliability requirement is larger than 90%. The nominal system parameters are listed in Table 4.1.

Fugure 6.5 shows the outage probability of different channel usage ratio ρ against the macrocell radius with the shared spectrum allocation, where $d_{sf} = 20$ meters. We consider the interference from macrocell and femtocells. The gain-oriented and random selection schemes are considered. It is shown that the two-tier interference significantly impacts the link reliability probability. As the macrocell radius D_M increases, the outage probability decreases because the interference from the macrocell decrease. In this figure, the lower channel usage ratio ρ can achieve lower outage probability and experience the interference from the others femtocells with lower probability. When we compare the gain-oriented selection scheme with random selection scheme, the gain-oriented selection scheme can achieve lower outage probability than random selection scheme when we use the same channel usage ratio.

Table 6.1 shows that the relationship between macrocell radius D_M and channel usage ratio ρ of femtocell. The table shows that the gain-oriented selection scheme can used more channel usage ratio ρ than randomly selected under the same macrocell radius D_M. If the macrocell radius D_M is shorter than 150 m, the both selection scheme makes the femtocells is outage even femtocells use only the channel usage ratio $\rho = 0.1$. In the same condition of macrocell radius $D_M = 200$ meters, femtocells can transmit with channel usage ratio $\rho = 0.3$ if femtocells use the gain-oriented selection scheme, and only $\rho = 0.1$ by random selection method. In other word, we can use triple subchannels by the gain-oriented selection scheme. In addition, the channel usage ratio will be limited by the interference from the others femtocells. Even we ignore the macrocell interference and consider the $D_M = \infty$, the fmetocell still cannot use all the bandwidth for transmission and limited by 90%.

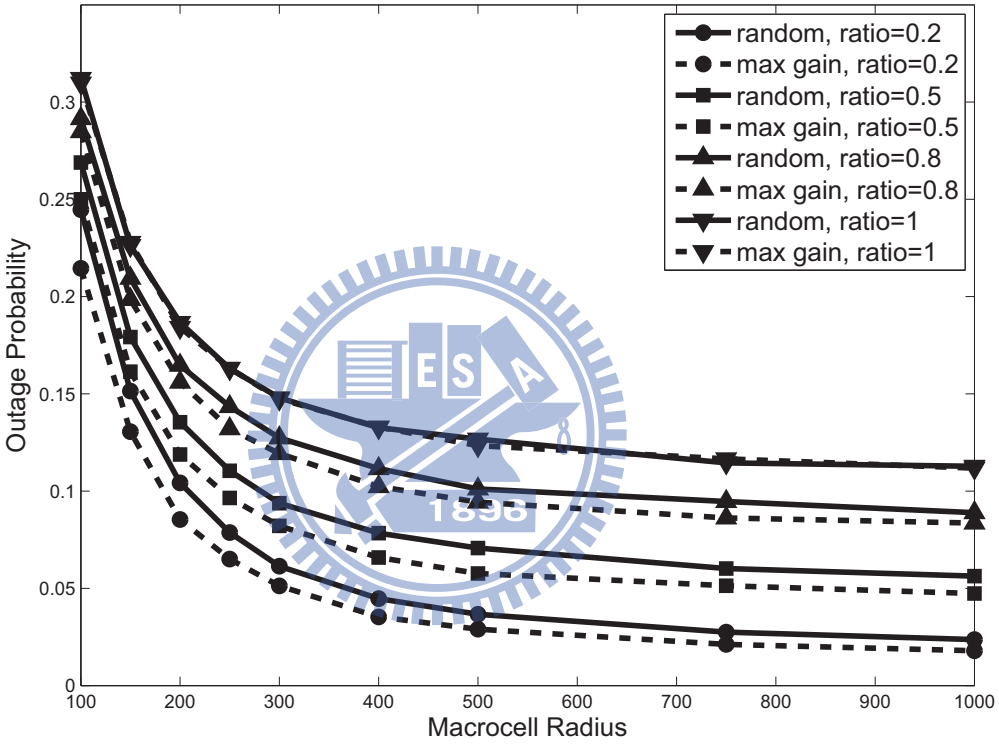

Figure 6.5: Outage probability in different macrocell radius.

Table 6.1: **Macrocell radius versus channel usage ratio with different selection method.**

Macrocell Radius (D_M)	**Channel Usage Ratio with Random Selecion (Ratio ρ)**	**Channel Usage Ratio with Maximal Channel Gain Selecion (Ratio ρ)**
100	x	x
150	x	x
200	0.1	0.3
250	0.4	0.5
300	0.5	0.6
400	0.7	0.7
500	0.7	0.8
750	0.8	0.8
1000	0.8	0.9
∞	0.9	0.9

Table 6.2 shows the relationship between channel usage ratio ρ and macrocell radius D_M. The table shows that the gain-oriented selection scheme is more suitable for femtocell in the same macrocell radius than randomly selected under the same channel usage ratio ρ that femtocell is used. If we request the channel usage ratio $\rho = 0.8$ the macrocell radius D_M has to be longer than 543.26 meters if the femtocell use the random selection scheme, and if the femtocell use the gain-oriented selection scheme, the macrocell radius D_M has to only be longer than 429.08 meters.

Table 6.2: **Channel usage ratio versus macrocell radius with different selection method.**

Channel Usage Ratio (ρ)	**Random Selecion on Macrocell Radius (D_M)**	**Maximal Channel Gain Selecion on Macrocell Radius (D_M)**
0.1	192.89	171.30
0.2	208.23	183.78
0.3	224.81	198.23
0.4	248.46	216.31
0.5	281.36	242.11
0.6	332.88	274.67
0.7	391.73	332.96
0.8	543.26	429.08
0.9	x	817.86
1	x	x

CHAPTER 7

Joint Sub-carrier Allocation and Power Control for Maximizing Energy Efficiency in OFDMA Based Femtocells

7.1 Introduction

Needless to say that the femtocells will be widely employed since the femtocells improve indoor capacity and coverage with low power and less cost in the next generation wireless networks . However, when the femtocells become popular, the femtocell users will suffer from the complicated two-tier interference, including the macrocell-to-femtocell and femtocell-to-femtocell interference. Therefore, the femtocells pose a many challenges on managing the interference in a autonomous and distributed manner. In this chapter, we investigate how to distributedly select the transmit power level and channel usage ratio for maximizing energy efficiency in OFDMA femtocells systems to reduce interference and to improve indoor capacity under a link reliability requirement. We develop the joint transmit power management and sub-carrier allocation principle. Simulation results show that the impact of channel usage ratio on the femtocell link reliability and capacity more significantly than increasing the power level. By using the joint transmit power management and sub-carrier allocation principle, femtocell can use the power in the most efficient way with the properly channel

usage ratio and the power level under the capacity and link reliability requirement.

7.2 Problem Formulation

Channel usage ratio ρ and transmit power level p_j are both essential factors in the joint transmit power management and sub-carrier allocation principle for the OFDMA-based femtocell systems. In the view point of channel usage ratio ρ, femtocell can achieve higher capacity by using higher channel usage ratio ρ. However, higher channel usage ratio also increase the probability that femtocells interfere with each other. From the viewpoint of transmit power level p_j, increasing the power level to a femtocell can increase the signal power to compete with the interference from macrocell. Nevertheless, increasing the power level to a femtocell is useless to overcome the interference from other femtocell. Increasing the power level to a femtocell also yields higher interference to other femtocells. Then the other femtocells have to increase the power level to compete with the increasing interference from the first femtocell. To achieve the higher energy efficiency, we formulate an optimization problem to determine the optimal the channel usage ratio and the properly power level of a femtocell. We aim to maximize the femtocell energy efficiency, and subject to the femtocell capacity and link reliability requirement of indoor and outdoor users.

The femtocell capacity C is defined as the aggregated throughput of a femtocell, which depends on the channel selection scheme, the number of used sub-channels, and the adopted MCS of each sub-channel. Let ε_j be the utility function. If the sub-channel j is selected to transmit data, $\varepsilon_j = 1$; otherwise, $\varepsilon_j = 0$. Consider that there are J data sub-channels. The sub-channel usage ratio is ρ, which is defined as the ratio of the number of used sub-channels to the total number of sub-channels. Thus, each femtocell can use ρJ sub-channels. The total femtocell power is equal to $\sum_{j=1}^{J} \varepsilon_j p_j$. Furthermore, according to the equivalent SINR $\gamma_{eff,j}$ from the EESM

calculation and Table 3.1, we can determine the used MCS and then the spectrum efficiency $SE_{EESM,j}$. Assume that B_j is the bandwidth of a sub-channel. Then, the femtocell capacity is equal to $C = \sum_{j=1}^{J} \varepsilon_j B_j SE_{EESM,j}$. The decision variable in the optimization problem is the channel usage ratio ρ and the transmit power level p_j. Based on these considerations, the energy efficiency maximization issue can be formulated as a nonlinear programming problem as expressed in the following as

$$\max_{0\le\rho\le 1, p_{\min}\le p_j\le p_{\max}} \frac{\sum_{j=1}^{J} \varepsilon_j B_j SE_{EESM,j}}{\sum_{j=1}^{J} \varepsilon_j p_j} \tag{7.1}$$

subject to:

$$\begin{aligned}
&\sum_{j=1}^{J} \varepsilon_j B_j \sigma_j \ge r_{th} \\
&\overline{P_{rel}} \ge Rel_{th} \\
&\varepsilon_j \in \{0,1\} && \forall j \\
&\rho = \frac{1}{J}\sum_{j=1}^{J} \varepsilon_j \\
&p_j \ge 0 && \forall j,
\end{aligned} \tag{7.2}$$

where $\varepsilon_j \in \{0,1\}$, and Rel_{th} and r_{th} are the link reliability and the femtocell capacity requirement for all the users.

7.3 Joint Sub-carrier Allocation and Power Control Principles

7.3.1 Impacts of transmission power on energy efficiency

Assume there are m power levels for a femtocell $p_1, p_2, p_3, ..., p_m$, and $p_1 < p_2 < p_3 < ... < p_m$. The minimal power level is p_1 and the maximal power level is p_m. For the same channel usage ratio is used in the femtocell, if there are five power levels (e.g. $p_{m-4}, p_{m-3}, p_{m-2}, p_{m-1}, p_m$) can ensure the capacity and the link reliability requirement. Then, p_{m-4} can achieve the highest energy efficiency than the other transmission power levels beacuse we can use lower power for transmission and ensure the capacity and the link reliability requirement. Moreover, lower transmit power is also the lower interference to the other femtocells.

7.3.2 Impacts of channel usage ratio on energy efficiency

Assume that there are n channel usage ratio for a femtocell $\rho_1, \rho_2, \rho_3, ..., \rho_n$, and $\rho_1 < \rho_2 < \rho_3 < ... < \rho_n$. The minimal channel usage ratio is ρ_1 and the maximal channel usage ratio is ρ_n. For the same transmission power level is used in the femtocell, if there are 5 channel usage ratio (e.g. $\rho_3, \rho_4, \rho_5, \rho_6, \rho_7$) can ensure the capacity and the link reliability requirement. Beacuse lower used channel usage ratio means the lower used transmit power, the ρ_3 can achieve the highest energy efficiency than the other channel usage ratio. We can ensure the capacity and the link reliability requirement with lower power. Moreover, lower channel usage ratio is also the lower probability to interfere the other femtocells.

7.3.3 Joint Sub-carrier Allocation and Power Control principle

We consider the joint transmit power management and sub-carrier allocation principle with two steps.

Step 1 : Find the channel usage ratio and power level can ensure the the capacity and the link reliability requirement.

Step 2 : Find maximal energy efficiency for femtocell with the channel usage ratio and power level under the the capacity and the link reliability requirement.

Table 7.1 shows the algorithm of the joint transmit power management and sub-carrier allocation principle. First, we have to know that if the transmit power p_i and the channel usage ratio ρ_i meet the femtocell capacity and link reliability requirement [13, 15, 28]. There are 4 different cases in the condition of the femtocell achieve capacity or link reliability requirement. In each case, we adjust the transmit power p_i and the channel usage ratio ρ_i refer from the algorithm in this table.

Figure 7.1 and 7.2 also show the flow chart of joint transmit power management and sub-carrier allocation principle. The maximal energy efficiency can be achieve in this algorithm.

Table 7.1: **Algorithm of the Joint Transmit Power Management and Subcarrier Allocation Principle.**

Step 1 :

Initial value $p_i \in \{p_1, p_{2,\ldots,p_m}\}$ $\rho_i \in \{\rho_1, \rho_{2,\ldots,\rho_m}\}$

While $(\sum_{j=1}^{J} \varepsilon_j B_j SE_{EESM,j} < r_{th})$ or $(\overline{P_{rel}} < Rel_{th})$

If $\sum_{j=1}^{J} \varepsilon_j B_j SE_{EESM,j} < r_{th}$

If $\overline{P_{rel}} \geq Rel_{th}$

$\rho_i = \rho_{i+1}$

else $\overline{P_{rel}} < Rel_{th}$

$\rho_i = \rho_{i+1}$

$p_i = p_{i+1}$

end

else $\sum_{j=1}^{J} \varepsilon_j B_j SE_{EESM,j} \geq r_{th}$

If $\overline{P_{rel}} < Rel_{th}$

$\rho_i = \rho_{i+1}$

end

end

end

Step 2 :

test p_{i-1}, ρ_i in (**Step 1**)

pass : $p_i = p_{i-1}$ and Go to (**Step 2**)

test p_i, ρ_{i-1} in (**Step 1**)

pass : $\rho_i = \rho_{i-1}$ and Go to (**Step 2**)

test p_{i-1}, ρ_{i+1} in (**Step 1**)

pass : $p_i = p_{i-1}$,$\rho_i = \rho_{i+1}$, and Go to (**Step 2**)

End of the Algorithm

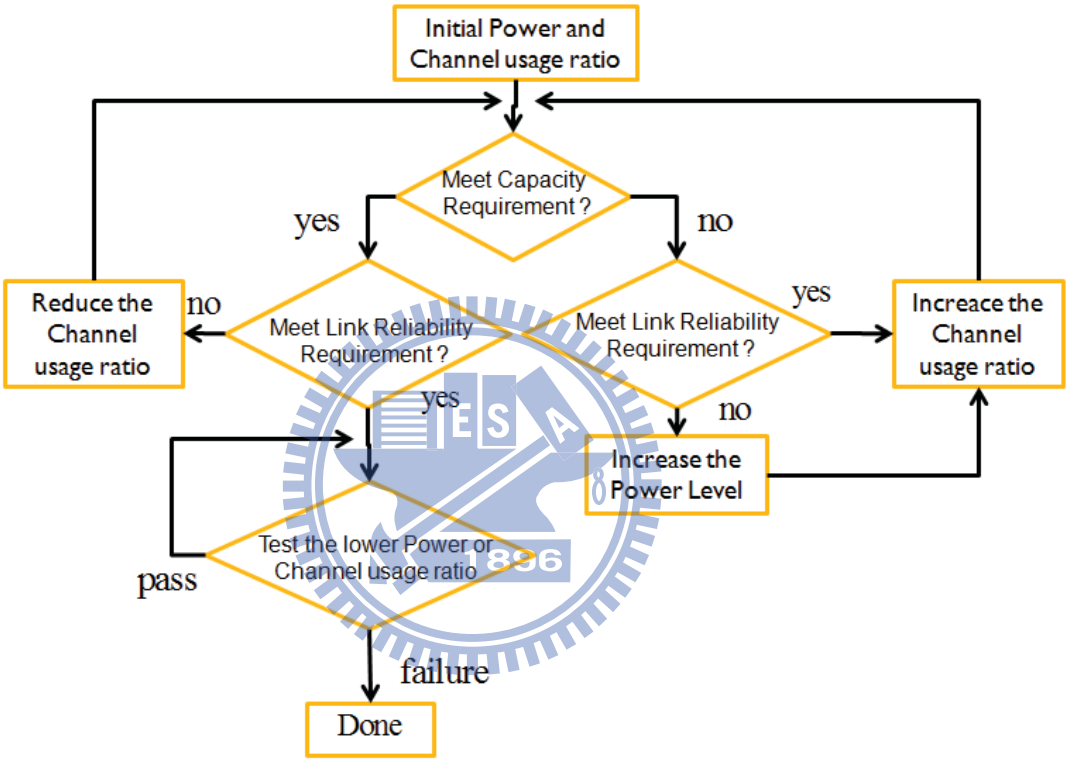

Figure 7.1: Flowchart of joint transmit power management and sub-carrier allocation idea.

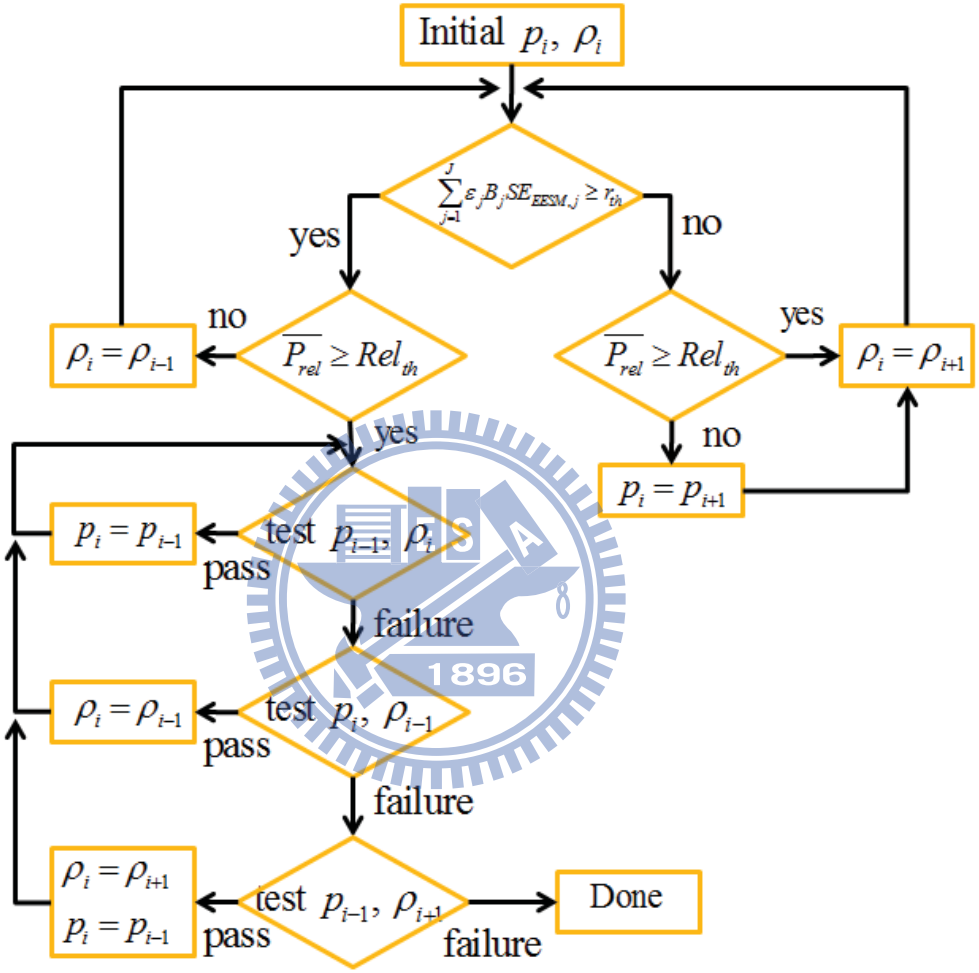

Figure 7.2: Flowchart of joint transmit power management and sub-carrier allocation principle.

7.4 Simulation Results

We investigate the downlink capacity and link reliability of the OFDMA-based femtocell. We consider the shared spectrum allocation and the exclusive spectrum allocation schemes for the femtocells and macrocell. We compare the different transmit power p_i and channel usage ratio ρ_i. We assume that the femtocell layout as shown in Fig. 3.1. There are 24 femtocells around the considered femtocell, and the group of 25 femtocells is uniformly distributed in a macrocell with the coverage of 500 meters. The separation distances between femtocells are $d_{sf} = 20$ m. The link reliability requirement is $Rel_{th} = 90\%$. The nominal system parameters are listed in Table 4.1.

7.4.1 Capacity in Shared Spectrum Allocation

Figure 7.4.3 shows the femtocell capacity for the various transmit power and channel usage ratio in the shared spectrum allocation scheme, where $d_{sf} = 20$ m. It is shown that femtocell can provide higher capacity by increasing the transmit power p and the channel usage ratio ρ. The higher transmit power can provide higher signal power to compete with the interference. The higher channel usage ratio can transmit data by more bandwidth, but it also increase the probability to interfere the other femtocells. From this figure, we know that increasing the channel usage ratio can achieve higher femtocell capacity more than increasing the transmit power. We can consider that the channel usage ratio allocate and limit the resource from whole wireless resource, and the power control allocates and adjusts the resource under the limited wireless resource.

7.4.2 Energy Efficiency in Shared Spectrum Allocation

Figure 7.4.3 shows the energy efficiency for the various transmit power and channel usage ratio in the shared spectrum allocation scheme, where $d_{sf} = 20$ m. It is shown that femtocell can achieve the highest energy efficiency by using the minimal transmit power p and the minimal channel usage ratio ρ. However, although the lower transmit power and lower channel usage ratio can achieve the highest energy efficiency, but it also serve the femtocell user with very low capacity. Therefore, to achieve the tradeoff between the maximal energy efficiency and capacity requirement, we develop the joint transmit power management and sub-carrier allocation principle to this problem.

7.4.3 Maximal Energy Efficiency in Shared Spectrum Allocation

Figure 7.4.3 shows the energy efficiency for the various transmit power and channel usage ratio in the shared spectrum allocation scheme, where $d_{sf} = 20$ m. In this figure, if the transmit power level and channel usage ratio cannot ensure the femtocell capacity or the link reliability requirement, then we put 0 in this figure. This figure also shows that the lower transmit power level and lower channel usage ratio may not ensure the femtocell capacity and the link reliability, and the higher transmit power and higher channel usage ratio will make the energy efficiency with a very low value. The joint transmit power management and sub-carrier allocation principle can be used in this problem. For example, if we request the link reliability have to greater than 90% and the femtocell capacity have to higher than 5 Mbps. In principle, we can find the best level of transmit power is 17 dB and the channel usage ratio is 0.4 by using the algorithm of joint transmit power management and sub-carrier allocation principle.

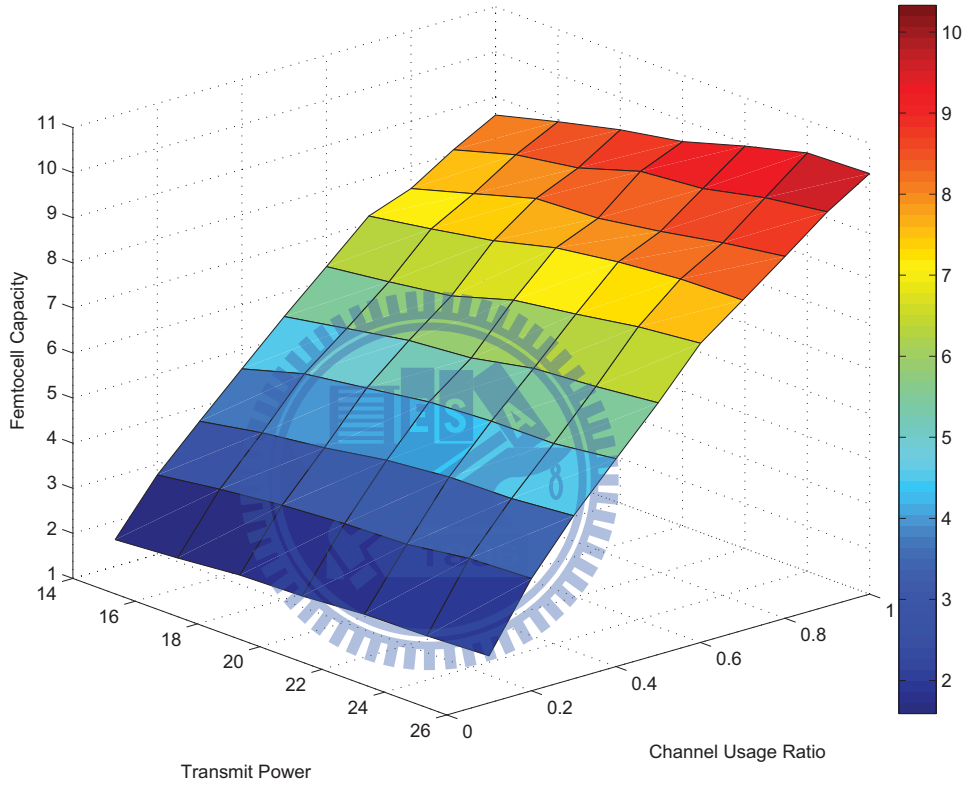

Figure 7.3: Femtocell capacity for various transmit power and channel usage ratio in the shared spectrum allocation scheme.

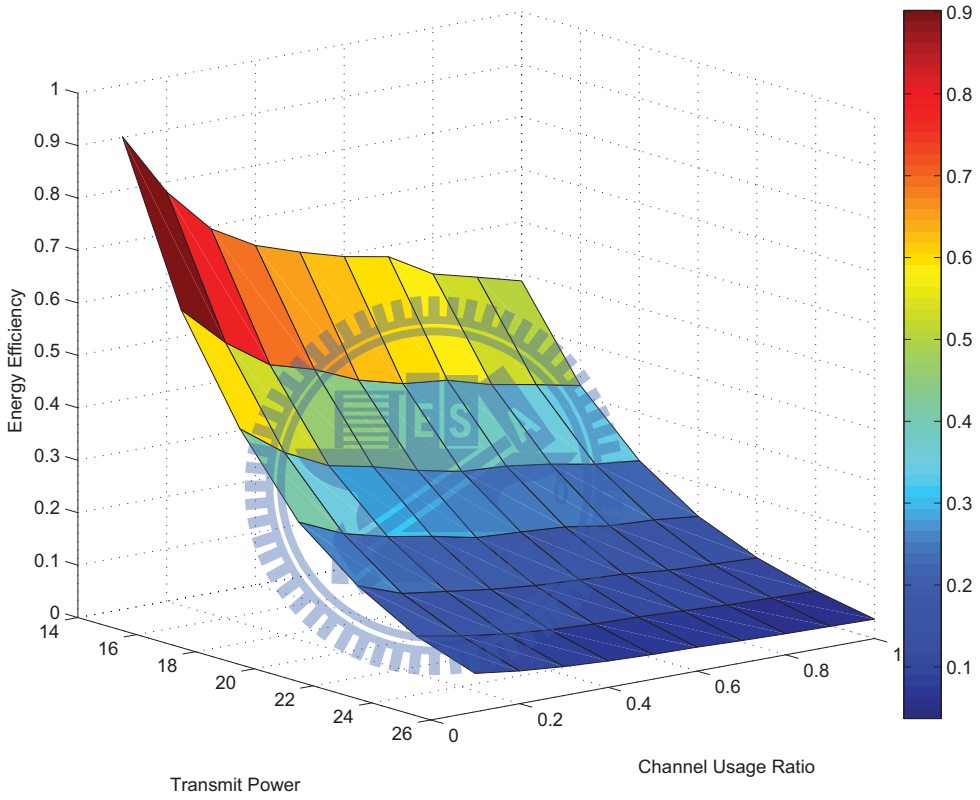

Figure 7.4: Energy efficiency for various transmit power and channel usage ratio in the shared spectrum allocation scheme.

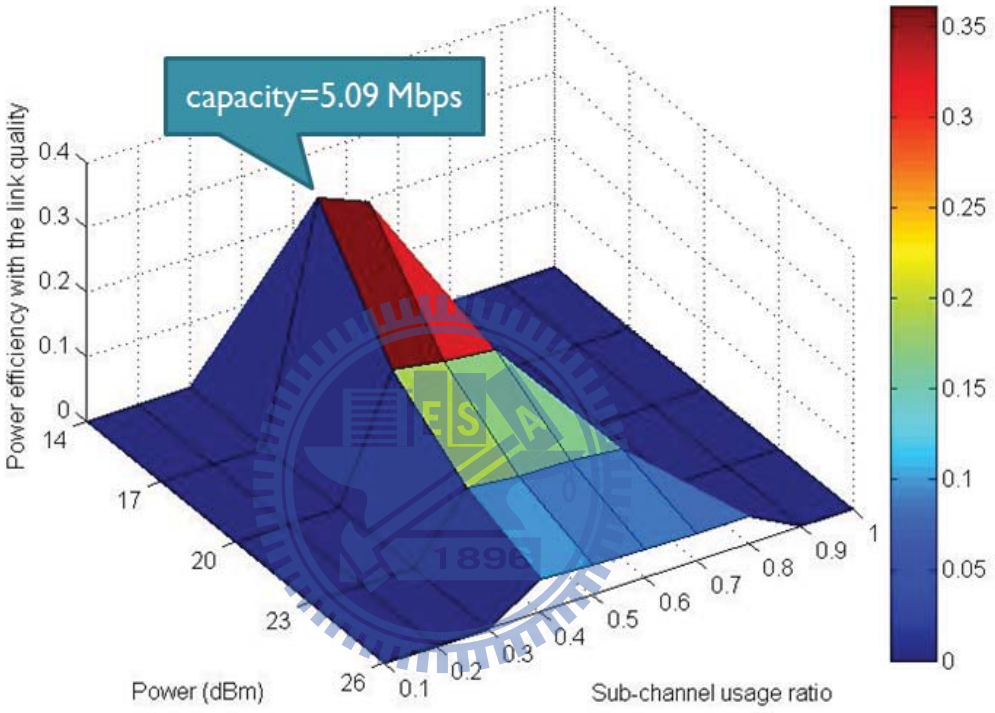

Figure 7.5: Energy efficiency for various transmit power and channel usage ratio in the shared spectrum allocation schemewith the femtocell capacity and link reliability requirement.

7.4.4 Impact of Adjusting Channel Usage Ratio First and Transmit Power First on Adjusting Times

Assume that there are 13 power levels for a femtocell from 14 dBm to 26 dBm, and 10 channel usage ratios for a femtocell 0.1 to 1. Four different case are simulated: femtocell with two-tier interference, macrocell interference only, femtocell interference only, and single femtocell environment. The two-tier interference environment is that there are 24 femtocells around the considered femtocell, and the group of 25 femtocells is uniformly distributed in a macrocell with the coverage of 500 meters. The separation distances between femtocells are $d_{sf} = 20$ m in the shared spectrum allocation scheme. The macrocell interference only environment can be considered the femtocell with sparse deployment (e.g. $d_{sf} = 1000$) in the shared spectrum allocation scheme. The femtocell interference only environment can be considered the exclusive spectrum allocation scheme and we do not consider the macrocell interference. The single femtocell environment means that there very low interference fro other femtocells or macrocell.

The purposed joint transmit power management and sub-carrier allocation principle is the channel usage ratio oriented method. We adjust the channel usage ratio first when the femtocell capacity and the link reliability is not achieved. We compare the joint transmit power management and sub-carrier allocation principle with the channel usage ratio oriented method and transmit power oriented method.

Table 7.4.4 shows that the number of adjusting times of these two different oriented methods. The higher value means the femtocell has to change the channel usage ratio and transmit power a lot to find the maximal energy efficiency point and ensure the femtocell capacity and link reliability requirement. In this table, adjusting times of the joint transmit power management and sub-carrier allocation principle with the channel usage ratio oriented method has lower value than transmit power

Table 7.2: **Adjusting Times of the Channel Usage Ratio Oriented and Transmission Power Oriented Joint Transmit Power Management and Sub-carrier Allocation Principle.**

	The Number of Adjusting Times	
	adjust channel usage ratio first	adjust transmit power level first
macrocell interference only	8.21	9.83
femtocell interference only	8.65	14.72
two-tier interference	6.71	13.78
single femtocell	9.73	10.83
Average	8.33	12.29

oriented method in each case. Simulations results show that the average adjusting times of the channel usage ratio oriented method is 8.83, and the average adjusting times of the transmit power oriented method is 12.29. That means the transmit power oriented method have to adjusting 39% times more than the channel usage ratio oriented method.

7.4.5 Improvement of Energy Efficiency

There are 13 power levels and 10 channel usage ratios are assumed as same as the Sec. 7.4.4. In Sec. 7.4.4, the joint transmit power management and sub-carrier allocation principle with the channel usage ratio and transmit power oriented methods

can adjust the power and channel usage ratio to a better level. However, we are also interest in the improvement of the energy efficiency by using the joint transmit power management and sub-carrier allocation principle. Under the same condition of capacity and link reliability requirement, we compare the joint transmit power management and sub-carrier allocation principle to the random selection method, witch select the power lever and channel usage ratio randomly.

Table 7.4.5 shows that the energy efficiency of the proposed principle and random selection. The higher value means the femtocell can serve to its user with higher energy efficiency and ensure the capacity and link reliability requirement. In this table, joint transmit power management and sub-carrier allocation principle achieve higher value than random selection in each case. Simulations results show that the average energy efficiency of joint transmit power management and sub-carrier allocation principle is 0.99 bits/s/mW, and the average energy efficiency of the random selection is 0.34 bits/s/mW. That means the joint transmit power management and sub-carrier allocation principle can achieve 191% higher energy efficiency than the random selection method.

Table 7.3: **Adjusting Times of the Channel Usage Ratio Oriented and Transmission Power Oriented Joint Transmit Power Management and Sub-carrier Allocation Principle.**

	Spectrum efficiency (bits/s/mW)	
	Joint Transmit PowerManagement and Sub-carrier Allocation Principle	Random Selection
macrocell interference only	1.07	0.38
femtocell interference only	0.83	0.24
two-tier interference	0.28	0.11
single femtocell	1.78	0.63
Average	0.99	0.34

CHAPTER 8

Conclusions

In this thesis, we develop the distributed channel selection principle to ensure the link reliability and improve capacity in the OFDMA-based femtocell systems. In the femtocell system, both the femtocell-to-femtocell and the macrocell-to-femtocell interference significantly degrade the link reliability. We develop gain-oriented and interference-avoidance-oriented channel selection principles to improve capacity and link reliability. Simulation results show that the developed channel selection scheme can achieve at most 121% higher capacity than the random selection scheme, under the link reliability requirement $Rel_{th} \geq 90\%$. It is also shown that the interference-avoidance-oriented selection scheme is suitable for femtocell with lower channel usage ratio. In addition, the gain-oriented selection scheme can be used to enhance capacity for femtocell with with higher channel usage ratio.

We also investigate the analytical approach for distributed channel selection principles for femtocell with two-tier interference. The outage probability of femtocell with the random selection and the gain-oriented schemes can be calculated. By using the order statistics method, we can analyze the femtocell outage of gain-oriented scheme. We also investigate the impacts of channel usage ratio ρ and the macrocell radius on the outage probability of femtocell users. Simulation results show the relationship between the femtocell channel usage ratio and the macrocell radius distance. For example, in Chapter 5, when we consider the macrocell radius $D_M = 250$

m, the random selection scheme can use only the channel usage ratio $\rho = 0.1$, the gain-oriented selection scheme can use the channel usage ratio $\rho = 0.5$. In this case, the five times bandwidth can be used in gain-oriented selection scheme than random selection scheme.

We develop the joint transmit power management and sub-carrier allocation principle. By using the joint transmit power management and sub-carrier allocation principle, femtocell can use the power in the most efficiency way with the properly channel usage ratio and the power level under the capacity and link reliability requirement. The channel usage ratio oriented method and transmit power oriented method of the principle are considered. Simulations results show that the average adjusting times of the channel usage ratio oriented method is 8.83, and the average adjusting times of the transmit power oriented method is 12.29. It is means that the transmit power oriented method have to adjusting 39% times more than the channel usage ratio oriented method.

Bibliography

[1] H. Claussen, L. Ho, and L. G. Samuel, "An overview of the femtocell concept," *Bell Labs Technical Journal*, vol. 13, pp. 221–245, 2008.

[2] C. Edwards, "The future is femto," in *IET*, Sep. 2008.

[3] S. Yeh, S. Talwar, S. C. Lee, and H. Kim, "WiMAX femtocells: a perspective on network architecture, capacity, and coverage." *IEEE Communications Magazine*, vol. 46, pp. 58–65, Oct. 2008.

[4] X. Li, L. Qian, and D. Kataria, "Downlink power control in co-channel macrocell femtocell overlay." IEEE CISS.

[5] C. Lee, L.-C. Wang, and J.-H. Huang, "Effect of two-tier interference in OFDMA femtocell systems with various sub-carrier allocation methods." IEEE Transaction Vehicular Technology, to be submitted.

[6] V. Chandrasekhar and J. G. Andrews, "Femtocell networks: A survey," *IEEE Communications Magazine*, pp. 59–67, Sep. 2008.

[7] H. Claussen, L. Ho, and L. Samuel, "Self-optimizationof coverage for femtocell deployments," in *WTS*. IEEE Wireless Telecomunications Symposium, Apr., p. 278 - 85.

[8] D. López-Pérez, A. Valcarce, G. Roche, and J. Zhang, "OFDMA femtocells: a roadmap on interference avoidance," *IEEE Communications Magazine*, pp. 41–48, Sep. 2009.

[9] *WiMAX System Evaluation Methodology*, V2.1 ed., WiMAX Forum, Jul. 2008.

[10] H. Zeng, C. Zhu, and W. P. Chen, "System performance of self-organizing network algorithm in wimax femtocells," in *WICON*, Nov. 2008.

[11] J. G. Andrews, A. Ghosh, and R. Muhamed, *Fundamentals of WiMAX*. Prentice-Hall, 2007.

[12] L.-C. Wang, S.-Y. Huang, and A. Chen, "On the throughput performance of CSMA-based wireless local area network with directional antennas and capture effect: A cross-layer analytical approach," *IEEE WCNC*, pp. 1879–1884, Mar. 2004.

[13] V. Chandrasekhar and J. G. Andrews, "Uplink capacity and interference avoidance for two-tier femtocell networks," *IEEE Transactions on Wireless Communications*, vol. 8, no. 7, pp. 3498–3509, Jul. 2009.

[14] *Proposed Change for the IEEE P802.16m/D1: Downlink Power Control for Femto ABS with Penetration Loss*.

[15] L.-C. Wang, K.-N. Yen, J.-H. Huang, A. Chen, and C.-J. Chang, "Cross-layer performance analysis of joint rate and power adaptation schemes with multiple-user contention in nakagami fading channels," *International Conference On Communications And Mobile Computing*, pp. 881 – 886, Oct. 2006.

[16] V.Chandrasekhar, J. Andrews, Z. Shen, T. Muharemovic, and A. Gatherer, "Power control in two-tier femtocell networks," *IEEE Transactions on Wireless Communications*, vol. 8, no. 8, pp. 4316–4328, Aug. 2009.

[17] *IEEE 802.16m System Description Document (SDD)*, IEEE 802.16 Broadband Wireless Access Working Group, IEEE 802.16m-09/0034r2, Sep. 2009.

[18] L. G. Garcia, K. I. Pedersen, and P. E. Mogensen, "Autonomous component carrier selection: Interference management in local area environments for LTE-advanced," *IEEE Communications Magazine*, pp. 110–116, Sep. 2009.

[19] *Usage Models*, IEEE 802.11n Working Group, IEEE 802.11-03/802r14, Mar. 2004.

[20] *Indoor MIMO WLAN Channel Models*, IEEE 802.11n Working Group, IEEE 802.11-03/162r2, Jul. 2003.

[21] *Simulating the SUI Channel Models*, IEEE 802.16 Working Group, IEEE 802.16.3c-01/53, Apr. 2001.

[22] *CINR measurement using EESM method*, IEEE 802.16 Working Group, IEEE 802.16e-05/141r3, Apr. 2005.

[23] C. Lee, L.-C. Wang, and J.-H. Huang, "Distributed channel selection principles for femtocells with two-tier interference." IEEE Vehicular Technology Conference, May. 2010.

[24] David Lopez-Perez and Guillaume Roche and Alvaro Valcarce and Alpar Juttner and Jie Zhang, "Interference avoidance and dynamic frequency planning for WiMAX femtocells networks," *International Conference on Computational Science*, pp. 1579–1584, Aug. 2008.

[25] H. Claussen, L. T. W. Ho, and L. G. Samuel, "Downlink power control in co-channel macrocell femtocell overlay," *IEEE International Communications Conference*, pp. 5604–5609, Oct. 2007.

[26] L.-C. Wang, A. Chen, and S.-Y. Huang, "A cross-layer investigation for the throughput performance of CSMA/CA-based wlans with directional antennas and capture effect," *IEEE Transactions on Vehicular Technology*, vol. 56, no. 5, pp. 2756–2766, Sep. 2007.

[27] J. Kim, S. H. Moon, and D. K. Sung, "Throughput estimation of downlink packet access systems using point mass approximation," *IEEE Transactions on Vehicular Technology*, vol. 4, May. 2010.

[28] V. Chandrasekhar and J. G. Andrews, "Spectrum allocation in tiered cellular networks," *IEEE Transactions on Communications*, vol. 57, no. 10, pp. 3059–3068, Oct. 2009.

Vita

Chiao Lee

He was born in Taiwan, R. O. C. in 1986. He received a B.S. in Electrical Engineering from National Chung Hsing University of Technology in 2008. From July 2008 to September 2010, he worked his Master degree in the Wireless System Lab in the Department of Communication Engineering at National Chiao-Tung University. His research interests are in the field of wireless communications.